Study on molecular breeding of yeast strain for bio-production based on flux balance analysis

Submitted to
Graduate School of Information Science and Technology, Osaka University

January 2019

Keisuke Morita

List of publications

1. Journal paper

[1-1] **Keisuke Morita**, Yuta Nomura, Jun Ishii, Fumio Matsuda, Akihiko Kondo, and Hiroshi Shimizu, "Heterologous expression of bacterial phosphoenolpyruvate carboxylase and Entner-Doudoroff pathway in *Saccharomyces cerevisiae* for improvement of isobutanol production" *Journal of Bioscience and Bioengineering*, Vol. 124, No. 3, pp. 263-270, (2017). (Chapter 2)

[1-2] Jun Ishii, **Keisuke Morita**, Kengo Ida, Hiroko Kato, Shohei Kinoshita, Shoko Hataya, Hiroshi Shimizu, Akihiko Kondo, Fumio Matsuda, "A pyruvate carbon flux tugging strategy for increased 2,3-butanediol production and reducing ethanol subgeneration in the yeast *Saccharomyces cerevisiae*" *Biotechnol Biofuels*, (2018). (Chapter 2 & 3)

2. International conferences

[2-1] **Keisuke Morita**, Fumio Matsuda, Jun Ishii, Akihiko Kondo, Hiroshi Shimizu, "Heterologous gene expression in *Saccharomyces cerevisiae* for higher isobutanol production", Metabolic Engineering XI, 2016, Awaji-shima, Japan, June 2016, Poster (Chapter 2)

[2-2] **Keisuke Morita**, Fumio Matsuda, Koji Okamoto, Kengo Ida, Jun Ishii, Akihiko Kondo, Hiroshi Shimizu, "Engineering of mitochondrial isobutanol production in *Saccharomyces cerevisiae*" 14th International Congress on Yeasts, 2016, Awaji-shima, Japan, June, Poster (Humanware Interdisciplinary Studies)

[2-3] **Keisuke Morita**, Fumio Matsuda, Jun Ishii, Akihiko Kondo, and Hiroshi Shimizu, "Dynamic regulation of ethanol production in yeast by inactive Cas9 system", i-BioS2017, 2017, Singapore, December, Poster (Chapter 3)

Abstract

Recently, computer-aided strain breeding of microorganisms has been actively performed to develop the productivities of useful substances. Flux balance analysis (FBA) has been used for the metabolic design suitable for chemical production as a comprehensive and cost-effective prediction method of metabolic state in the microbial cell. Yeast *Saccharomyces cerevisiae* is a great industrial host for bio-ethanol production due to its robustness to pH stress and fermentation ability and also applied for some production of chemicals. However in the computer-aided yeast metabolic engineering approaches, the result of metabolic simulation and the yield of actually constructed strains are often different, thus improvement of the approach is desired. In this thesis, to improve the computer-aided yeast breeding approach, strains were constructed FBA simulation result and investigated the current model prediction capacities and the strain breeding approaches. In strain breeding, additional engineering was also conducted to complement the factors that are ignored in FBA simulation according to the design-build-test-learn cycle of metabolic engineering. Then, a yeast FBA metabolic model was reconstructed including the constraint of the factor which was considered from the comparison, to propose the method for searching the suitable target metabolite for the bio-production in *S. cerevisiae*. Using the reconstructed model, selection of the target metabolites that suitable for the yeast bio-production was tried and verified by the strain breeding.

This thesis consists of the following four chapters:

Chapter 1: Background and objective of the research are described.

Chapter 2: Metabolic simulation based on FBA for isobutanol production was carried out. FBA results suggested that the improvement of cofactor imbalance of

NADPH and inhibition of ethanol by-production were important for high yield of isobutanol production. The engineered strain which was introduced the metabolic pathway helping the regeneration of NADPH increased isobutanol yield 1.45 times compared to the wild-type strain (1.1%). Then, in order to suppress the ethanol production, ethanol non-producing yeast strain with multiple knockouts of pyruvate decarboxylase (PDC) genes was constructed. The strain also improved the isobutanol yield to 2.9%, however it was too small compared with the metabolic simulation result (54%). From these results, the iron-sulfur cluster (ISC) dependent reactions were considered as the common factor of low active metabolic pathways causing a metabolic bottle-neck.

Chapter 3: the FBA metabolic model was reconstructed based on the results from chapter 2. Introduction of the constraint for ISC to the FBA metabolic model resulted in a decrease of the gap between simulation results to experimental values of constructed strains (decreased to 11.7%). Using the reconstructed metabolic model, isobutanol production requiring the ISC was suggested as an unsuitable target in yeast. On the other hand, metabolites such as 2,3-butanediol were turned out to be producible in yeast. Then engineered strains based on reconstructed FBA result were achieved high 2,3-butanediol yield (58%) that value was close to simulation results (58.9).

Chapter 4: General conclusion and future perspective of this study are described.

Table of contents

Chapter 1: Introduction

1-1 Highlights

- Microbial bioproduction of chemicals is focused on recently.
- Metabolic simulation based on flux balance analysis (FBA) has been developed for the rational metabolic engineering to improve the productivities of target products.
- Yeast *Saccharomyces cerevisiae* is one of the useful host microorganism for bioproduction, however, there are several targets with very low production yield of bred strains compared to the FBA metabolic simulation results.
- The general objective of this study was an improvement of the FBA based computer-aided yeast breeding approach to filling in a gap between the simulation results and the experimental results.

1-2 Microbial fermentation of foods and chemicals

The microorganism is a generic term for microscopic organisms that are too small to observe their structure and shape on our eyes without using a microscope. Microorganisms exist everywhere in the natural environment and also in our body, directly relate to the maintenance of our physical condition and diseases. Human beings have used microorganisms before we realized their existences. For example, *Japanese-sake* is brewed from rice converting starch to glucose by *Aspergillus oryzae* and then converting glucose to ethanol by yeast *Saccharomyces cerevisiae*. In a similar way, fermented foods such as beer, wine, miso, cheese, and yogurt have been produced by

microbial bio-processes for a long time [1]. In the 20th century, production of monosodium glutamate (one of the amino acid known as *umami*) has been carried out using *Bacillus subtilis* by Ajinomoto Company (Japan) Kyowa Hakko Company (Japan).

Bio-processes performed by microorganisms were also used in the field of medicine. The bioprocesses have high reaction specificity of the substrate and can produce highly complex and functional substances. Antibiotics are natural medicines produced by microorganisms. For example, penicillin produced by the fungus *Penicillium chrysogenum* discovered by Fleming in the 1920s saved many people's lives from the infection during the war [2]. Streptomycin produced by *Streptomyces griseus* was also used against tuberculosis which was a fatal disease at that time.

Bio-processes had been mainly focused on the production of foods and some antibiotics. However, emerging of new problems such as depletion of oil and global warming with the development of chemical processes, recently, movements have become active to reduce the burden on the environment by replacing a part of chemical processes to bioprocesses. The most representative example is the production of bio-ethanol using yeast strain for alternative fuel from corns. This process was actually carried out in industrial scales. However, this approach has faults because the use of corns is competing with the demand as food. Furthermore, ethanol is a simple structural chemical with low energy density and high hydrophilicity, it cannot be used with gasoline in current engines. Therefore, more complicated chemicals with higher energy density have been tried to be produced for the use of fuels and raw materials of polymers. Actually, the bio-production of 1,3-propanediol (DuPont Tate and Lyle Bioproducts Company (USA)), 1,4-butanediol (Genomatica Inc. (USA)) and succinate (Myriant Corporation) were achieved in industrial scales. Bio-processes are still widely contributing to human society and further

development is desired for constructing a sustainable material production process with low environmental burden [3].

1-3 Molecular breeding of microorganisms and metabolic engineering

An important thing for the development of bioprocess is the molecular breeding of microbial strains directly involved in the chemical conversion. Until the 1980s, when the sequences and function of genes of organisms were unknown, the general methods of strain breeding were the isolation of microbial strains with the desired character from the nature and the recombination of the genome by crossing the strains of different traits. In addition, random mutation methods by ultraviolet rays or chemical mutation induction were performed with cycles of screening and selections to obtain strains with a higher growth rate, stress tolerance, and productivity. These methods can be applied to any kind of microorganisms regardless of species and knowledge with appropriate screening conditions and selective pressures. Therefore, they are still contributing to the improvement of productivity of antibodies, amino acids, and alcohols. Although these methods are powerful for the strain breeding, it takes a long time to obtain the desired strain. It was also difficult to identify what kind of mutations were responsible for the strain improvement due to the random mutations and to apply the knowledge to other organisms and chemical productions.

In recent years, the DNA structure and whole genome sequences of several organisms such as *S. cerevisiae* and *Escherichia coli* were elucidated by the development of molecular biology. It has been contributed to constructing a database of amassed data that include gene sequences, functions, enzymatic activities and so on. [4, 5, 6].

Gene modification technology and gene cloning technology have also greatly

developed. Discovering the plasmid vectors allowed the over-expression of genes [7]. A plasmid is a circular nucleic acid molecule that exists separately from the genome in the microbial cell, cloned and inherited to cells in the same manner of genome DNA. High-throughput modification of microbial metabolism by expression of metabolic enzyme became possible by the combination of the expression cassettes composed by a promoter and a terminator and a gene on plasmids. It was also possible to knock out the entire gene of the target or introduce a single mutation at an arbitrary position on the genome. As a result of enabling large-scale modification of metabolic genes using such new technologies, a field of metabolic engineering was established [8, 9].

Metabolism is a series of intracellular chemical reactions that convert carbon sources and nitrogen sources to energy and other chemical substances required for construction of their cells in their life cycles. The goal of metabolic engineering is optimizing a system of these metabolic reactions for the target bio-production. Microbial cells can be considered as factories that produce the final products from the raw materials on a belt conveyor by continuous machine processing. Cells gradually convert the substrates such as glucose by a number of reactions catalyzed by enzymes, acquiring the metabolites and energy necessary for cell growth and cell maintenance, then, finally excrete the final product (Figure 1-3-1). An example of the factory shown in figure 1-3-1(A), in order to maximize the production of Product A, the production of other products (Product B and Product C) lines should be reduced. The same approach can be applied to the microbial metabolism. To maximize the biosynthesis of Product A in cells figure 1-3-1(B), deletion of the genes for metabolic reactions necessary for the production of Product B, cell components and energy were the most effective approach. If it is necessary, expressing the enzyme genes for new metabolic reactions to increase the number of lines

(increasing the number of enzymes) was also effective. However, different from the factory described in figure 1-3-1(A), the factory can receive energy from the outside for operations, whereas the microbial cells must acquire the all energy and cell components within the metabolism in the cell. That is, if reactions for cell components and energy production are completely stopped, the metabolic system itself cannot be maintained due to the cell death. Also, if the new metabolic reactions requiring the energy metabolites are introduced, the balance between energy consumption and regeneration might be collapsed and also resulted in a decrease of productivity and growth ability.

The tasks of metabolic engineering are designing the optimal metabolism for target metabolite production while ensuring the cell component and energy production necessary for growth and cell maintenance and breeding the microbial strains for the target production. However, intracellular metabolic pathways are composed of thousands of chemical reactions and metabolites and interact intricately through the energy transfer metabolite such as ATP, NADH, and NADPH. Therefore, it was very difficult to rationally predict which metabolic enzyme gene should be expressed or destroyed to improve the productivity of the target metabolite.

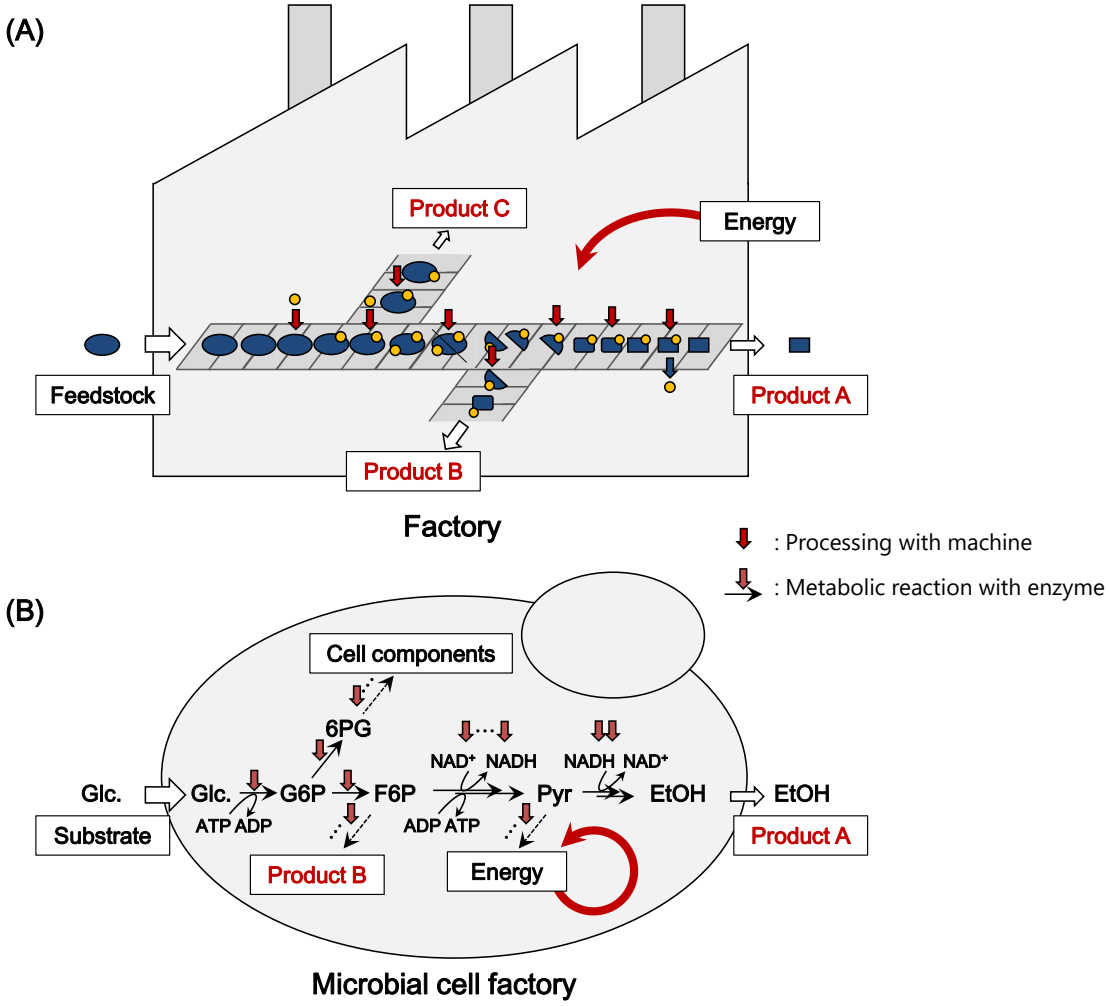

Figure 1-3-1 Similarities and differences of (A) the factory and (B) the microbial cell factory

(A) In the factory, machines produce products by the successive process of raw materials using energy supplied from outside. (B) In the microbial cell factory, metabolic enzymes catalyze the substrate successively to produce the cell components and energy necessary for the cell growth and maintenance, then, other products are produced using surplus carbons and energy.

1-4 Metabolic simulation based on flux balance analysis

Recently, metabolic simulation techniques have been developed as a result of the accumulation of knowledge of metabolic enzymes, pathways, and genes [10,11]. Actions of metabolic reactions in the cell involve many factors such as stoichiometry, metabolite concentration, reaction rate, and thermodynamics. Taking all of these factors into consideration, construction of dynamic metabolic models have been attempted [12,13,14,15,16,17,18]. These models calculate the flux of the metabolic reactions and the time course of metabolite concentrations using the experimental parameters such as Km values, Gibbs free energies, and metabolite concentrations. (Figure 1-4-1). These methods have been developed for predicting the localized metabolic flux to analyze the metabolite pool change, the expression level of the enzyme, and the effect of feedback regulation by the product. However, for the construction of dynamic models, experimental values of all parameters related to reactions such as Michaelis-Menten constant values are necessary. Furthermore, it cannot represent the entire metabolic network yet due to the problem of calculation cost. In recent years, the method called the ensemble modeling has been studied to represent the metabolism by integrating the hundreds of results from models given a random parameter to reactions with no experimental data [19]. It is also difficult to estimate a genome-wide metabolic network because of the large calculation cost.

In the 1990s, metabolic simulation approach based on flux balance analysis (FBA) was established [20,21,22]. In FBA, metabolism is considered as a steady state when the cell growth maximized for growth in a mid-log growth phase. With these constraints, entire metabolic flux distributions are calculated by linear programming

using a static model constructed by the stoichiometric reactions only. In this method, factors such as metabolite concentration, enzyme amount, thermodynamic are eliminated. Therefore, FBA can calculate the metabolic flux of complex genome-wide metabolic networks with small calculation cost.

Since the report of Varma *et al.*, metabolic simulation based on FBA has been actively carried out. Many metabolic models and tools for calculation on computers were also developed [23, 24, 25, 26, 27, 28, 29, 30, 31]. FBA can investigate the effect of the changes in culture conditions on the growth ability and behavior of metabolism. It can also investigate the behavior of whole reactions when the reactions are deleted or newly introduced to metabolism. Metabolic reactions include metabolites called coenzymes such as ATP, NADH, and NADPH that served as energy currency in the cell, and their consumptions and regenerations make the metabolism more complicated. However, it becomes possible to compute the cofactors collectively by FBA, metabolic designs for maximizing the productivity of the target metabolite can be easily calculated on the computer. That is, what reaction should be deleted or added can be predicted in advance for the strain breeding. Much more rational metabolic engineering can be conducted by FBA compared to modifying the genes in a blinded manner, therefore successful examples that improved the productivity of several metabolites in several organisms such as *E. coli* and *S. cerevisiae* have been reported [32, 33, 34, 35, 36, 37]

Of course, FBA is a simplified approach using static model, ignoring feedback control, reaction kinetics and so on, so the cases that the experimental results are mismatched to the FBA results often occur. For that reason, in metabolic engineering based on FBA, cycles of design-build-test-learn are required, corresponding to the design of metabolic network based on the simulation (Design), the breeding of strains (Build),

the fermentation test and the analysis (Test) and discovery of the problems for further improvement of design and breeding (Learn) (Figure 1-4-2). This approach is actively conducted in computer-aided metabolic engineering, especially in the field of synthetic biology to improve the efficiency of engineering. Metabolic engineering design based on FBA does not consider the kinetic factors of reactions, therefore breeding of microbial strain is also important such as releasing the feedback regulations, searching for highly active enzymes, and optimizing the metabolism by adaptive laboratory evolution (ALE) experiments. In fact, improvement of succinate production in *E.coli* was reported that the high yields of succinate close to FBA results were achieved by releasing the feedback control by optimization of metabolism through the ALE [38].

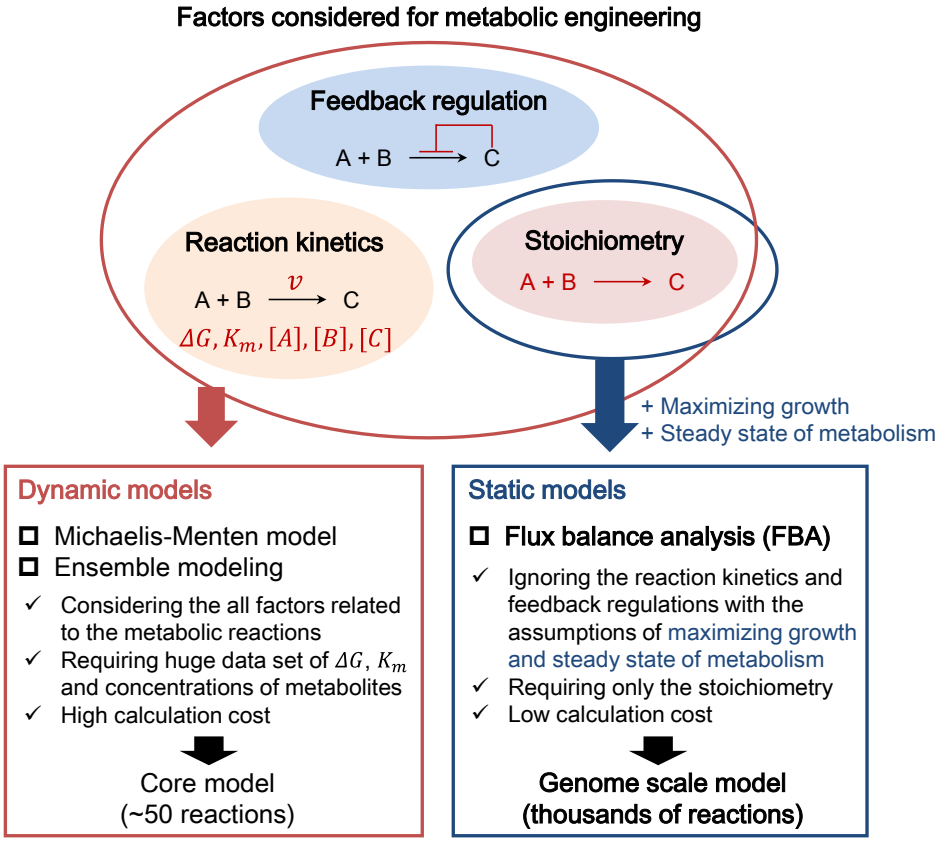

Figure 1-4-1 Factors involved in the metabolic reactions and characters of metabolic simulation approaches.

There is two mainstream of approaches, one is the dynamic models considering all factors for metabolic reactions. The other is static models represented by FBA using stoichiometry only. Due to the low calculation costs and data availabilities, FBA is often used for metabolic engineering to calculate the genome-scale metabolic flux distributions.

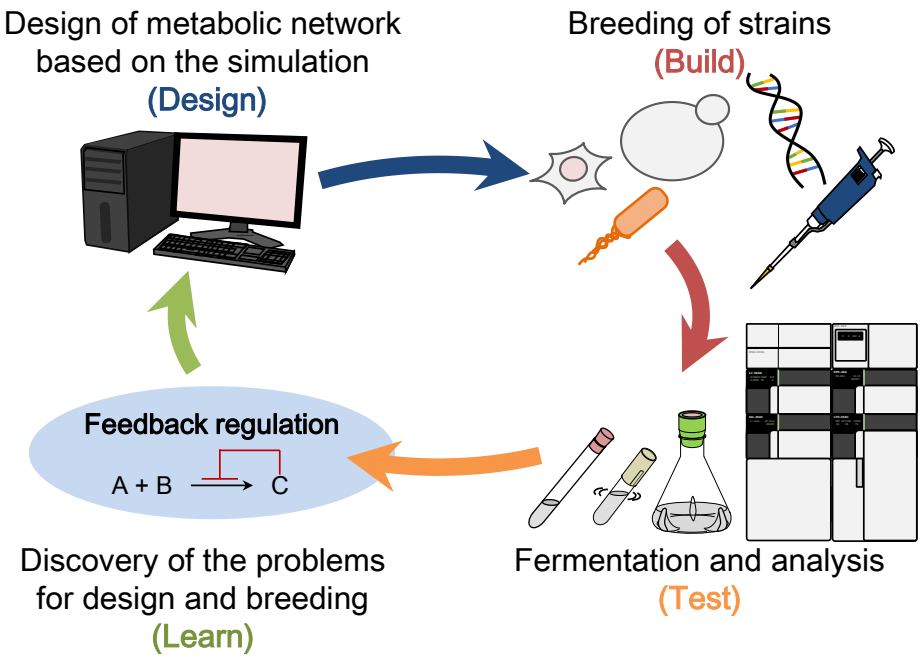

Figure 1-4-2 Design-build-test-learn cycle conducted in metabolic engineering for improvement of the target productivity.

Design, build, test and learn corresponding to the design of metabolic network based on the simulation, the breeding of strains, the fermentation test and the analysis, and discovery of the problems for further improvement of design or breeding.

1-5 Metabolic engineering of yeast based on flux balance analysis

Yeast *Saccharomyces cerevisiae* is one of the useful host microorganism for bioproduction. Table 1-5-1 shows the advantages and disadvantages of yeast as the bio-production host comparing to the representative bacterial organism of *E. coli*. *S. cerevisiae* is the first eukaryote whose genome was fully sequenced in the genome project in the 1990s, besides a lot of genetic and physiological knowledge is accumulated as model organisms [4]. In yeast, a lot of genetic engineering tools are also established for metabolic engineering. Compared to bacterial hosts such as *E. coli*, yeast has been used for brewing to produce drink alcohol for a long time because of its high alcohol

fermentation ability and high growth ability, tolerance to fermentation stress such as pH stress and osmotic pressure. *S. cerevisiae* has been used for bio-ethanol production in industrial scale because of its safety viewpoint guaranteed in the record of the long history for using food production. Furthermore, *S. cerevisiae* is a physically robust microorganism to endure the shear stress of microbial fermenter and repeated fermentation process. It is applied to both of the growth-coupled fermentation process and the non-growth fermentation process. The non-growth fermentation process can reduce the fermentation cost because the bacterial cells once increased, it can be used repeatedly by inoculating the grown cells to fresh medium. Unlike the bacterial hosts, yeast has no risk to fatal phage virus contamination which requiring complete washing and sterilization of the culture tank. On the other hand, the complexity of yeast cell structure is higher than the bacterial cells due to the eukaryotic cell nature such as mitochondria, cytosol, nucleus, and vacuoles. The complexity of yeast cell might cause unexpected metabolic bottle-neck in the form of the rate limiting of metabolite transport and localization of enzymes, metabolite, and cofactors. These factors make the yeast metabolic engineering difficult, however, from the benefits described above, expansion of further applications of *S. cerevisiae* for the bio-production host is desired.

Molecular breeding of *S. cerevisiae* strain for bioproduction of chemical materials such as bio-ethanol, other alcohols, proteins, antibodies and secondly metabolites has been studied for a long time. Recently, Metabolic engineering of *S. cerevisiae* based on FBA has been studied as well as other bacterial hosts such as *E. coli*, many metabolic models have been constructed and updated [39, 40, 41, 42, 43, 44]. These metabolic models were published after the validation of the growth rates and metabolic flux distributions in several culture conditions. Some examples have been

reported that engineering of yeast based on FBA successfully improved several target metabolites production [45, 46, 47, 48]. However, there are also several targets with very low yield compared to the FBA metabolic simulation results. For example, one of the C4 alcohol, isobutyl alcohol (isobutanol) was achieved 86% (mol mol-glucose^{-1}) of production yield in *E. coli*, by the introduction of metabolic genes necessary for biosynthesis, knockout of the competitive pathway genes, and improving the cofactor redox imbalance [49]. In yeast, the yield of isobutanol was predicted more than 50% from the results of FBA metabolic simulation. [50].Although similar approaches with *E. coli* were conducted in *S. cerevisiae* to construct the isobutanol production strain, the yield was up to only 4% [51].

This situation might be the result of the overestimation of target yield due to the low prediction capacity of the current yeast FBA model, or the low productivity due to the imperfection of the strain breeding. Either way, the current situation of the difference between the simulation results and the experimental results of bred yeast strains is unfavorable because it lowers the reliability of metabolic engineering based on FBA in yeast. Therefore, it is necessary to investigate the cause for this problem and solve for the further improvement of a computer-aided metabolic engineering approach to achieve the goal of target production avoiding the useless approaches and reducing the experimental costs.

Table 1-5-1 Features of *E. coli* and *S. cerevisiae* as the production hosts

Features	*E. coli*	*S. cerevisiae*
Knowledge	◎	◎
Growth ability	◎	◎
pH tolerance	~5	~3
Physical robustness of cell	○	◎
Repeated fermentation	◎	◎
Risk of phage contamination	High	No risk
The complexity of cell structure	Low	High
Ease of engineering	◎	○

1-6 General objective and the outline of this thesis

The general objective of this thesis was an improvement of the FBA based computer-aided yeast breeding approach to filling in a gap between the simulation results and the experimental results. To investigate the current model prediction capacities or the strain breeding approaches are insufficient or not, strains were constructed based on FBA simulation result. In strain breeding, additional engineering was also conducted for enhancing the expression of enzymes, releasing the feedback regulations and optimizing the metabolism by adaptive laboratory evolution to complement the factors lacked in FBA design according to the design-build-test-learn cycles of metabolic engineering. Then, a yeast FBA metabolic model was reconstructed including the constraint of a factor which was considered from the comparison, to propose the method for searching the suitable target metabolite for the bio-production in *S. cerevisiae*. Using the reconstructed model, selection of the target metabolites that suitable for the yeast bio-production was tried and verified by the strain breeding.

The thesis consists of 4 chapters, and a schematic outline of the thesis is shown in Figure 1-6-1.

Chapter 1 describes the general introduction of this thesis. The background about the microbial process and metabolic engineering of yeast based on FBA are summarized in this chapter. The objectives and schema of this thesis are also described.

Chapter 2 describes the investigation of the availability and limitation of metabolic engineering based on FBA to estimate the unknown factor responsible for the low yield

of isobutanol production in *S. cerevisiae*. In this chapter, isobutanol production was focused on as an example because of its low production yield record. According to the FBA simulation results, the introduction of several metabolic pathways increasing the NADPH supply (phosphoenolpyruvate carboxylase (PPC) and Entner–Doudoroff (ED) pathway) were suggested to improve the isobutanol production yield. The knockout of ethanol biosynthesis pathway which is a competitive pathway for isobutanol production was also suggested for improving isobutanol yield. Then, metabolically engineered isobutanol production strains were constructed for the fermentation test to verify the production yield. As a result, the introduction of PPC improved the yield of isobutanol to 1.1%, on the other hand, no improvement was observed with the introduction of the ED pathway. Knockout of multiple pyruvate decarboxylase genes responsible for ethanol production significantly decreased cell growth. Therefore ALE experiment was conducted to improve the growth. Evolved strain SD145-2 with *ILV6* deletion responsible for feedback regulation of isobutanol production pathway achieved 2.9% of isobutanol yield. This was the comparable result of isobutanol production in yeast in test tube scale culture. However, the value was much lower than the FBA result (54%) suggesting that the activity of the isobutanol biosynthesis pathway itself was terribly low. Both of the ED pathway and isobutanol biosynthetic pathway were involving reactions that required an iron-sulfur cluster (ISC) for the catalytic reaction. In the thesis, these ISC dependent reactions were considered as the bottle-neck of yeast metabolism that not included in the current FBA metabolic models.

Chapter 3 describes the reconstruction of the yeast FBA metabolic model iMM904 considering the new constraint of ISC dependent reactions. In the reconstructed model

iMM904-ISC, the sum flux value of ISC dependent reactions of wild-type strain in decided fermentation conditions was calculated to fix the upper limit of ISC synthesis. Then the flux distributions for bio-production was computed with gene deletions and addition of heterologous pathways. Firstly the metabolic simulation for isobutanol production was re-calculated with the reconstructed model, it was found that the simulation yield was largely decreased compared to the results shown in chapter 2 (11.7% from 54%). It was suggested that the isobutanol might be unsuitable target metabolite to be produced in *S. cerevisiae*. Secondly, favorable target metabolite which can be produced in yeast was investigated using the reconstructed model. Then, several targets including 2,3-butanediol were found for mass production in *S. cerevisiae*. For the validation of the simulation results, 2,3-butanediol production strains were constructed for the fermentation test. The production yields of constructed strain in the growth-coupled phase (58.0%) was almost reached to the FBA results (58.9%). For further improvement of the production strain, the construction of a regulation system for yeast ethanol production was attempted, however, it was found that more improvement was necessary to decrease the ethanol by-production.

Chapter 4 describes the general conclusion and future perspective of this research.

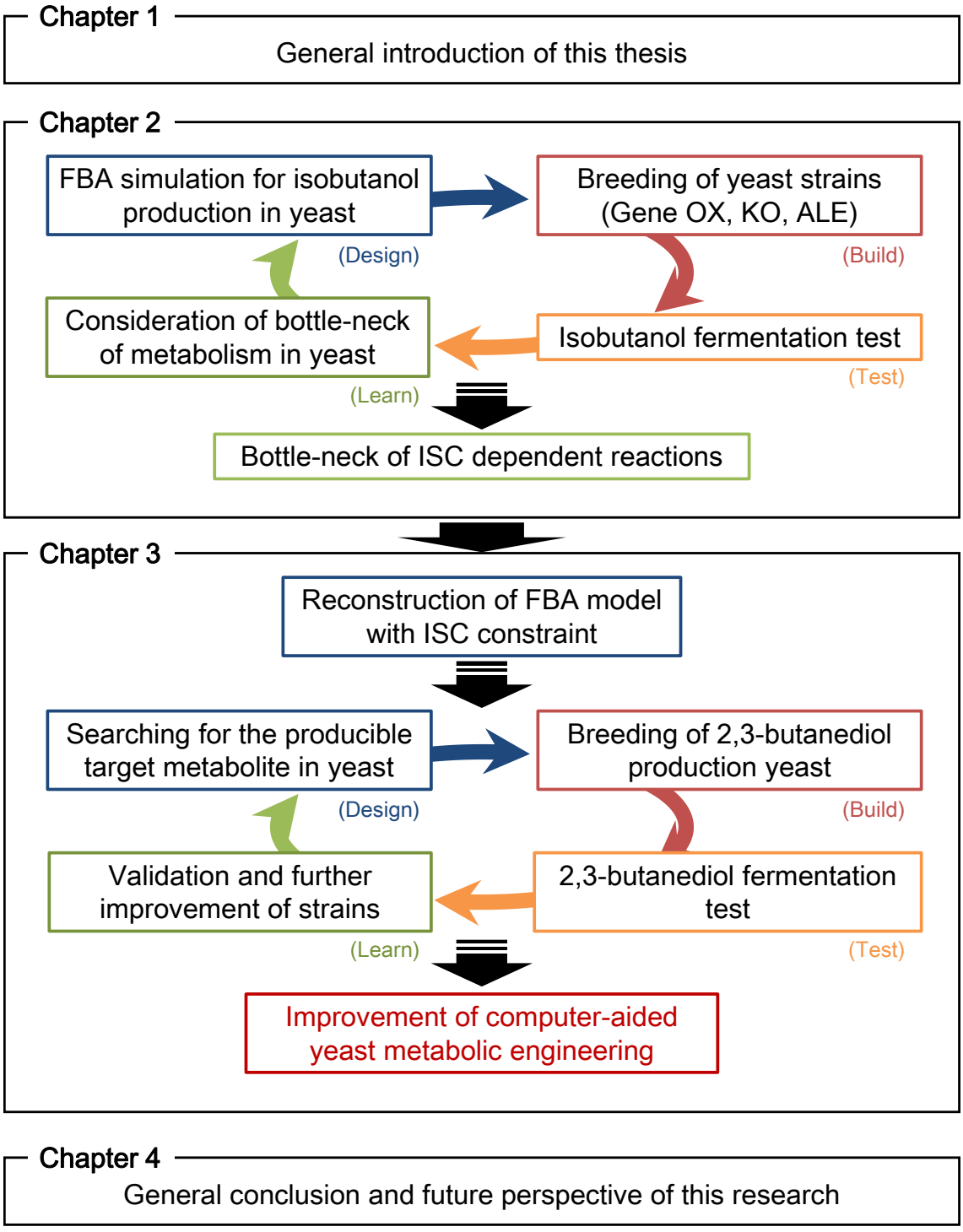

Figure 1-6-1 The outline of this thesis.

Abbreviations are defined as follows. FBA: flux balance analysis, OX: overexpression, KO knockout, ALE: adaptive laboratory evolution.

Chapter 2: Availability and limitation of metabolic engineering based on flux balance analysis in yeast for isobutanol production

2-1 Highlights

- Focusing on the isobutanol production in *S. cerevisiae*, strains were constructed based on the metabolic designs based on the flux balance analysis (FBA)
- The overexpression of the *syn*6803 phosphoenolpyruvate carboxylase gene improved the yield 1.4 times higher than that of control strain (1.13 % mol mol-glucose^{-1}).
- Introduction of the Entner-Doudoroff pathway was no effect for isobutanol production.
- Growth improved ethanol non-producible strain was achieved through the adaptive laboratory evolution (SD145-2 strain, growth rate: 0.59 h^{-1}).
- Isobutanol production of SD145-2 strain was improved by releasing of feedback regulation of valine biosynthesis, achieving the comparable yield of the world record in test tube culture (knockout of *ILV6*, 2.9%).
- The experimental results were far from the simulated yield (54%)
- The iron-sulfur cluster (ISC) dependent reactions were estimated as the factor to decrease isobutanol production yield in *S. cerevisiae*.

2-2 Introduction

2-2-1 Isobutanol production by microbial hosts

Isobutyl alcohol (isobutanol) is one of the chemicals that many researchers tried to increase the productivity in *S. cerevisiae*. Isobutanol is branched chain alcohol consisted of four carbon atoms and expected as a biofuel due to high energy density and low hygroscopicity [52]. Microorganisms do not have the ability of the mass production of isobutanol in nature. Therefore, Atsumi *et al*. focused on the 2 step reactions of 2-keto acid decarboxylase (KDC) and alcohol dehydrogenase (ADH). These reactions were known as the Ehrlich pathway which could convert the isobutanol from the 2-ketoisovalerate (an intermediate metabolite of valine biosynthesis pathway). They cloned the *kivd* derived from *Lactococcus lactis* encoding KDC and *ADH2* derived from *S. cerevisiae encoding* ADH respectively, then introduced to *E.coli* for the construction of artificial isobutanol production strain for the first time in the world. In this report, a strain which overexpressed *ilvIHCD* and knocked-out of genes involved in the competitive pathway (*adhE*, *ldhA*, *frdAB*, *fnr*, *pta*) achieved 51% isobutanol production yield in a 24-hour fermentation. In addition, overexpression of *alsS* derived from *Bacillus subtilis* and knockout of the competitive pathway gene *pflB* resulted in 86% isobutanol production yield [49]. After that report, artificial Ehrlich pathway has been introduced to various bacterial hosts to achieve several isobutanol production strains [53, 54, 55, 56, 57, 58, 59, 60, 61, 62]. In particular, Bastian *et al.* focused on the redox balance of cofactors (NADPH) that supplies the reducing power for isobutanol biosynthesis. The major cofactors supplied from the glucose metabolism of the glycolysis is NADH, however, isobutanol production requires NADPH. Therefore, they improved the cofactor redox

imbalance by overexpression of the transhydrogenase which converts NADH to NADPH. They also engineered the cofactor requirement of isobutanol biosynthesis pathway to the NADH from the NADPH, then great isobutanol yield was achieved in *E. coli* which close to the theoretical maximum yield of isobutanol.

2-2-2 Isobutanol production by *Saccharomyces cerevisiae*

Isobutanol production strain of *S. cerevisiae* has also been achieved by the expression of the artificial Ehrlich pathway in the cytosol as well as bacterial hosts (Kondo *et al*., 0.52% mol mol-glucose^{-1}, Table 2-2-1, figure 2-2-1) [63]. Chen *et al.* achieved 6 times higher isobutanol yield compared to the wild-type strain by the overexpression of *ILV2*, *ILV5*, and *ILV3* to enhance the valine biosynthetic pathway in the mitochondria (0.94% mol mol-glucose^{-1}) [64]. Cytosol of *S. cerevisiae* cell is compartmented by cell organelles such as mitochondrion and lysosome. The valine biosynthetic pathway exists in the mitochondrion. Therefore, Avalos *et al.* constructed the Ehrlich pathway in mitochondrion to integrate the whole isobutanol production pathway, then 1.54% mol mol-glucose^{-1} of isobutanol yield was achieved [65]. There are also many reports for the isobutanol production in *S. cerevisiae* [50, 66, 67, 68, 69] Recently, Matsuda *et al.* constructed the whole isobutanol biosynthetic pathway in the cytosol and improved the cofactor redox imbalance by the overexpression of the transhydrogenase-like shunt pathway. Furthermore, with the *LPD1* knockout encoding the competitive pathway of isobutanol synthesis pathway, isobutanol yield was reached at 2.9% and 3.94% mol mol-glucose^{-1} in test tube scale fermentation and high-density culture respectively [51].

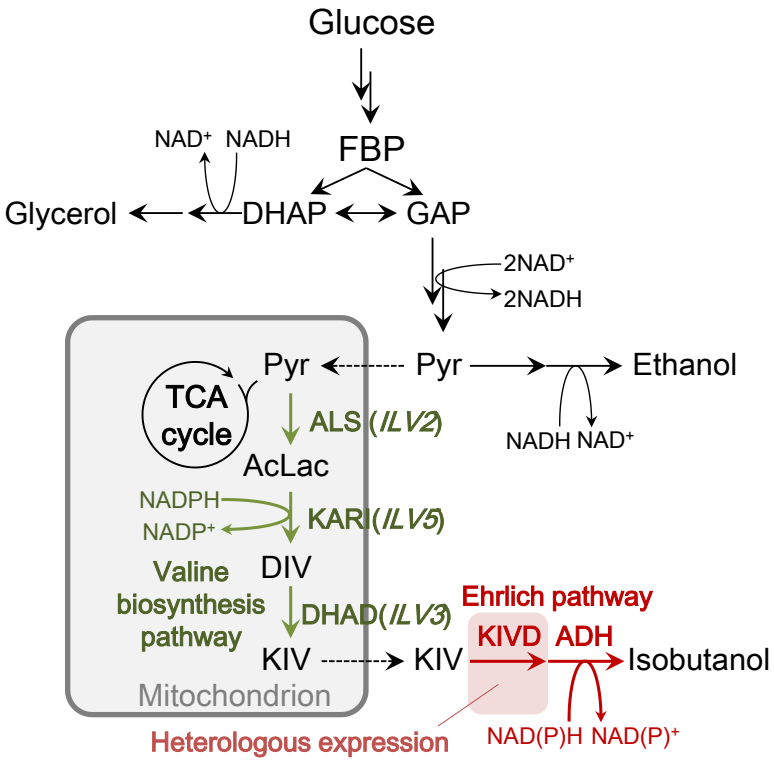

Figure 2-2-1 Biosynthesis pathway of the isobutanol in *S. cerevisiae*.

Metabolites and pathway map of *S. cerevisiae* with isobutanol production pathway. One mol of isobutanol was produced from the one mol of glucose *via* the valine biosynthesis pathway (shown in green) and Ehrlich pathway (shown in red). Abbreviations are defined as follows. FBP: fructose bis-phosphate, GAP: glyceraldehyde 3-phosphate, DHAP: dihydroxyacetone phosphate, Pyr: pyruvate, AcLac: acetolactate, DIV:2,3-dihydroxy isovalerate, KIV: α-ketoisovalerate, ALS: acetolactate synthase, KARI: ketol-acid reductoisomerase, DHAD: dihydroxy acid dehydratase, KIVD: 2-ketoisovalerate decarboxylase, ADH: alcohol dehydrogenase.

Table 2-2-1 Reports of the Isobutanol production in *S. cerevisiae*

Strain	Overexpressed genes	Gene knockout	Carbon source (g/L)	Medium	Fermentation conditions	Titer (mg/L)	Yield (% mol/mol C-source)	Ref.
YPH499	*ILV2, ^{Ll}kivD,ADH6*	*pdc1*	Glucose (20)	Defined	Microaerobic	43	0.52	[63]
CEN.PK2-1C	*ILV2, ILV3,ILV5*	None	Glucose (40)	Defined	Aerobic	n.i.	0.94	[64]
BY4741 x Y3929 (diploid)	*LV2, ILV3,ILV5, ARO10-TS, ^{Ll}adhARE1-TS*	None	Glucose (100)	Complex	Semi-aerobic	635	1.54	[65]
D452-2	*ILV2Δ55,ILV3Δ20,ILV5Δ34, ^{Ll}kivD*	None	Glucose (40)	Complex	Microaerobic	151	0.92	[66]
YPH499	*ILV2, ILV2Δ54,ILV3Δ41,ILV5Δ47, LlkivD,ADH6*	None	Glucose (20)	Defined	Microaerobic	63	0.77	[67]
CEN.PK2-1C	*^{syn}ILV2Δ54,^{syn}ILV3Δ19,^{syn}ILV 5Δ48*	*ilv2*	Glucose (40)	Defined	Aerobic	630	3.83	[68]
CEN.PK2-1C	*^{syn}ILV2Δ54,^{syn}ILV3Δ19,^{syn}ILV 5Δ48,ARO10, ADH2,TAL1, XKS1,^{synCp}xylA*	*ilv2*	Xylose (20)	Defined	Aerobic	1.36	0.02	[69]
YPH499	*LV2, ILV2Δ54, ILV3Δ41, ILV5Δ47, ^{Ll}kivD, ADH6, MAE1*	*lpd1*	Glucose (20) Glucose (100)	Defined	Microaerobic	230 1620	2.91(Test tube) 3.94(High density)	[51]

syn: synthesized gene

2-2-3 Objective in this chapter

Metabolic engineering based on the flux balance analysis (FBA) has been reported with successful results in bacterial hosts by increasing the cofactor supply and knockout of the competing pathway for bioproduction. However, there are few reports that the productivity of products has greatly improved in *S. cerevisiae* compared to bacteria host researches by introducing similar approaches described above. In this chapter, microbial isobutanol production was focused on. In bacterial hosts such as *E. coli*, metabolic theoretical maximum yield was achieved by the overexpression of biosynthetic pathway genes, deletion of the competing pathway genes and improving the redox imbalance of cofactors. With the similar approaches, isobutanol yield in yeast was also predicted more than 50% by metabolic simulation based on FBA. However, in *S. cerevisiae*, the yield of isobutanol production is still at an elementary level. These result suggested that the possibility of overestimation of the current yeast model due to the low prediction capacity, or incompletion of strain breeding due to the unpredicted reason in *S. cerevisiae* making the isobutanol production difficult, unlike bacterial metabolic engineering.

In this chapter, focusing on the isobutanol production in *S. cerevisiae*, strains were constructed based on the metabolic designs based on the flux balance analysis (FBA) metabolic simulations. FBA suggested that the addition of a metabolic pathway for improvement of redox imbalance of NADPH and deletion of the ethanol biosynthetic pathway related gene competing to isobutanol production were effective for the increase of the isobutanol yield. Triple gene knockout of pyruvate decarboxylase responsible for the ethanol production disturbed the metabolic state of yeast and resulted in the significant

decrease of growth ability. For that reason, adaptive laboratory evolution (ALE) was conducted to improve the growth of non-ethanol producing yeast strains. In FBA simulation, feedback regulation of the isobutanol biosynthesis pathway is ignored for the convenience of calculation. Therefore, *ILV6* gene responsible for feedback regulation of isobutanol production pathway was knocked out to complement the weakness of FBA. Assuming that the strain breeding with complementing the ignored factors in FBA can be a breakthrough of the low productivity, isobutanol yield of constructed strains and the simulation results were compared to verify the availability and limitation of metabolic engineering based on FBA. When the yield does not improve based on the assumption, estimation of the unknown factor responsible for the low yield of isobutanol production in *S. cerevisiae* is discussed.

2-3 Methods

2-3-1 Principle of flux balance analysis

In the following, the calculation of flux distribution by flux balance analysis (FBA) was explained using the example of the simple metabolic network shown in Figure 2-3-1.

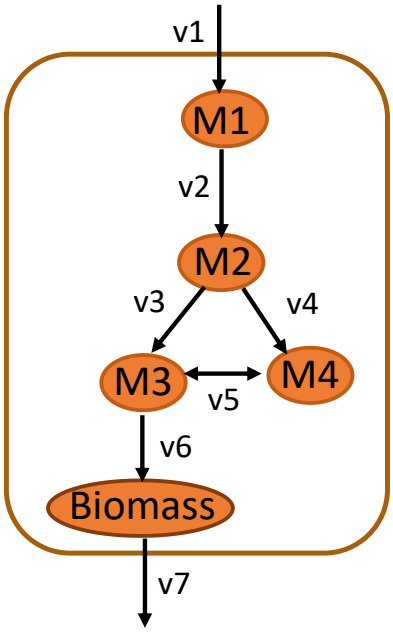

Figure 2-3-1 Example of metabolic network

M*i* and v*j* represent metabolites and metabolic flux respectively (*I*, *j*: integer number).

Stationary state of metabolism

In the case of the simple metabolic network shown in Figure 2-3-1, the temporal change of the concentration of each metabolite M_i can be written by flux v_j as follows. The unit of v_j is mmol gDCW^{-1} h^{-1}

$$\frac{\mathrm{d}[M1]}{\mathrm{dt}} = v_1 - v_2 \quad \text{(Equation 1.1a)}$$

$$\frac{\mathrm{d}[M2]}{\mathrm{dt}} = v_2 - v_3 - v_4 \quad \text{(Equation 1.1b)}$$

$$\frac{\mathrm{d}[M3]}{\mathrm{dt}} = v_3 + v_5 - v_6 \quad \text{(Equation 1.1c)}$$

$$\frac{\mathrm{d}[M4]}{\mathrm{dt}} = v_4 - v_5 \quad \text{(Equation 1.1d)}$$

$$\frac{\mathrm{d}[Biomass]}{\mathrm{dt}} = v_6 - v_7 \quad \text{(Equation 1.1e)}$$

In FBA, steady state of intracellular metabolism is considered. This means that the concentration of each metabolite does not dynamically change. Assuming a steady state of the metabolic reactions, the above equations are shown as follows.

$$\frac{\mathrm{d}[M1]}{\mathrm{dt}} = v_1 - v_2 = 0 \quad \text{(Equation 1.2a)}$$

$$\frac{\mathrm{d}[M2]}{\mathrm{dt}} = v_2 - v_3 - v_4 = 0 \quad \text{(Equation 1.2b)}$$

$$\frac{\mathrm{d}[M3]}{\mathrm{dt}} = v_3 + v_5 - v_6 = 0 \quad \text{(Equation 1.2c)}$$

$$\frac{\mathrm{d}[M4]}{\mathrm{dt}} = v_4 - v_5 = 0 \quad \text{(Equation 1.2d)}$$

$$\frac{\mathrm{d}[Biomass]}{\mathrm{dt}} = v_6 - v_7 = 0 \quad \text{(Equation 1.2e)}$$

Then, these constraint equations can be represented by determinants as follows.

$$\begin{pmatrix} 1 & -1 & 0 & 0 & 0 & 0 & 0 \\ 0 & 1 & -1 & -1 & 0 & 0 & 0 \\ 0 & 0 & 1 & 0 & 1 & -1 & 0 \\ 0 & 0 & 0 & 1 & -1 & 0 & 0 \\ 0 & 0 & 0 & 0 & 0 & 1 & -1 \end{pmatrix} \begin{pmatrix} v_1 \\ v_2 \\ v_3 \\ v_4 \\ v_5 \\ v_6 \\ v_7 \end{pmatrix} = \begin{pmatrix} 0 \\ 0 \\ 0 \\ 0 \\ 0 \\ 0 \\ 0 \end{pmatrix} \quad \text{(Equation 1.3)}$$

Assuming that the matrix on the left (stoichiometric matrix) and the vector of metabolic flux are S and v respectively, the above equation can be rearranged to as follows.

$$S \cdot v = 0 \quad \text{(Equation 1.4)}$$

The above equation is a constraint equation expressing the steady state of intracellular metabolism in FBA.

Restrictions on the upper and lower limits of each metabolic flux

Limiting the upper bound and the lower bound for each metabolic flux, the various condition of metabolic conditions can be expressed, for example, the reversibility of reactions, the consumption rate of nutrient sources and the gene deletions.

In Figure 2-3-1, the metabolite M_1 flows in from outside the cell. If the uptake rate of this metabolite M_1 is 20 mmol gDCW^{-1} h^{-1} at the maximum, the following constraint equations can be built for v_1.

$$0 \leq v_1 \leq 20 \quad \text{(Equation 1.5a)}$$

Considering the reactions that convert metabolite M_1 to M_2 and M_4 to M_3, they are

an irreversible reaction and a reversible reaction, the following constraint equations about v_2 and v_5 are described .

$$0 \leq v_2 \leq \infty \qquad \text{(Equation 1.5b)}$$

$$-\infty \leq v_5 \leq \infty \qquad \text{(Equation 1.5c)}$$

Regarding the upper bound value and the lower bound value of the metabolic flux v_j as ${v_j}^{max}$ and ${v_j}^{min}$, the constraint equations can be described as follows.

$${v_j}^{\min} \leq v_j \leq {v_j}^{max} \qquad (\forall i = R) \qquad \text{(Equation 1.6)}$$

From the above constraint equation, it is possible to represent the upper and lower bound values of each metabolic flux in FBA.

Maximizing the cell growth

Using the steady state of intracellular metabolism and the constraint of the upper and the lower bound of each metabolic flux, the metabolic flux distributions can be calculated to some extent. However, in many cases, there are a lot of solutions of the flux distributions satisfying these constraints. Therefore, FBA metabolic simulation requires one more condition, maximizing cell growth. This condition is based on the concept that cells optimize their metabolism to maximize their own duplication for surviving. In figure 2-3-1, the flux representing the biomass formation is v_7. In general, the biomass formation is often expressed as v_{growth}. Maximizing the cell growth is described as follows

maximize v_{growth} (Equation 1.7)

Summary of FBA

As described above, in FBA, the metabolic flux distribution can be calculated as a linear optimization problem based on the three conditions of the steady state of intracellular metabolism, the upper and the lower limits of each metabolic flux and the maximization of cell growth. The linear programming problem expressing FBA can be described as follows.

Maximize (max) (v)	v_{growth}	
Subject to (s.t.)	$S \cdot v = 0$	$(\forall i = M)$
	${v_j}^{\min} \leq v_j \leq {v_j}^{max}$	$(\forall i = R)$

Each letter corresponds to the following.

v_j : Metabolic flux of reaction *j*

${v_j}^{max}$: Upper limit of the metabolic flux of reaction *j*

${v_j}^{min}$: Lower limit of the metabolic flux of reaction *j*

v_{growth} : Biomass biosynthesis rate

$S_{i,j}$: Coefficient for metabolite *i* in reaction *j*

M : Set of metabolites

R : Set of reactions

Solving this linear programming problem, all the metabolic flux distributions v can be calculated. Geometrically, the solution space of each metabolic flux is determined by the two constraints such as the steady state of intracellular metabolism and the limitation of the upper and lower limits of each metabolic flux. Then, with the third constraint of maximizing the cell growth rate, the optimal solution of FBA appears on the boundary in the solution space (Figure 2-3-2).

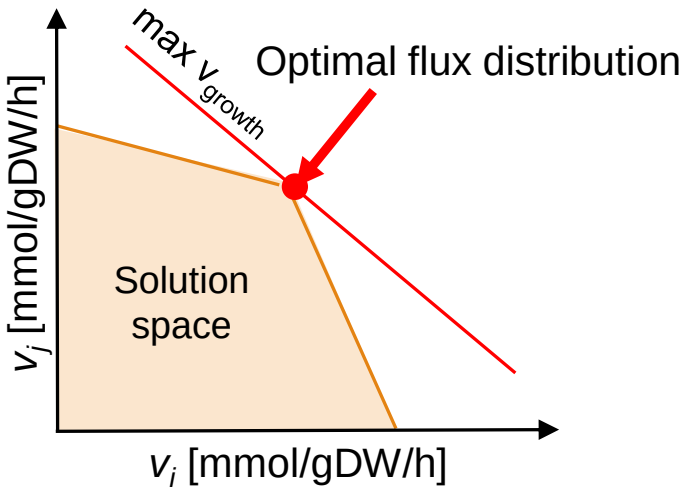

Figure 2-3-2 The optimal solution of FBA in the solution space.
v*i* and v*j* represent metabolic flux (*i*, *j*: integer number).

2-3-2 Calculation method for flux balance analysis

Metabolic model

For flux balance analysis (FBA) metabolic simulations of *S. cerevisiae*, the yeast genome-scale model iMM904 was used. The model iMM904 is composed of 904 genes, 1577 reactions and 1226 metabolites [44]. The added reactions to the model iMM904 were shown in appendix table A3 page 130 for the simulation of isobutanol production.

Conditions for calculation

For all calculations, the COBRA toolbox on MATLAB 2013a (MathWorks Inc., Natic, MA, USA) was used [31]. In addition, GLPK (GNU Linear Programming Kit) was used for a linear programming solver. For the calculations of flux distributions, the glucose uptake rate and oxygen uptake rate were set to 10 mmol $gDW^{-1}\,h^{-1}$ and 0.5 mmol $gDW^{-1}\,h^{-1}$, respectively (the default value of the model iMM904).

2-3-2 Strains and plasmids and yeast transformation

The yeast strains and plasmids used in this study are listed in appendix table A1 and table A2 page 125 and page 128 respectively. The lithium-acetate method was used for all yeast transformations. All strains were cultured in yeast extract peptone dextrose (YPD) medium (1% bacto yeast extract, 2% bacto peptone, 2% glucose) and synthetic dextrose (SD) medium (6.7% yeast nitrogen base without amino acids and 2% or 0.5% glucose, as necessary, 0.06% leucine, 0.03% lysine hydrochloride, 0.02% histidine, 0.02% uracil, 0.04% tryptophan and 0.04% adenine hydrochloride) for transformations.

2-3-3 Fermentation test

For the isobutanol fermentation test, transformants were cultured for 72 hours at 30°C with shaking at 150 rpm in 5 mL of SD medium containing 20 g/L glucose and required amino acids in test tubes. The initial OD_{600} value for the main culture was set at 1.0, with OD_{600} levels determined using a spectrophotometer (UVmini-1240, Shimadzu, Kyoto, Japan).

2-3-4 Analytical methods for culture broth

To determine the concentrations of glucose, ethanol, isobutanol, acetate, glycerol, and pyruvate in the culture broth, supernatant of culture was applied to a gas chromatograph (GC) (Agilent 7890A GC; Agilent Technologies, Santa Clara, USA) and high-performance liquid chromatography (HPLC) system (Shimadzu, Japan).

Gas chromatography analysis

The alcohol concentration of the culture broth was determined by the gas chromatography (GC). The GC was operated with the following conditions: column, Stabilwax 60 m × 0.32 mm ID × 1 μm (Restek, Bellefonte, USA); carrier gas, helium; flow rate, 6.5 mL min^{-1}; injection volume, 1 μL; split ratio, 1:10; oven temperature, raised at 10°C/min from 50℃ for 5 min, 30°C/min from for 5 min and kept at 250°C for 4 min; flame ionization detector (FID) temperature, 250°C.

High- performance liquid chromatography analysis

Glucose, glycerol, and acetate concentration of the culture broth were determined by the high-performance liquid chromatography (HPLC) system. The HPLC system was equipped with an Aminex HPX-87H column (7.8 mm, 300 mm, Bio-Rad, USA), UV/vis detector (SPD-20A, Shimadzu, Kyoto, Japan), and refractive index detector (RID-10A, Shimadzu, Kyoto, Japan). The column temperature was set at 65°C, and 1.5 mM H2SO4 was used as the mobile phase with a flow rate of 0.5 mL min^{-1}. The flow cell temperature of the refractive index detector was set at 40°C.

2-3-5 ^{13}C metabolic flux ratio analysis

In carbon labeling experiments, SD medium (6.7 g/L yeast nitrogen base without amino acids and 0.5% [1-^{13}C] glucose) containing the required amino acids was used. Yeast cells from the plate medium were cultured in 5 mL of SD medium at 30°C with shaking at 150 rpm. The cells were inoculated into 50 mL of SD medium in 500-mL Sakaguchi flasks. In the main culture, cells were incubated at 30°C with shaking at 120 rpm. The initial OD_{600} values were set at 0.1.

[1-^{13}C] glucose (99%) was purchased from Cambridge Isotope Laboratories (Andover, MA, USA). To analyze alanine derived from cellular proteins, 2 mL of broth was taken from the culture flask at OD_{660} = 1.0, and cells were collected by centrifugation at 15,000 rpm at 4°C for 5 min. The cell pellet was washed twice with 0.9% NaCl and was hydrolyzed in 2 mL 6 *N* HCl at 105°C for 18 h. After filtration (Cosmonice Filter W; pore size, 0.45 μm; filter diameter, 13 mm; Nacalai Tesque, Kyoto, Japan), 10 μL of the internal standard (600 μM cycloleucine) was added to the hydrolysate and evaporated to dryness. The dried residue was dissolved in 50 μL acetonitrile and 50 μL *N*-(tert-butyldimethylsilyl)-*N*-methyl-trifluoroacetamide containing 1% of tert-butyldimethyl-chlorosilane and incubated at 105°C for 1 h. After cooling overnight, the supernatant was applied for gas chromatography-mass spectrometry (GC-MS) analysis.

The mass isotopic distributions of ion clusters at mass to charge (m/z) ratios of [M-57] and [M-85] derived from alanine were determined using GC-MS (Agilent 7890A GC and 5975C Mass Selective Detector; Agilent Technologies, Santa Clara, USA); column, DB-5MS+DG; 30 m × 0.25 mm ID × 0.25 μm; (Agilent Technologies, Santa Clara, USA); carrier gas, helium; flow rate, 1.0 mL/min; detection mode, selected ion

monitoring; ion source temperature, 230°C; electron impact ionization, 70 eV; injection volume, 1 μL; split ratio, 1:10; oven temperature, 150°C for 2 min, increased by 3°C/min to 270°C, then increased at a rate of 10°C/min to 300°C, and maintained at that temperature for 5 min.

The metabolic flux ratio of upper glycolysis, including the Embden-Meyerhof (EM), pentose phosphate (PP), and Entner-Doudoroff (ED) pathways were determined by the mass isotopic distributions of the alanine derived from the pyruvate. [1-^{13}C] glucose metabolized through the EM or ED pathway resulted in equal amounts of non-labeled and C1-labeled pyruvate or non-labeled and C3-labeled pyruvate, respectively, although the ^{13}C label was removed as a form of CO_2 in the PP pathway, resulting in only 5/3 molecules of non-labeled pyruvate. The flux ratio of each pathway was determined by the mass isotopic distributions of the *m/z* ratios of alanine [M-57] and [M-85] which is directly converted from pyruvate. In other words, the relationship between the flux ratios of pathways is represented in the following equations (Equation 2.1 to Equation 2.3):

$$a : b = x + \frac{5}{3}y + 2z : x \qquad \text{(Equation 2.1)}$$

$$c : d = x + \frac{5}{3}y + z : x + z \qquad \text{(Equation 2.2)}$$

$$1 = x + y + z \qquad \text{(Equation 2.3)}$$

a, b, c, and d represented the normalized mass isotopic distributions of fragments M_0 and M_1 of alanine [M-85] and alanine [M-57], respectively. x, y, and z also represented the flux ratios in the EM, PP, and ED pathways. Flux ratios (x, y, and z) is

represented by the following equations (Equation 2.4 to Equation 2.6):

$$x = \frac{5b(c+d)}{(a+b)(3c+2d)} \quad \text{(Equation 2.4)}$$

$$y = \frac{3(c-d)}{3c+2d} \quad \text{(Equation 2.5)}$$

$$z = 1 - x + y \quad \text{(Equation 2.6)}$$

2-3-6 Protein analysis by sodium dodecyl sulfate polyacrylamide gel electrophoresis (SDS-PAGE)

Cells were harvested at 20 or 24 hours after the start of fermentation (OD_{660} = 2.0), and yeast cell pellets were obtained. Pellets were washed with 50 mM Tris-HCl (pH 7.5) on ice. After centrifugation, pellets were suspended in 30 µL of sample buffer (2% SDS, 80 mM Tris-HCl (pH 6.8), 1.5% dithiothreitol) and immediately heated at 100°C for 3 min and held at -30°C until extraction. Proteins were extracted by adding 0.1 g of 2 mm glass beads and vortexing for 3 min. Seventy microliters of sample buffer was added, and the mixture was vortexed for 1 min and heated at 100°C for 1 min. The protein concentration of the supernatant was determined based on the method of Bradford using the Bio-Rad Protein Assay Dye Reagent. Five or Fifteen microgram of protein in loading buffer (2% SDS, 60 mM Tris-HCl (pH 6.8), 10% glycerol, 2.5% 2-mercaptoethanol, 0.1 mg/mL bromophenol blue) was loaded onto a 7.5% or 12.5% SDS-PAGE gel, and proteins were separated. A WIDE-VIEW™ Prestained Protein Size Marker III (Wako Pure Chemical Industries) or low-range marker (SP-0110, APRO SCIENCE) were used to identify PPC from *Synechocystis* sp. PCC6803 (118.9 kDa), 6PGD (64.6 kDa) and KDPGA (22.3 kDa) from *E. coli*.

2-3-7 Laboratory adaptive evolution of yeast strains

The subculture of YSM021 strain in 20g/L glucose SD medium was carried out for a laboratory adaptive evolution. The cells were continuously cultured in a test tube with 5 mL of SD medium under the semi-aerobic conditions in the five independent culture series. Each of independent culture series was repeatedly transferred to the new medium when the cell growth was saturated. The experiment was continued for around 125 days (3000 hours) until further growth improvement was not observed. The glycerol stocks of the culture series 1 at day 43 and 125 were spread to plate medium, then strains from isolated colonies were obtained (SD75 and SD145 strains).

2-3-8 Genome re-sequencing for evolved strains

Genome DNA of YPH499, YSM021, and 6 evolved strains (SD75-1 to SD75-3 and SD145-1 to SD145-3 strains) were prepared by using the QIAGEN Genomic-tip 100/G (Qiagen, Venlo, Netherlands) for next-generation sequencing of the whole genomes. The genomes were sequenced by pair-end sequence (250 bp) by Illumina HiSeq2000 using MiSeq reagent 500 cycle kit v2 (Illumina, San Diego, CA, USA). Each sample yielded a fastq file including approximately 25 million reads, and the average quality scores per base were higher than 20. Reads were mapped to a reference genome sequence of S288C strain obtained from *Saccharomyces* Genome Database using Bowtie2 [70]. Variations in the genome sequence were identified using SAMtools [71]. The mapping results were confirmed by the Integrative Genomics Viewer (IGV) [72].

2-4 Results and discussions

2-4-1 Metabolic pathway design of *S. cerevisiae* for isobutanol production based on flux balance analysis

Metabolic simulation based on flux balance analysis (FBA) was conducted using a genome-scale model iMM904 to increase the isobutanol production yield in *S. cerevisiae*. In the calculation, the glucose consumption rate and oxygen uptake rate were set to 10 and 0.5 mmol gDW^{-1} h^{-1} respectively, to represent the microaerobic condition. As a result, most of the glucose was converted to ethanol and isobutanol was not produced in the natural metabolic model iMM904. For isobutanol biosynthesis, two molecules of NADPH were required as cofactors, however, in *S. cerevisiae*, two molecules of NADH were commonly generated by glucose metabolism of glycolysis. Then the cofactor redox balance of NADH was maintained by the consumption in ethanol biosynthesis. In order to increase the supply of NADPH for isobutanol production, two unnatural metabolic pathways in *S. cerevisiae*; the phosphoenolpyruvate carboxylase (PPC) pathway and Entner-Doudoroff (ED) pathway (EDP) were introduced to the model iMM904 (Figure 2-4-1, Table 2-4-1). Then, the calculation with the model iMM904-PPC which added the PPC reaction and the model iMM904-EDP which introduced the EDP reactions, isobutanol production yield were not observed. This is because of the by-production of the ethanol. In the glucose metabolism, it is more efficient and balance of cofactors was closed for cells using the glycolysis (EM pathway) with two ATP and NADH generations rather than using ED pathway with one ATP generation or using PPC to convert NADH to NADPH.

Therefore, models that the ethanol biosynthesis reaction was deleted from each

model were constructed. In *S. cerevisiae*, the ethanol is converted from the pyruvate which was produced by the glucose metabolism, by two-step reactions of pyruvate decarboxylase (PDC) and alcohol dehydrogenase (ADH). There are three PDC genes and seven ADH genes in *S. cerevisiae* genome, considering the difficulty to construct the gene knockout strains, deletion of PDC reaction was selected to construct the model without ethanol production (iMM904-pdcΔ, iMM904-PPC-pdcΔ, and iMM904-EDP-pdcΔ). The flux distributions were calculated using these models, 28.3%, 22.1% and 54.2% of isobutanol production yields were obtained for each model, respectively. In these calculations, of course, no constraint for the PPC and ED pathway reactions were set. However, supposing to the carbon flux was drawn in their pathway, that is, in the case of the overexpression of these enzymes, the isobutanol yields were increased along with the flux of PPC and ED pathway (Table 2-4-1). Therefore it was suggested that the overexpression of these pathways, might increase the isobutanol yield. In the following section, *S. cerevisiae* strains were constructed based on the above three approaches; introduction of PPC, the introduction of the ED pathway and knockout of three PDC genes. Considering the difficulties of the construction of PDC knockout strains, the introduction of pathways and PDC knockout approaches were verified separately.

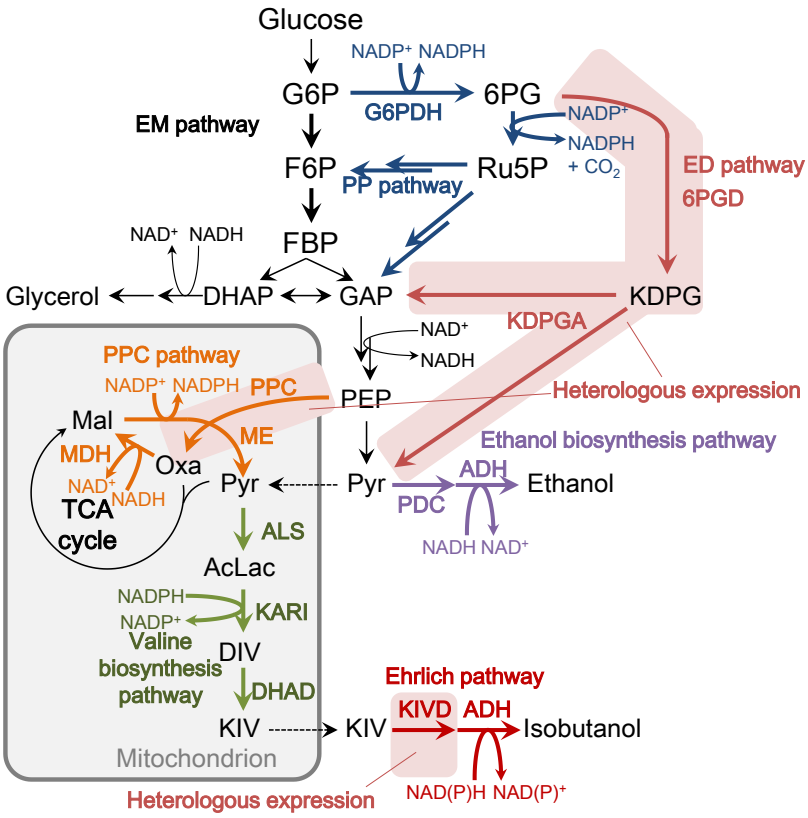

Figure 2-4-1 Pathways introduced to yeast metabolism by FBA

The phosphoenolpyruvate carboxylase (PPC) improves NADH consumption and NADPH generation required for isobutanol production. The Entner-Doudoroff (ED) pathway also provides sufficient NADPH for isobutanol production without the loss of carbon, unlike the pentose phosphate (PP) pathway. Abbreviations are defined as follows. G6P: glucose 6-phosphate, 6PG: 6-phosphogluconate, FBP: fructose bis-phosphate, GAP: glyceraldehyde 3-phosphate, DHAP: dihydroxyacetone phosphate, PEP: phosphoenolpyruvate, Pyr: pyruvate, AcCoA: acetyl-CoA, Oxa: oxaloacetate, Mal: malate, KDPG: 2-dehydro-3-deoxy-phosphogluconate, AcLac: acetolactate, DIV:2,3-dihydroxy isovalerate, KIV: α-ketoisovalerate, G6PDH: glucose-6-phosphate dehydrogenase, 6PGDH: 6-phosphogluconate dehydrogenase, 6PGD: 6-phosphogluconate dehydratase, KDPGA: 2-dehydro-3-deoxy-phosphogluconate aldolase, MDH: malate dehydrogenase, ME: malic enzyme, ALS: acetolactate synthase, KARI: ketol-acid reductoisomerase, DHAD: dihydroxyacid dehydratase, KIVD: 2-ketoisovalerate decarboxylase, ADH: alcohol dehydrogenase.

Table 2-4-1 Simulation result based on flux balance analysis

Models	Growth rate (h^{-1})	Ethanol yield (%)	Glycerol yield (%)	Isobutanol yield (%)
iMM904	0.23	170.01	0.00	0.00
iMM904-pdcΔ	0.13	0.00	0.00	28.31
iMM904-PPC	0.30	141.62	0.00	0.00
iMM904-PPC-pdcΔ	0.29	0.00	0.00	22.06
*iMM904-PPC(2)-pdcΔ	0.18	0.00	0.00	52.34
iMM904-PPC(4)-pdcΔ	0.21	0.00	0.00	50.52
iMM904-PPC(6)-pdcΔ	0.23	0.00	0.00	48.70
iMM904-PPC(8)-pdcΔ	0.25	0.00	0.00	41.01
iMM904-EDP	0.23	170.01	0.00	0.00
iMM904-EDP-pdcΔ	0.16	0.00	0.00	54.15
iMM904-EDP(2)-pdcΔ	0.15	0.00	0.00	62.00
iMM904-EDP(4)-pdcΔ	0.15	0.00	0.00	69.85
iMM904-EDP(6)-pdcΔ	0.14	0.00	0.00	77.69
iMM904-EDP(8)-pdcΔ	0.13	0.00	0.00	85.54

* Models shown like iMM904-PPC(2)-pdcΔ means the simulation results that flux of introduced pathway (PPC and EDP) were set in the values described in brackets (in this case, the flux of PPC was set to 2 mmol $gDCW^{-1}$ h^{-1}).

2-4-2 Expansion of metabolic network by the introduction of phosphoenolpyruvate carboxylase

Phosphoenolpyruvate carboxylase

The phosphoenolpyruvate carboxylase (PPC) is a metabolic enzyme which catalyzes a reversible reaction of the phosphoenolpyruvate (PEP) to oxaloacetate by the fixation of carbon dioxide and the hydrolysis of a phosphate group (Figure 2-4-2). This metabolic enzyme is widely present in bacterial cells, however, it does not exist in *S. cerevisiae*. There is a similar enzyme of PPC which is called phosphoenolpyruvate carboxykinase encoded by *PCK1* in *S. cerevisiae*. This enzyme is used for gluconeogenesis, for decarboxylation of oxaloacetate and phosphorylation to produce PEP, though there is no reverse reaction. Heterologous expression of PPC converting PEP to oxaloacetate (Oxa) was expected to increase the supply of NADPH and pyruvate (Pyr) because the Oxa produced could be converted to Pyr by regenerating NADPH with a metabolic bypass that includes malate dehydrogenase (MDH) and malic enzyme (ME) in *S. cerevisiae* (Figure2-4-3).

- **Phosphoenolpyruvate carboxylase**

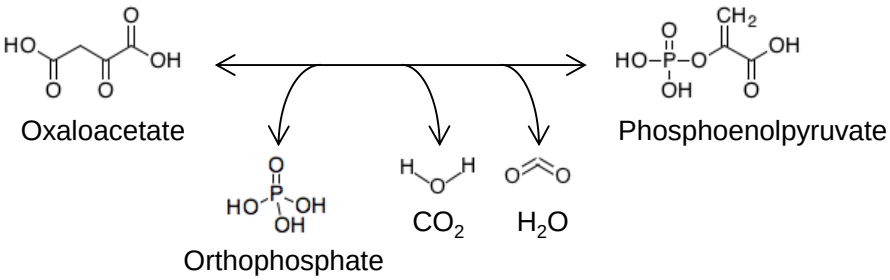

Figure 2-4-2 Metabolic reaction catalyzed by phosphoenolpyruvate carboxylase (PPC)

PPC catalyzes the reversible reaction producing one molecule of phosphoenolpyruvate from one molecule of oxaloacetate.

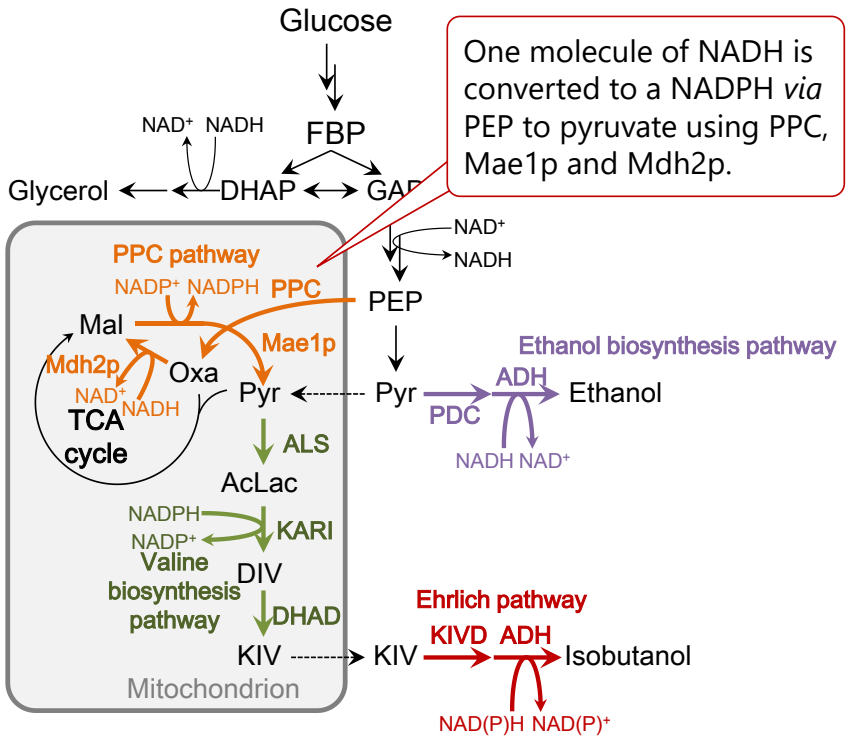

Figure 2-4-3 Metabolic pathway converting the NADH to the NADPH by PPC.

One molecule of NADH is converted to the NADPH *via* PEP to pyruvate using PPC, Mae1p, and Mdh2p.

Construction of the isobutanol production strains based on FBA

In *S. cerevisiae* metabolism, 2-ketoisovalerate carboxylase (Kivd) does not exist which is required for the isobutanol production to convert the 2-ketoisovalerate to isobutyraldehyde. The plasmid vector pATP426-kivd-ADH6-ILV2 was constructed in the previous study which simultaneously overexpressing the *kivd* derived from *Lactococcus lactis* encoding Kivd, *ADH6* derived from *S.cerevisiae* encoding an alcohol dehydrogenase (ADH) which converts isobutyraldehyde to isobutanol, and *ILV2* derived from *S. cerevisiae* encoding an acetolactate synthase (ALS) which converts a pyruvate to acetolactate, the first step reaction of isobutanol biosynthesis pathway. To obtain the isobutanol production strains, the vector ATP426-kivd-ADH6-ILV2 and two empty vectors (pGK422 and pGK423) were introduced to *S. cerevisiae* YPH499 strain (YKP003). The constructed strains were cultivated in 5 mL of SD medium with 20g/L glucose under semi-anaerobic conditions. The isobutanol titer of the control strain (YKP003) at 48 h of cultivation was 64.2 ± 3.2 mg/L, this was 0.78±0.04% mol mol-glucose^{-1} yield (Figure 2-4-4). This yield was the similar value to which was reported in previous research (0.55% mol mol-glucose^{-1}) obtained by overexpressing a similar gene in the YPH499 strain [51].

For the additional overexpression of *ppc* genes derived from *E. coli* (*Ecppc*, pGK422-PPCec plasmid), *Corynebacterium glutamicum* (*Cgppc*, pGK422-PPCcg plasmid) and *Synechocystis sp.* PCC6803 (^{Sy}*ppc*, pGK422-PPCsy plasmid), three plasmids were constructed. These *ppc* genes were available in our laboratory. Introduction of pGK422-PPCec and pGK422-PPCcg had no effect on isobutanol production (strain YKP004, 56.9 ± 7.6 mg/L (0.69±0.09%) and strain YKP005, 67.5 ± 1.7 mg/L(0.82±

0.02%), respectively). However, the isobutanol production level of strain YKP006, which introduced pGK422-PPCsy was 93.2 ± 1.6 mg/L(1.13±0.02%), or 1.45-fold greater than that of the control strain. Focusing on the growth, OD values of the YKP003 strain (the control strain) reached to 2.6±0.1 at 48 hours, though that of the YKP004, YKP005 and YKP006 strains increased to 3.1±0.2, 2.9±0.1, and 2.9±0.2, respectively, which were higher than the YKP003 strain. The Amino acid auxotrophy was not different in those strains so this growth improvement was the effect of the *ppc* expression. FBA simulation result also suggested the growth improvement, this fermentation result was supported by these simulation result.

PPC expression was investigated by the SDS-PAGE of crude protein extracts from all three strains. The result showed that only the YKP006 strain expressing ^{Sy}*ppc* showed a band corresponding to PPC (118.9 kDa) (Figure 2-4-5). There was no band of PPC in strain YKP004 (99.1 kDA) and YKP005 (103.2 kDa), indicating a poor heterologous expression and translation of PPC from ^{Ec}*ppc* and ^{Cg}*ppc* or their instability in *S. cerevisiae* cells. However, the growth rates of the strains were improved by the introduction of ^{Ec}*ppc* and ^{Cg}*ppc*, they were expressed in some level but too small to be observed in SDS-PAGE. Although an experimental validation is needed, the result suggested that the expression of PPC derived from *syn*6803 promoting NADPH supply required for isobutanol production in cooperation with malic enzyme and malate dehydrogenase.

In this section, the increase of isobutanol production yield was tested by the improvement of the NADPH supply. Overexpression of the PPC pathway gene in the constructed strain, it was possible to improve the production yield of isobutanol slightly without the deletion of the ethanol biosynthesis pathway. Of course, the yields were much

lower than the simulation result combined with PDC deletion, suggesting that knockout of ethanol biosynthesis was essential for more improvement.

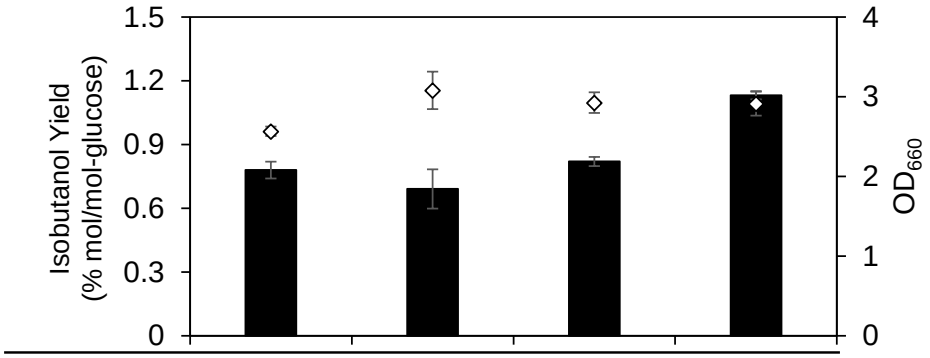

Strain	YKP003	YKP004	YKP005	YKP006
^{LI}*kivd, ADH6, ILV2*	+	+	+	+
ppc	-	*PPCec*	*PPCcg*	*PPCsy*

Figure 2-4-4 The isobutanol production yields (%mol/mol-glucose) and OD660 values in the culture broth at 48 hours from the start of the fermentation test. The black bars represent the production yield of isobutanol, and the open diamonds represent the OD_{660} values. Error bars also showed the standard error of N = 3 independent experiments.

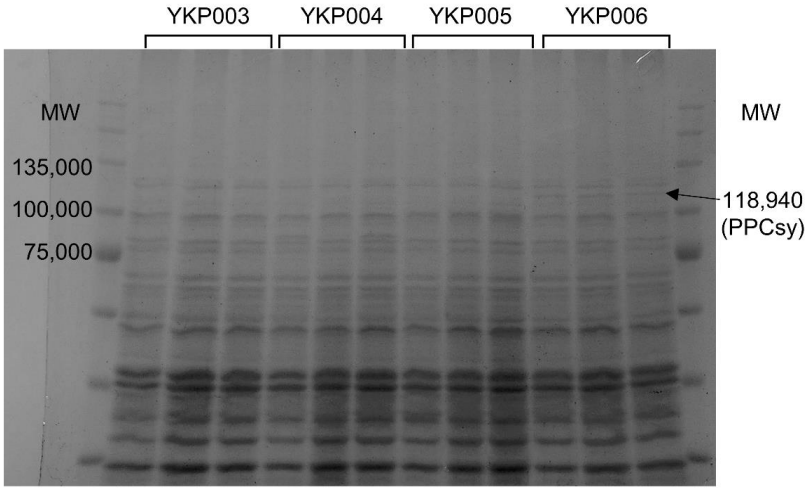

Figure 2-4-5 SDS-PAGE of crude proteins extracted from YKP003 to 006 strains after 24 hours fermentation. MW means a molecular weight.

2-4-3 Expansion of metabolic network by the introduction of the Entner-Doudoroff pathway

Entner-Doudoroff pathway

The reactions for the regeneration of NADPH in the metabolic pathway of *S. cerevisiae* were less than that of bacteria. One example is the Entner-Doudoroff pathway (ED pathway). ED pathway is widely preserved in bacteria species such as *E. coli* for the glucose metabolism as well as the Embden-Meyerhof-Parnas pathway (EMP pathway) and the oxidative pentose-phosphate pathway (PP pathway) (Figure 2-4-6) [73]. The ED pathway is consisted by two reactions; 6-phosphogluconate (6PG) dehydratase converting the 6PG to the 2-dehydro-3-deoxy-6-phosphogluconate (KDPG) and KDPG aldolase converting the KDPG to the glyceraldehyde 3-phosphate (GAP) and the pyruvate. This pathway is not normally used in bacteria because of the lower energy efficiency of ATP production than the EMP pathway (Two or one ATP molecules were produced from one molecule of glucose by EMP or ED pathway respectively). However, the ED pathway could convert the coenzyme $NADP^+$ to NADPH in glucose metabolism without the carbon loss by the decarboxylation, unlike the PP pathway. In addition, since the ED pathway could reduce one molecule of $NADP^+$ and the PP pathway could reduce two molecules of $NADP^+$ per one molecule of glucose, the use of these pathways give the flexibility to regulate the redox balance of intracellular NADPH (Figure 2-4-7).

- **6-Phospho-D-gluconate dehydratase**

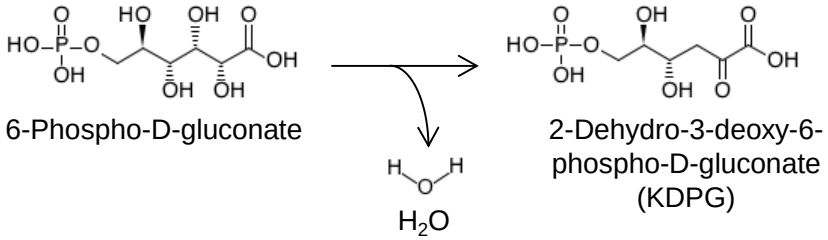

- **2-dehydro-3-deoxy-6-phospho-D-gluconate aldolase**

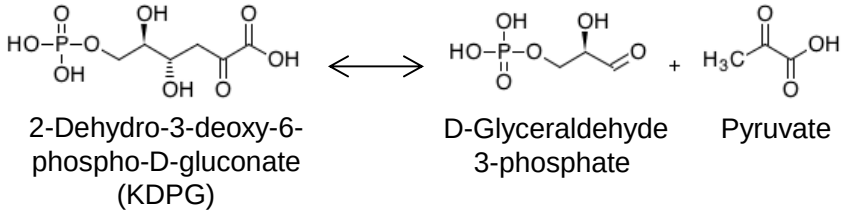

Figure 2-4-6　Reactions constituting the Entner-Doudoroff pathway

One molecule of 6 PG generates one molecule of GAP and pyruvate.

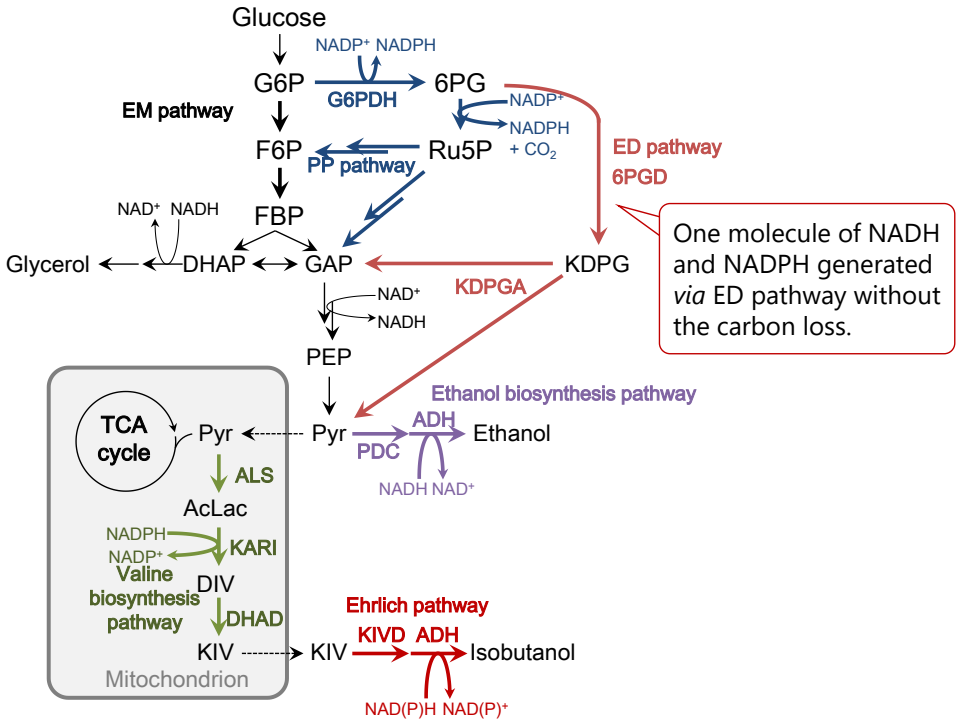

Figure 2-4-7 Metabolic map of the entrance ED pathway and surrounding pathways.

The EMP pathway branches at G6P and the PP pathway and the ED pathway branches at 6PG.

Introduction of the Entner-Doudoroff pathway to S. cerevisiae

In order to introduce the enzymes of the Entner-Doudoroff (ED) pathway in *S. cerevisiae*, the genes *edd* and *eda*, which encode 6PGD and KDPGA, respectively, were amplified from the genomic DNA of *E. coli* (^{Ec}*edd*, and ^{Ec}*eda*, respectively) to construct the expression plasmids (pGK423-Eceda and pGK425-Ecedd). These plasmids were introduced into strain YPH499 pATP426-ILV2-kivd-ADH6 (YED010 strain). The isobutanol and ethanol yields and OD_{660} levels at 48 hours after the start of fermentation were shown in figure 2-4-8. The isobutanol yields of strains YED007 and YED008, which lacked isobutanol biosynthesis-related genes, were less than 0.21% (about 20 mg/L). Isobutanol yields increased to 0.88±0.17% (72.1±13.6 mg/L) with the expression of isobutanol biosynthesis-related genes. The proteins were successfully expressed and translated because the SDS-PAGE of crude protein extracts of strain YKM027 expressing ^{Ec}*edd* and ^{Ec}*eda* genes showed two bands corresponding to 6PGD (64.6 kDa) and KDPGA (22.3 kDa) (Figure 2-4-9). However, additional expression of enzymes of the ED pathway failed to increase isobutanol production in the fermentation test (0.79±0.04%, 65.2 ± 3.3 mg/L).

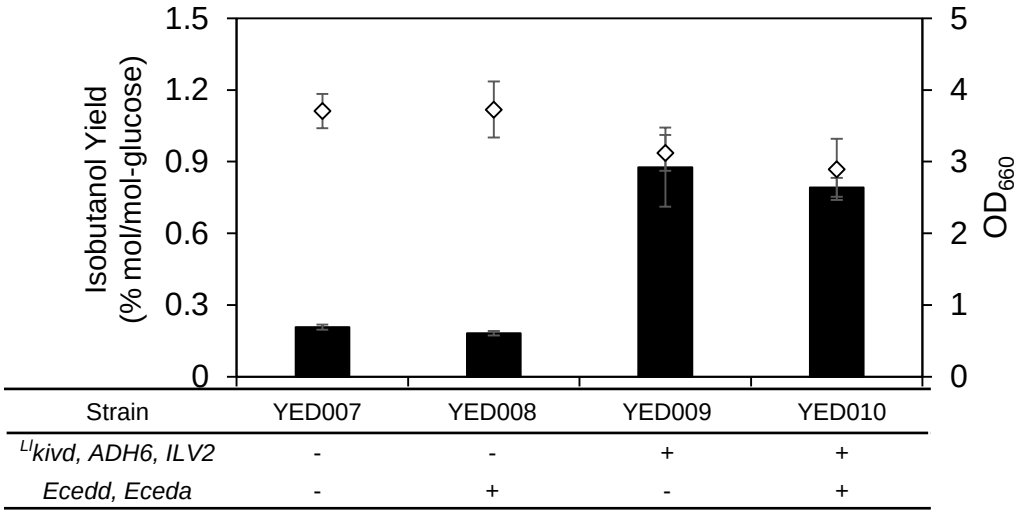

Figure 2-4-8 The isobutanol production yields (%mol/mol-glucose) and OD660 values in the culture broth at 48 hours from the start of the fermentation test. The black bars represent the production yield of isobutanol, and the open diamonds represent the OD_{660} values. Error bars also showed the standard error of N = 3 independent experiments.

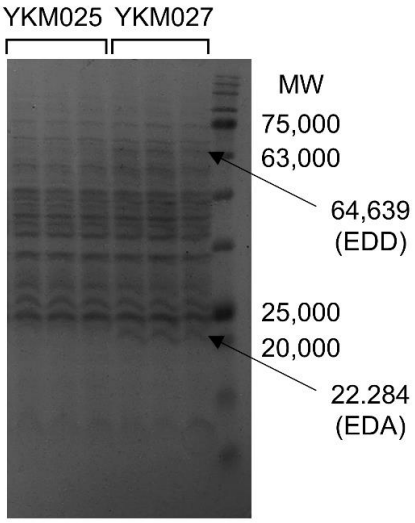

Figure 2-4-9 (a) SDS-PAGE of crude proteins extracted from YKM025 and YKM027 strain after 24 hours fermentation. MW means a molecular weight.

13-C metabolic flux ratio analysis

SDS-PAGE analysis confirmed that the enzymes of the ED pathway-related genes were successfully expressed. In this section, the effect of ^{Ec}*edd* and ^{Ec}*eda* expression on the *S. cerevisiae* phenotype was further investigated using laboratory *S. cerevisiae* BY4742 strain with four amino acid auxotrophy. 6-phosphogluconate (6PG) is a branch point metabolite for the PP pathway and ED pathway (Figure 2-4-7), and 6PG is converted to ribulose 5-phosphate (Ru5P) by the reaction of 6PG dehydrogenase (6PGDH) in the PP pathway. Thus, to increase the precursor supplies for ED pathway, BY4742 *gnd1Δ* strain was used whose *GND1* gene encoding a major isoform of 6PGDH was deleted. Plasmid pGK423-Eceda and pGK425-Ecedd were introduced into BY4742 and BY4742 gnd1Δ strains to obtain the YKM015 and YKM027 strains. While the *GND1* knockout also decreased the specific growth rate to 0.19±0.01 h^{-1} (YKM025), it recovered to 0.22±0.004 h^{-1} with the expression of additional ED pathway genes (YKM027) (Table 2-4-2). Furthermore, higher optical densities (OD_{660}) after 30 hours of fermentation were observed in these strains, indicating that overexpression of genes in the ED pathway affected the growth phenotype. Moreover, the codon-optimized version of *edd* and *eda* derived from *Zymomonas mobilis* (^{Zm}*eddOp* and ^{Zm}*edaOp*) were synthesized for the construction of overexpression vectors. Since the specific growth rate of strain YKM040 (BY4742 gnd1Δ /pGK423-ZmedaOp/pGK425-ZmeddOp/pGK426) was 0.22±0.005 h^{-1}, which was similar to that of YKM027 (BY4742 gnd1Δ /pGK423-Eceda/pGK425-Ecedd/pGK426), this phenotype may not be specific to the *edd* and *eda* genes from *E. coli*.

The metabolic flux levels of ED pathways were estimated in a carbon-labeling

experiment using a stable isotope (^{13}C)-labeled glucose. When *S. cerevisiae* cells are cultivated in the medium containing [1-^{13}C] glucose as a sole carbon source, one molecule of [3-^{13}C] pyruvate and one molecule of non-labeled pyruvate are produced by glycolysis via the EM pathway. On the other hand, only non-labeled pyruvate is produced via the PP pathway, because ^{13}C carbon is discarded by 6PGDH in the PP pathway. Glycolysis via the artificial ED pathway produced one molecule of [1-^{13}C] pyruvate and one molecule of non-labeled pyruvate. This indicates that the metabolic flux levels of ED pathways can be determined from the ^{13}C labeling patterns of pyruvate or pyruvate-derived metabolites such as alanine using mass spectrometry. *S. cerevisiae* strains were cultivated in 50 mL of SD medium with [1-^{13}C] glucose under aerobic conditions. Cells collected at the mid-log growth phase were acid hydrolyzed to obtain ^{13}C labeled alanine from cellular proteins. The mass spectrum of *tert*-butyldimethylsilyl-alanine was determined using GC-MS, and the flux ratios of the ED pathways were estimated from the mass isotopic distributions of $[M-85]^+$ (including C2-C3 carbons) and $[M-57]^+$ (including C1-C3 carbon) fragments. Table 2-4-3 shows the estimated flux ratios of the ED pathways in the metabolically engineered strains. The estimated flux ratios of the ED pathways in the wild-type strain (YKM013) were 0.005 ± 0.002, indicating that 0.5% of the incorporated glucose was catabolized to pyruvate via the ED pathway. The flux ratios of the ED pathways in the YKM015 strain expressing ED pathway-related genes from *E. coli* were slightly increased to 0.006 ± 0.001. On the other hand, the flux ratios of the ED pathway in the BY4742 gnd1Δ strain were increased from 0.002 ± 0.001 (YKM025) to 0.011 ± 0.0004 (YKM027, harboring ED pathway-related genes from *E. coli*) and 0.007 ± 0.001 (YKM040, harboring ED pathway-related genes from *Z. mobilis*), respectively. These result suggested that the introduced ED pathway worked in BY4742 gnd1Δ strains and

should have some effect on the growth phenotype. However, compared to the EMP pathway, the metabolic flux of the ED pathway was extremely small, so it is unlikely that a slight flux of the ED pathway had a large effect on growth. Therefore, these results indicated that the improvement of the growth rate observed in BY4742 gnd1Δ strains might not be the result of the function of the ED pathway but another function of the ED pathway-related genes.

The above results were suggested that the ED pathway was hardly functioning as the original pathway *in S. cerevisiae*. A previous study has reported that the enzyme activities of 6PG dehydratase and KDPG aldolase derived from *E. coli* could not be detected in the cytoplasm of *S. cerevisiae* [74]. Some metabolic reactions require an iron-sulfur cluster (ISC) as a cofactor to have the activity as a catalyst. Among the two metabolic enzymes consisting of the ED pathway, 6PG dehydratase is ISC protein which requires [4Fe-4S] iron-sulfur cluster. However, in most of the eukaryotes such as *S. cerevisiae,* ISCs were synthesized in small cell compartment known as the mitochondrion. Therefore, it is considered that the ED pathway does not function in the cytosol of *S. cerevisiae* because of the deficient of ISC for the activity of 6PG dehydratase. In this section, analysis of the function of the ED pathway introduced into *S. cerevisiae* was tried at the flux level and proved that this pathway has little function. Lack of ISC in the cytosol is considered to be a major cause for the low activities of the ED pathway, thus there are many problems in trying to operate the reactions requiring ISC in yeast. It should be avoided to use this ISC required pathway for metabolic engineering of *S. cerevisiae*.

Table 2-4-2 Growth rate of constructed strains

Strain	Growth rate(h^{-1})
YKM013: WT	0.21±0.01
YKM015: WT+EcEDP	0.19±0.01
YKM025: gnd1Δ	0.19±0.01
YKM027: gnd1Δ+EcEDP	0.22±0.004
YKM040: gnd1Δ+ZmEDP	0.22±0.005

Table 2-4-3 Flux ratio of each pathway to glucose uptake rate

Strain	EM pathway	PP pathway	ED pathway
YKM013: WT	0.958±0.003	0.037±0.002	0.005±0.002
YKM015: WT+EcEDP	0.964±0.006	0.030±0.005	0.006±0.001
YKM025: gnd1Δ	0.969±0.007	0.029±0.007	0.002±0.001
YKM027: gnd1Δ+EcEDP	0.999±0.013	-0.010±0.013	0.011±0.0004
YKM040: gnd1Δ+ZmEDP	0.967±0.005	0.026±0.004	0.007±0.001

2-4-4 Triple gene knockout of pyruvate decarboxylase

S. cerevisiae and ethanol fermentation

The ethanol fermentation in *S. cerevisiae* is one of the most important ability for the yeast to obtain fast growth. Under the high glucose concentration conditions, the aerobic ethanol fermentation is strongly promoted in *S. cerevisiae* by the Crabtree effect which is suppressing the expressions of genes for the respiration. In the ethanol fermentation, one molecule of glucose is converted to two molecules of pyruvate producing two molecules of NADH and ATP, then pyruvate is converted to ethanol *via* acetaldehyde by two reactions catalyzed by pyruvate decarboxylase (PDC) and alcohol dehydrogenase (ADH). ADH reaction requires NADH for reducing power, thus the balance of coenzyme NADH and NAD^+ is kept constant by the consumption and the regeneration of NADH in the ethanol production and the glucose metabolism (Figure 2-4-10). This system had been acquired in the process of evolution in *S. cerevisiae* for consuming the glucose rapidly and growing faster, and preventing the growth of competitors by the toxic ethanol production.

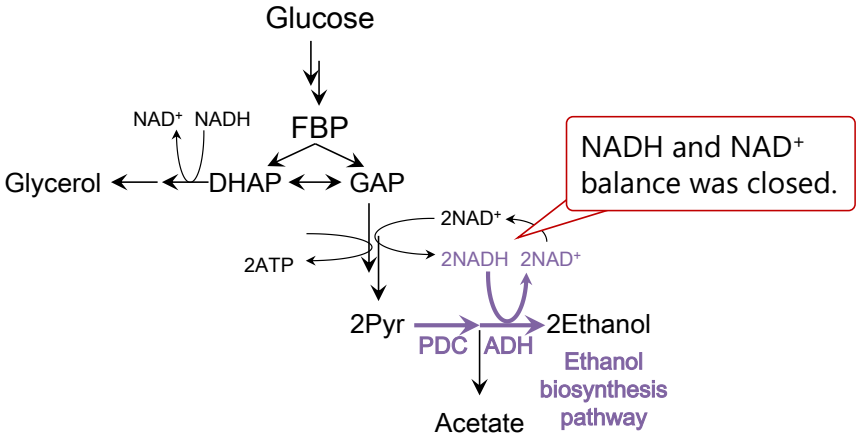

Figure 2-4-10 Schematic diagram of ethanol fermentation

The ethanol fermentation is very important for *S. cerevisiae*, many isozymes for PDC and ADH reactions exist. There are three genes; *PDC1*, *PDC5*, and *PDC6* for the PDC reaction and six genes; *ADH1*, *ADH2*, *ADH3*, *ADH4*, *ADH5*, *SFA1* for the ADH reaction. *ADH6* and *ADH7* also exist for ADH reaction that specialized for the production of branched-chain alcohols. The ethanol fermentation is one of a major problem to produce useful chemical substances using *S. cerevisiae* because although the introduction of a metabolic pathway for bioproduction of certain target metabolite, *S. cerevisiae* turns the most of carbon sources to the ethanol. Therefore, many researchers have attempted to construct the multiple gene knockout strains of ethanol biosynthesis related genes. Ida *et al.* constructed multiple gene knockout strain for ethanol production which disrupted six ADH genes (*ADH1*, *ADH2*, *ADH3*, *ADH4*, *ADH5*, and *SFA1*) and one PDC gene (*PDC1*) and two glycerol production related genes of *GPD1* and *GPD2*. Then, they constructed the lactate production strains that inhibited the production of ethanol and glycerol and achieved the high yield of lactate production (2 mol-lactate mol-glucose^{-1}) which was the same value of the theoretical maximum yield [75]. Kim *et al.* constructed triple gene deletion strains of PDC reaction (*PDC1*, *PDC5*, and *PDC6*) for the 2,3-butanediol production. This PDC knockout strain was impossible to grow on a glucose minimal medium, an adaptive laboratory evolution experiment was conducted to obtain the trains that can grow on glucose medium. The result of the reverse engineering of the acquired strains, the lack of the phosphorylation site of Mth1p constituting the glucose sensor (*MTH1-ΔT*) was discovered to become possible *S. cerevisiae* to grow on glucose medium [76]. These ethanol non-producing strains were very important for the metabolic engineering of *S. cerevisiae*. However, these strains also had problems of the low growth ability and the poor availability of amino acid auxotrophy markers.

In this section, triple gene knockout strains encoding PDC were newly constructed based on a laboratory *S. cerevisiae* YPH499 strain to eliminate the ethanol by-production for isobutanol production.

Adaptive laboratory evolution of ethanol non-producing yeast strain

Ethanol non-producing yeast *S. cerevisiae* strains have been constructed by multiple gene knockout of pyruvate decarboxylase (PDC) and alcohol dehydrogenase (ADH). However, these strains showed very low growth abilities and have few availabilities of amino acid auxotrophic markers, so there are problems that the handling of the strains required much times and markers must be recycled every time to carry out the multi-step of metabolic engineering [75,76].

Triple PDC gene knockout strains were constructed based on the laboratory yeast strain of *S. cerevisiae* YPH499 (*MATa ura3-52 lys2-801 ade2-101 trp1-Δ63 his3-Δ200 leu2-Δ1*) harboring the 6 amino acid auxotrophic markers by URA-blaster method. An ethanol non-producing yeast strain YSM021 (YPH499::*pdc1Δpdc5Δpdc6 ΔMTH1-ΔT*) was constructed by the triple gene knockout of *PDC1*, *PDC5*, and *PDC6* with *MTH1* mutation (*MTH1-ΔT*) reported in a previous study [76]. This strain was confirmed that it did not produce ethanol, but its growth rate and the final OD was very low in the glucose medium (Figure 2-4-11). Thus, a subculture of YSM021 strain in 20g/L glucose SD medium was carried out for the adaptive laboratory evolution (ALE) to obtain a strain which improved the growth rate in the glucose medium (Figure 2-4-12). The cells were continuously cultured in a test tube with 5 mL of SD medium under the semi-aerobic conditions in the five independent culture series. Each of independent culture series was repeatedly transferred to the fresh medium when the optical cell density was saturated. At

43 days after the stat of sub-culture, growth improvement of the cells in series 1 was observed. The experiment was continued for around 125 days (3000 hours) until further growth improvement was not observed. The glycerol stocks of the culture series 1 at day 43 and 125 were spread to plate medium, strains from isolated colonies were obtained (SD75 and SD145 strains).

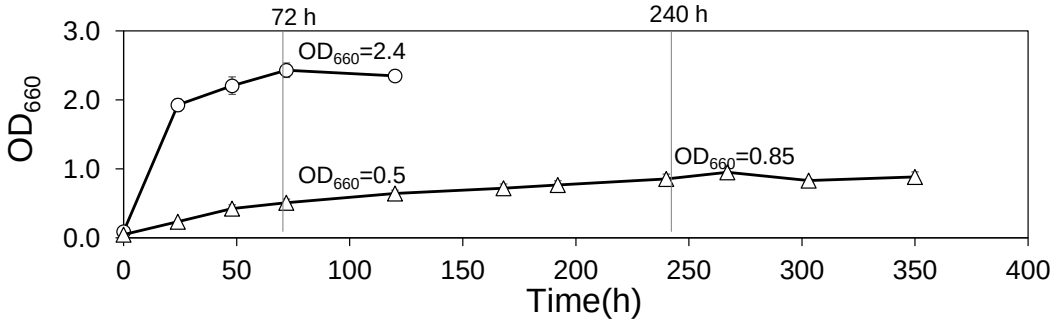

Figure 2-4-11 Growth curves of YSM021 strain and YPH499 strain

Cultivation under the microaerobic condition with 20 g/L glucose SD medium. White circles represent YPH499 wild strain, the triangles represent YSM021 strain (PDCΔ strain). OD600 value of YPH499 strain saturated at 72 hours from the start of the culture and reached to 2.4, though the OD600 value of YSM 021 strain reached to 0.5, and even at 240 hours it reached to only 0.9.

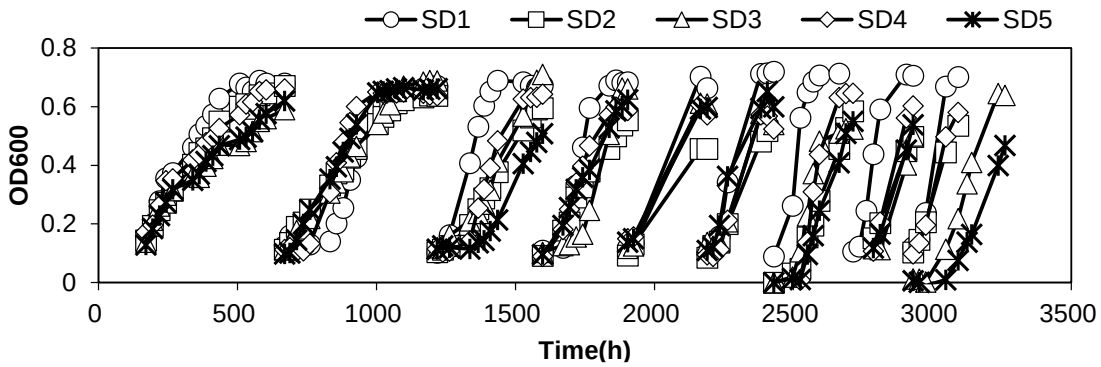

Figure 2-4-12 Growth curves of five series of culture during the ALE

Sub-cultivation results of YSM021 strains in five independent series. Growth improvement was seen especially in the SD1 series from the third subculture.

Validation of growth rate

Each colony of the six growth improved strains (SD75-1, SD75-2, SD75-3, SD145-1, SD145-2, SD145-3) was cultured in 5 mL of SD medium to compare their growth rate to the parental YSM021 strain and YPH499 wild strain (YSM001 strain) (Figure 2-4-13). Three strains (SD75-1, SD75-2, and SD75-3) obtained from the freeze stock SD-75 reached at 2 of OD_{600} value at 120 hours from the start of culture. This was three times higher OD_{600} value compared to YSM021 strain (original strain before the evolution experiment). On the other hand, three strain (SD145-1, SD145-2, and SD145-3) obtained from the frozen stock SD-145 reached 2.5 of OD_{600} value at 120 hours. This value was 4 times higher than that of the YSM021 strain and the same value compared to YSM001 strain (no PDC gene deletion). In addition, the growth rate of the laboratory evolved strain was calculated. (Table 2-4-4). Three strains acquired from stock SD145 showed higher growth rate than that of from stock SD75. Since the YSM021 strain was not observed log-growth phase, the growth rate could not be calculated. Although the data was not shown, culture broth of six evolved strains was obtained and analyzed by gas

chromatography, then no ethanol production was confirmed. In addition, the acquired evolved strain was observed with an electric microscope (Figure 2-4-14). All of the cells were an elliptical shape, and the budding traces which were characteristics in *S. cerevisiae* was observed, so it was concluded that these strains were not contaminated with other bacterial cells but pure *S. cerevisiae* strains.

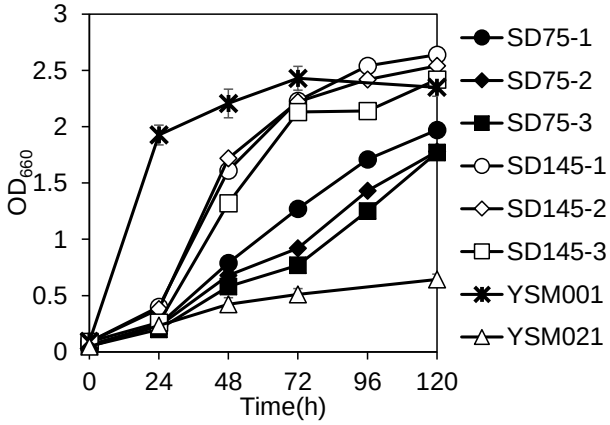

Figure 2-4-13 Growth curve of single colonized strains

A black circle, diamond, and square symbols represented the colonies obtained from the stock SD75 (43 days) and a similar open symbol represented the colonies obtained from the stock SD415 (125 days). In addition, asterisk indicated a wild-type strain (YPH499) and open triangles indicated YSM021 strain.

Table 2-4-4 Specific growth rate (0 to 48 hours) of single colonized strain.

Name	SD75-1	SD75-2	SD75-3	SD145-1	SD145-2	SD145-3
Growth rate (μ^{-1})	0.054	0.051	0.051	0.060	0.062	0.056

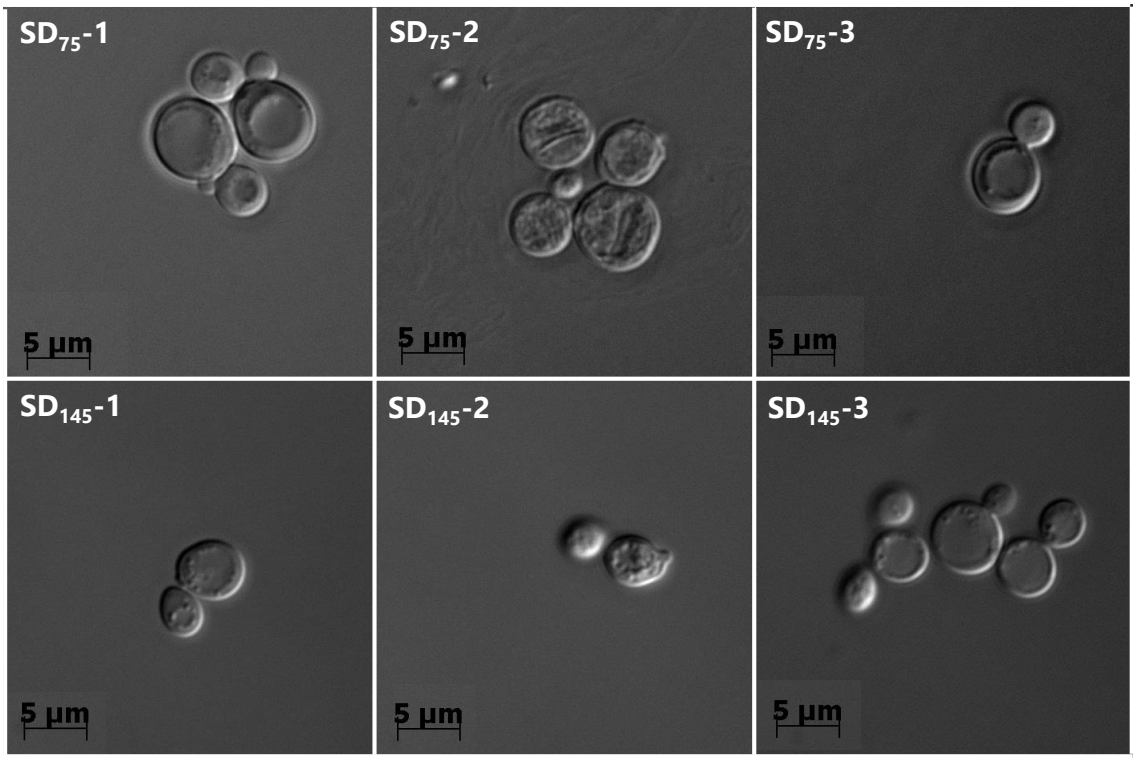

Figure 2-4-14 Microscopic image of the laboratory evolved strain observed with an electric microscope (1000 times enlarged image).

All of the cells were an elliptical shape, and the budding traces which were characteristics in *S. cerevisiae* was observed.

Observation of the fermentation profiles

The SD145-2 strain, one of the most growth improved strain in six evolved strains was cultured in test tubes to investigate the fermentation profiles (Figure 2-4-15). Fermentation was carried out by using SD medium containing 20 g/L glucose as a sole carbon source, the culture broth was analyzed by high-performance liquid chromatography to determine the concentration of glucose and organic acids. The YSM001 strain (control wild strain) represented by open circles in figure 2-4-15 reached to 2.9±0.1 of OD_{600} value in 48 hours, and most of the glucose in the medium was consumed (9.6±1.0 mM remained). Most of the products were ethanol and glycerol that

concentrations were 137.6±5.9 mM and 10.0±0.6 mM, respectively. The YSM021 strain (triple gene knockout strain of PDC) represented by open squares reached to 1.0±0.01 of OD_{600} value at 72 hours, and none of the glucose in the medium was consumed. This strain did not produce the ethanol and glycerol but 4.9±0.3 mM of pyruvate was produced. The SD 145-2 strain (the laboratory evolved strain) represented by the diamond was reached to 2.8±0.2 of OD_{600} value at 72 hours, this is the same value as the YSM001 strain. Although the growth rate was slower than that of the YSM001 strain, it was greatly improved compared to the YSM021 strain. Glucose concentration in the culture medium was 10 mM consumed but no ethanol was produced, though 0.8±0.04 mM of glycerol was produced. The concentration of pyruvate decreased to 2.1±0.5 mM compared to the YSM021 strain. This result indicated that in the laboratory-evolved strains, most of the consumed glucose was used for the growth while taking in glucose in the medium very slowly without a Crabtree effect or catabolite suppression. The glycerol production was increased compared to YSM021 strain, it was suggested that the NADH re-oxidation by glycerol production was required because of the increase of glucose metabolism.

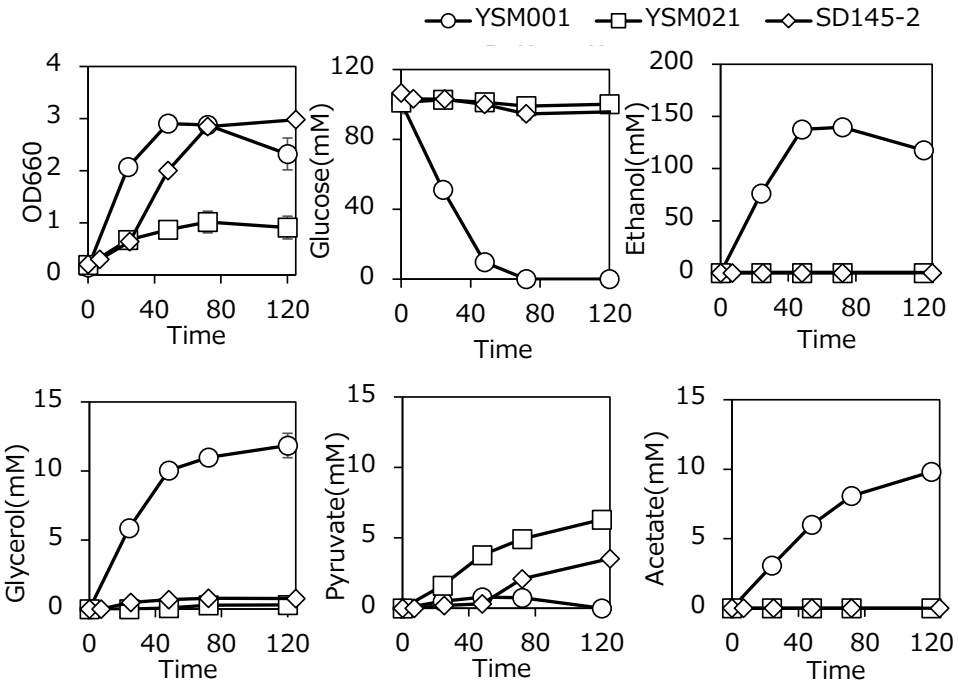

Figure 2-4-15 Fermentation profiles of laboratory-evolved strain SD145-2 strain, YSM001 strain, and YSM021strain

The open circles, squares, and diamonds represented the YM001 strain, the YSM021 strain, and the SD145-2 strain respectively.

Genome resequencing of evolved strains

The genomes of the laboratory-evolved strains were re-sequenced using the next generation sequencer to identify what kind of mutation was introduced into the genes. Reads were mapped to a reference genome sequence of S288C strain obtained from *Saccharomyces* Genome Database using Bowtie2 or BWA. Variations in the genome sequence were identified using SAMtools, then The mapping results were confirmed by the Integrative Genomics Viewer (IGV) (Table 2-4-5). In three strains obtained from stock SD75 in the middle stage of subculture, two nonsynonymous substitutions were identified in *YAK1* and *MCT1*. *MCT1* is a gene predicted to encode malonyl-CoA ACP transferase

involved in mitochondrial fatty acid synthesis. On the other hand, *YAK1* is a gene related to the glucose sensor like *MTH1* identified in the previous study, mutation of this gene might be responsible for growth improvement. In the three strains obtained from stock SD145 at the end of subculture, four nonsynonymous substitutions were found in *ECM21* and *SUP19* in addition to the same mutations in *YAK1* and *MCT1* described above. *ECM21* is known as a gene involved in endocytosis control of cell membrane proteins, and *SUP19* is encoding serine transfer RNA. From these results, it was suggested that the mutations of one or both of *YAK1* and *MCT1* are responsible for the growth improvement of these laboratory-evolved strains. Furthermore, it is considered that the growth ability of the final laboratory evolved strain (SD145-2 strain) was acquired by additional mutations of *ECM21* and *SUP19*.

Table 2-4-5 Non-synonymous substitution on genes identified in genome re-sequencing

Chromosome	Site (bp)	Gene	Site in gene (bp)	Before		After	Types of mutations	Strains
chr10	148844	YAK1	1547	GTT Val	→	GAT Asp	Non-synonymous	SD75, SD145
chr15	756954	MCT1	605	G Gly	→	A Val	Non-synonymous	SD75, SD145
chr2	27308	ECM21	991	T Val-Ser	→	- Val-Phe	Frameshift	SD145
chr5	288490	SUP19	35	C Ser	→	G Stop	Non-synonymous	SD145

Isobutanol fermentation test

In this section, we constructed metabolically engineered *S. cerevisiae* strains for isobutanol production based on the laboratory evolved non-ethanol producing SD145-2 strain (Figure 2-4-16). First, the PDY001 strain harboring the plasmid pATP426-kivd-ADH6-ILV2 and the PDY005 strain harboring the plasmid pATP426-mtkivdOp-mtADH7Op-ILV2 were constructed. The constructed strains were cultivated in 5 mL of 20g/L glucose SD medium under semi-anaerobic conditions (Figure 2-4-17 (A)). The isobutanol titer of the PDY001 and PDY005 strains at 72 hours of cultivation were 2.8 mg/L and 1.7 mg/L respectively. The isobutanol concentrations of these strains were terribly low, and final OD values of both strains decreased to 1.5 compared to SD145-2 strain. In addition, the isobutanol production yields could not be calculated because the consumed glucose amount was too small to detect. To enhance the isobutanol biosynthesis pathway, a plasmid pILV532cytL was introduced to PDY001 to construct the PDY007 strain. The plasmid pILV532cytL was the overexpression plasmid which is expressing three valine biosynthesis pathway-related genes (*ILV2*, *ILV3*, and *ILV5*) derived from *S. cerevisiae*, however, their mitochondrial transport signal sequences were truncated for the expression in the yeast cytosol. In addition, a PDY055 strain was constructed with the knockout of *ILV6* which is responsible for the feedback repression of *ILV2*. The isobutanol production concentrations of the PDY007 was 0.4 mg/L, in contrast, the PDY055 strain produced 17.4±9.5mg/L of isobutanol (Figure 2-4-17 (B)). This result showed that the release of feedback regulation was important for isobutanol production. For more enhancement of the isobutanol production pathway, PDY082, PDY074 and PDY079 strains harboring the plasmid pATP426-kivd-ADH6-ALSLpOp, pATP425-

ILV5c-DhadZm-AlsLpOp and pATP425-KariKp-ILV3c-AlsLpOp were constructed respectively. Each vectors expressing three valine biosynthesis genes in cytosol derived from several organisms; ALS gene of codon optimized *als* from *Lactococcus Plantarum*, KARI genes of truncated *ILV5* from *S. cerevisiae* or *kari* from *Klebsiella pneumoniae*, and DHAD genes of truncated *ILV3* from *S. cerevisiae* or *dhad* from *Zymomonas mobilis*. The PDY082 strain was also constructed introducing the plasmid pILV532cytL. The fermentation test revealed that the strain PDY074, PDY079, and PDY082 were shown low isobutanol titers (about 5 mg/L). Figure 2-4-18 (A) showed the isobutanol production yields of PDY055, PDY074, PDY079, and PDY082 strain. The isobutanol yield of PDY055 strain was 2.90±0.60% mol/mol-glucose, this was the highest yield in this thesis. On the other hand, yields of PDY074, PDY079, and PDY082 strain were 0.46±0.06% mol mol-glucose^{-1}, 0.48±0.22% mol mol-glucose^{-1} and 0.32±0.03% mol mol-glucose^{-1} respectively, however in these strains, a lot of acetoin by-production was observed which is converted from acetolactate (Figure 2-4-18 (B)). The acetoin yield of PDY074, PDY079, and PDY082 strain were 12.28±3.77% mol mol-glucose^{-1}、15.48±3.37% mol mol-glucose^{-1} and 14.57±5.29% mol mol-glucose^{-1} respectively, though that of the PDY055 strain was 7.30±1.30% mol mol-glucose^{-1}. The acetoin by-production in these strains indicated the low activity of the reactions of the downstream of the isobutanol biosynthetic pathway from the acetolactate. In particular, the DHAD is an iron-sulfur cluster requiring protein, thus it is considered that the isovalerate converted from the acetolactate was accumulate due to the low activity of DHAD and the carbon flux was overflowed to the acetoin biosynthesis.

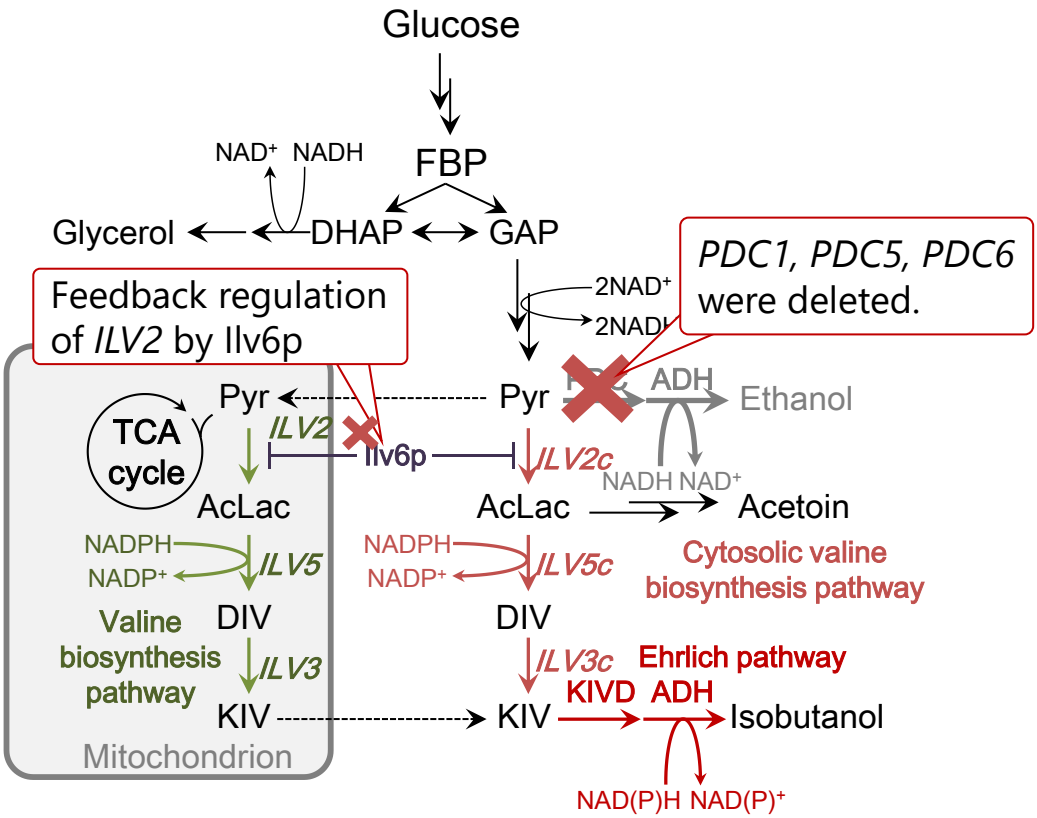

Figure 2-4-16 Metabolic map of isobutanol production pathway

The first step reaction of ethanol biosynthesis pathway (PDC reaction) was eliminated. The gray line represented the acetoin production pathway (by-product).

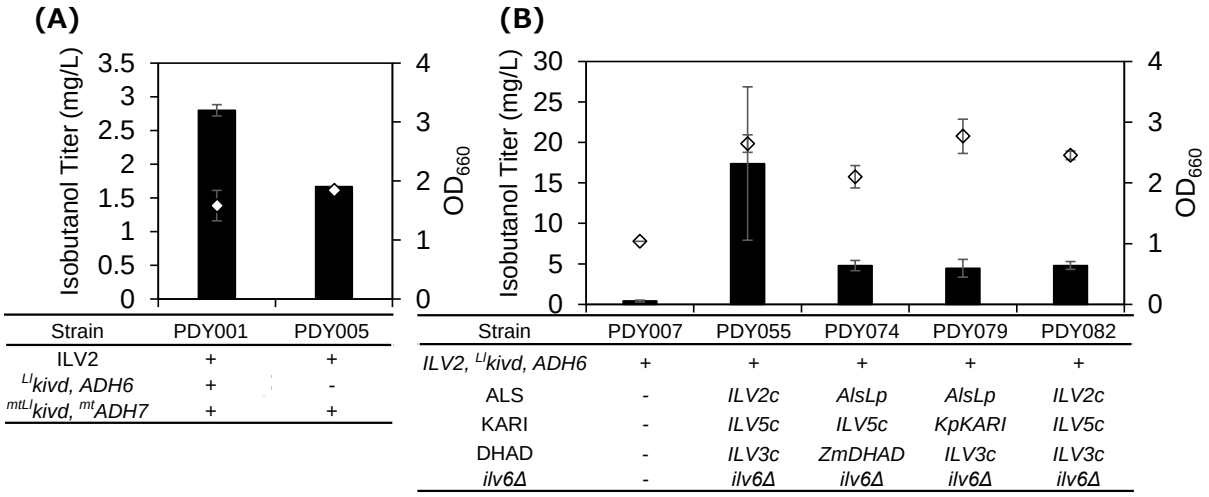

Strain	PDY001	PDY005
ILV2	+	+
LIkivd, ADH6	+	-
mtLIkivd, mtADH7	+	+

Strain	PDY007	PDY055	PDY074	PDY079	PDY082
ILV2, LIkivd, ADH6	+	+	+	+	+
ALS	-	*ILV2c*	*AlsLp*	*AlsLp*	*ILV2c*
KARI	-	*ILV5c*	*ILV5c*	*KpKARI*	*ILV5c*
DHAD	-	*ILV3c*	*ZmDHAD*	*ILV3c*	*ILV3c*
ilv6Δ	-	*ilv6Δ*	*ilv6Δ*	*ilv6Δ*	*ilv6Δ*

Figure 2-4-17 Concentration of isobutanol and the OD_{600} values at 72 hours from the start of the fermentation test. (A) showed the results of PDY001 strain and PDY005 strain, and (B) showed the results of PDY007 strain, PDY055 strain, PDY074 strain, PDY079 strain, and PDY082 strain.

The black bar represented the isobutanol concentrations and the open diamond represented the OD values. Error bars also represented the standard error of N=3 independent experiments.

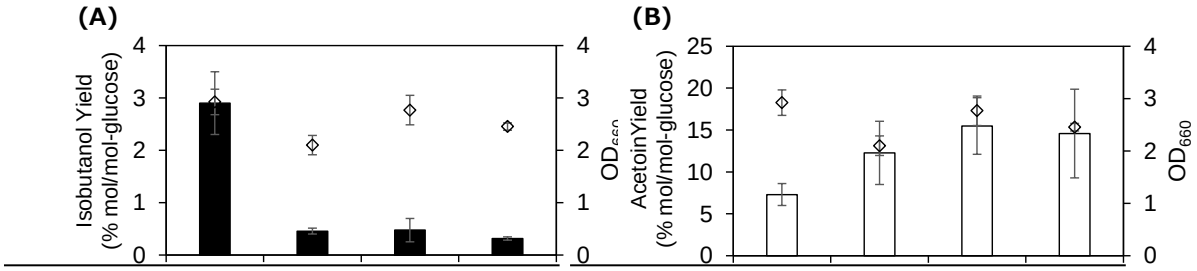

Strain	PDY055	PDY074	PDY079	PDY082
ILV2, LIkivd, ADH6	+	+	+	+
ALS	*ILV2c*	*AlsLp*	*AlsLp*	*ILV2c*
KARI	*ILV5c*	*ILV5c*	*KpKARI*	*ILV5c*
DHAD	*ILV3c*	*ZmDHAD*	*ILV3c*	*ILV3c*
ilv6Δ	*ilv6Δ*	*ilv6Δ*	*ilv6Δ*	*ilv6Δ*

Strain	PDY055	PDY074	PDY079	PDY082
ILV2, LIkivd, ADH6	+	+	+	+
ALS	*ILV2c*	*AlsLp*	*AlsLp*	*ILV2c*
KARI	*ILV5c*	*ILV5c*	*KpKARI*	*ILV5c*
DHAD	*ILV3c*	*ZmDHAD*	*ILV3c*	*ILV3c*
ilv6Δ	*ilv6Δ*	*ilv6Δ*	*ilv6Δ*	*ilv6Δ*

Figure 2-4-18 OD_{600} values and (A) isobutanol production yield and (B) acetoin production yield at 72 hours from the start of the fermentation test.

The black bar represented the isobutanol concentrations and the white bar represented the acetoin concentrations. Error bars also represented the standard error of N=3 independent experiments.

2-5 Conclusion

In this chapter, assuming that the strain breeding with complementing the ignored factors in FBA can be a breakthrough of the low isobutanol yield, experimental results of constructed yeast strains and the simulation results were compared to verify the availability and limitation of metabolic engineering based on FBA. FBA results suggested that the introduction of PPC pathway and ED pathway could increase the isobutanol yield because of the improvement of NADPH supply which was required in the isobutanol production pathway. Knockout of pyruvate decarboxylase genes related to ethanol biosynthesis could also improve the isobutanol yield because of the decrease of the ethanol by-production.

The isobutanol yield of constructed strain which introduced the PPC gene derived from *syn*6803 was improved 1.4 times higher than that of control strain (improved to 1.13±0.02% from 0.78±0.04%). In this strain ethanol production was not inhibited, the yield was much lower than the predicted value of FBA result (maximally 52%). However, as FBA suggested, it is important that the enhancement of NADPH supply for isobutanol production. In addition, the PPC gene derived from *syn*6803 which was found in this thesis is considered to be useful for improving the yield of other target products requiring the NADPH in yeast.

However, no improvement of isobutanol yield was observed with the introduction of the ED pathway. Although the isotopic tracer experiments using [1-^{13}C] glucose suggested that the ED pathway hardly functioned as a metabolic pathway in *S. cerevisiae*. It was confirmed that the enzymes (EDD and EDA) involved in this pathway were expressed by SDS-PAGE analysis. The EDD constituting the ED pathway is an

enzyme whose activity depends on the coordination of iron-sulfur cluster (ISC), so it was considered that the no function of ED pathway was due to the lack of ISC in the cytoplasm of the yeast cell.

Ethanol non-producing yeast was constructed whose pyruvate decarboxylase (PDC) genes were completely knocked out. As a result of the inhibition of ethanol production, metabolism in this strain was seriously disturbed, thus the growth ability was also remarkably decreased. Through the adaptation laboratory evolution (ALE) experiment, ethanol non-producing yeast strain SD415-2 with high growth ability was achieved by optimizing the metabolic state with no ethanol production. In this strain, the mutation was introduced to the gene involved in the glucose uptake system in addition to the *MTH1* mutation. This indicated that the entrance of metabolism (glucose uptake) was down-regulated to prevent the jam of the metabolism.

The expression of *ILV2* for the first reaction of valine biosynthetic pathway involved in isobutanol production is known to be repressed by feedback regulation mediated by the *ILV6*. This factor was not considered in FBA simulation. The experimental results also showed the very low isobutanol concentration in strains without *ILV6* knockout. Therefore, the PDY055 strain with *ILV6* knockout was constructed based on the SD145-2 strain (Figure 2-4-19). The PDY055 strain achieved 2.90±0.60% mol/mol-glucose of isobutanol yield. This was the comparable value to the highest isobutanol production yield in test tube scale culture without high-density fermentation process (2.91% Matsuda *et al.*, 2013, Table 2-2-1) However, this result was 18.5 times lower value than the result obtained from the FBA (54% mol/mol-glucose) although the considerable factors lacking in FBA simulation were complemented by the strain breeding such as feedback regulation and optimization of metabolism by ALE.

These result indicated that the low isobutanol yield was due to the low activities of isobutanol biosynthesis pathway itself. The KIVD coded by *kivd* derived from *L. lactis* in the downstream of the biosynthesis pathway used in this thesis was shown the sufficient activity in a study using a bacterial host such as *E. coli*. Of course, the activity of *kivd* should be different in *E. coli* and *S. cerevisiae* cell, there was no report mentioned about the low activity of this enzyme in *S. cerevisiae*. *ADH6* and other all upstream pathway genes, *ILV2, ILV5,* and *ILV3* were derived from *S. cerevisiae* itself, therefore, it was hard to see their activities were extremely low. However, there is one point to pay attention to this metabolic pathway. DHAD coded by *ILV3* in valine biosynthesis pathway is an ISC dependent enzyme. This is the same kind of enzyme-like EDD consisting of the ED pathway which showed no improvement for the isobutanol production. In the metabolic engineering for the target mass production, the production pathway must be a high activity for large flux. However, similar to the EDD of the ED pathway that did not function in the cytosol in yeast cell due to the lack of ISC, the overexpressed DHAD might also show little activity due to depletion of ISC in mitochondria. In fact, the construction of the whole isobutanol biosynthesis pathway in cytosol resulted in the increase of acetoin by-production. Acetoin is a by-product of valine biosynthesis pathway made from acetolactate which was the substrate of KARI, upstream reaction of DHAD. Therefore, an increase of acetoin production was considered to be caused by the overflow of acetolactate due to the mismatch of fluxes. The downstream flux of DHAD reactions could not catch up with the upstream metabolic flux of ALS and KARI due to its low activity (Figure 2-4-19).

In eukaryote such as yeast, cellular ISC was produced in mitochondria and transported to the cytosol [77], however, DHAD and most of other ISC dependent

proteins originally existed in mitochondria. This is because the cytosolic space is larger than the mitochondrion, so it is hard to keep the ISC concentration high in the cytosol because of the diffusion of ISC. Therefore, the functioning of the ISC dependent enzymes such as DHAD and EDD must be difficult in the cytosol of *S. cerevisiae*. On the other hand in the mitochondrion, DHAD is used for the valine and isoleucine biosynthesis, however, it might be strongly regulated by the ISC biosynthesis. Because it seemed that the cell was regulated not to produce an excessive amount of ISC necessary for cell growth and maintenance. In other words, ISC is produced only required amount for cell growth in *S. cerevisiae* cells, thus ISC dependent enzymes compete to acquire few ISC and could not show above the certain activities. Therefore the bottle-necks of the metabolism that was not simulated in FBA has occurred because ISC is not included in the stoichiometry of the FBA model.

In this chapter, the bottle-neck of ISC dependent reactions was estimated that brought the difference between the simulation result based on FBA and the experimental result of bred strain. The question is whether this bottle-neck can be improved by breeding like a feedback regulation or not. The ISC biosynthesis system is very complicated and hardly engineered. That is, in order to solve this problem, too much labor will be required. There is also a possibility that it cannot be applied for the cytosolic pathway because of the diffusion and dilution of ISC in the cytosol. Therefore, it is not a good idea to deal with these approaches related to ISC generation. However, the design of pathways including the ISC dependent reactions using current FBA model, it would result in the large differences of results between the simulation and the constructed strains. Such gaps are not preferable for the strategic planning of metabolic engineering based on FBA because it would cause an increase in experimental costs and lead us to wrong approaches.

Therefore, in order to reduce such costs and failure approaches, the new FBA metabolic model should be considered to avoid the pathways that include the ISC dependent enzymes for metabolic engineering of *S. cerevisiae*.

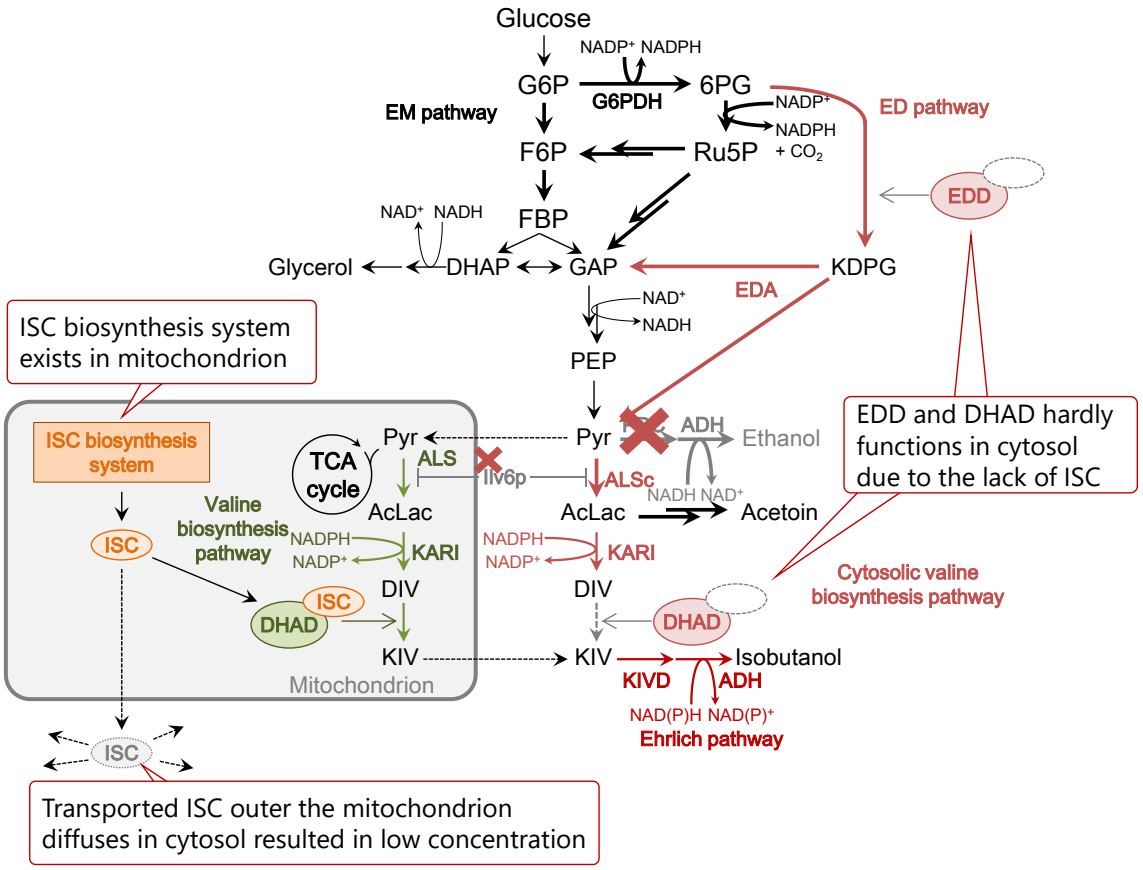

Figure 2-4-19 Metabolic map of isobutanol production pathway

Intracellular ISC is synthesized in the mitochondrion. Outer the mitochondrion, ISC is diffused to the cytosol and ISC dependent reaction hardly functions due to the absence of ISC. The acetoin production might be enhanced by the decrease of DHAD reaction.

Chapter 3: Reconstruction of flux balance analysis metabolic model and improvement of yeast strain for 2,3-butanediol production

3-1 Highlights

- The current FBA models of *S. cerevisiae* include iron-sulfur cluster (ISC) dependent reactions, however, there is no constraint for the amount of ISC in the yeast cell.
- Metabolic model iMM904-ISC was reconstructed considering the ISC constraint to limit the summed flux of ISC dependent reactions by the simulation result of wild-type metabolic distribution of iMM904 (< 2.2 mmol gDW^{-1} h^{-1} when glucose and oxygen uptake rate set to 10 and 0.5 mmol gDW^{-1} h^{-1}, respectively).
- A metabolic simulation using iMM904-ISC showed that the isobutanol production yield was greatly decreased (54.2% to 11.7%), indicating that the isobutanol was unsuitable metabolite to be produced in yeast.
- Searching for the suitable target for *S. cerevisiae* bioproduction using iMM904-ISC, several metabolites such as 2,3-butanediol was found (58.9%).
- 2,3-butanediol production strains resulted in high 2,3-butanediol yield that its values were close to the simulation result (58.0%).
- For further improvement of 2,3-butanediol productivity, repression system of ethanol fermentation was tried to be constructed.

3-2 Introduction

3-2-1 Limitation of the current metabolic engineering based on flux balance analysis

In the metabolic engineering strategy of microorganisms to improve the production of target metabolite, the cofactor redox balance such as NADH and NADPH has been often discussed. In this thesis, intracellular NADPH balance was focused on for the isobutanol production in *S. cerevisiae*. Engineered strains were constructed based on the metabolic design by the FBA metabolic simulation. The introduction of phosphoenolpyruvate carboxylase (PPC) improved isobutanol yield. On the other hand, the introduction of the Entner-Doudoroff (ED) pathway did not achieve the improvement of isobutanol yield because the introduced pathway itself was hardly functioning. 6-phosphogluconate dehydratase (6PGD or EDD) constituting the ED pathway is an iron-sulfur cluster (ISC) dependent protein for its activity. Therefore, the ED pathway could not function probably due to the low concentration of ISC in the cytoplasm. Although the possible metabolic engineering approaches such as the adaptive laboratory experiment and the removing of the feedback regulation were conducted, the isobutanol yields of the non-ethanol producing strains were 18 times smaller than that of predicted values by the FBA simulation. It was suggested that the activity of the isobutanol biosynthesis pathway itself was terribly low. The ketoisovalerate dehydratase (DHAD) which consists the isobutanol production pathway is known as the ISC dependent protein like 6PGD. Therefore it is considered that the use of metabolic pathway requiring the ISC is difficult in *S. cerevisiae* cells for overexpression.

3-2-2 Demand of the reconstruction of the metabolic model for flux balance analysis

The gaps between the simulation results and the experimental results of constructed strains are not preferable. In the metabolic engineering approaches based on the FBA, there are possibilities to generate many candidates of approaches that cannot be realized in *S. cerevisiae*. Then, a lot of constructed strains would be in vain, resulting in failure to achieve the target yield value or loss of time and resources. As described above, the DHAD and the 6PGD consisting of the isobutanol biosynthesis pathway and ED pathway are ISC dependent enzymes for its catalytic activities. Thus the deficiency of ISC in cytosol must cause a decrease of enzymatic activity. However, the current FBA based metabolic simulations have not concerned about ISC supply and requirement. As a result, unrealistic large fluxes were calculated on the cytosolic isobutanol biosynthesis pathway and the cytosolic ED pathway. These problems did not emerge in bacterial metabolic engineering such as *E. coli* because they have no compartments in the cell-like mitochondrion. However, it cannot be ignored in the metabolic engineering of eukaryotes such as *S. cerevisiae*. Therefore improvement of the conventional FBA model is necessary in order to acquire more accurate metabolic designs.

3-2-3 Objective in this chapter

In this chapter, the genome-scale model iMM904 was reconstructed to take into account the constraint of ISC dependent reactions. Isobutanol production yield was examined how the metabolic simulation results were varied depending on the constraint of ISC. In addition, production yields of several target metabolite were calculated using the reconstructed metabolic model to investigate what kind of targets were suitable to be

produced in *S. cerevisiae*. Then through the breeding of 2,3-butanediol production strain, which was one of the candidates obtained from simulation results, reconstructed FBA model was validated. In addition, the ethanol non-producing yeast constructed in chapter 2 remarkably decreased the growth ability due to the gene knockout. Therefore, as an approach to decrease the ethanol production with high growth ability, expression system using the mutant type of Cas9 protein was constructed for the repression of ethanol production aiming to improve the 2,3-butanediol productivity.

3-3 Methods

3-3-1 Reconstruction of FBA metabolic model with iron-sulfur cluster

Metabolic model and reactions

For the FBA metabolic simulations of *S. cerevisiae*, the yeast genome-scale model iMM904 was used. In order to introduce the constraint of ISC dependent reactions, the model iMM904 was modified in the following manner.

First, the reactions required ISC shown in appendix table A4 page 131 were removed from the original genomic scale model iMM904 (Figure 3-3-1). Then, the reactions in appendix table A5 page 132 that newly including the terms of ISC were added to the model. In the new ISC reactions, all of the reversible reactions in the original model were described as the different reactions that consume ISC either of positive reaction or reverse reaction (Model iMM904-ISC). In this thesis, reconstructed ISC dependent reactions were mainly including the dehydratases, succinate dehydrogenase, NADH dehydrogenase and respiratory chain enzymes involving Ubiquinone. In this model iMM904-ISC, sum flux of ISC dependent reactions is equal to the flux of reaction ISCsynth which represented the ISC biosynthesis in table A5.

In the calculation, firstly, the upper bound of reaction ISCsynth was set to free. FBA metabolic simulation was conducted under certain conditions of glucose uptake rate and oxygen uptake rate that were wanted to be examined (Figure 3-3-2). Then, sum flux of all ISC dependent reactions is calculated as the value of reaction ISCsynth. Secondly, this value is used as the upper bound of the reaction ISCsynth for following simulations with genes knockout or introduction of heterologous pathways.

Conditions for calculation

For all calculations, the COBRA toolbox on MATLAB 2013a (MathWorks Inc., Natic, MA, USA) was used [31]. In addition, GLPK (GNU Linear Programming Kit) was used for a linear programming solver. The added reactions for the metabolic simulation of target production to the model were shown in appendix table A3 page 130.

For the calculations of flux distributions, the glucose uptake rate and oxygen uptake rate were set to 10 mmol gDW^{-1} h^{-1} and 0.5 mmol gDW^{-1} h^{-1}, respectively (the default value of the model iMM904). The linear programming problem expressing FBA was described as follows.

Maximize (max) (v)	v_{growth}	
Subject to (s.t.)	$S \cdot v = 0$	$(\forall i = M)$
	$v_j{}^{\min} \leq v_j \leq v_j{}^{max}$	$(\forall i = R)$

Each letter corresponds to the following.

v_j : Metabolic flux of reaction j

$v_j{}^{max}$: Upper limit of the metabolic flux of reaction j

$v_j{}^{min}$: Lower limit of the metabolic flux of reaction j

v_{growth} : Biomass biosynthesis rate

$S_{i,j}$: Coefficient for metabolite i in reaction j

M : Set of metabolites

R : Set of reactions

In the calculation of the reconstructed model, firstly, the upper limit value of the reaction ISCsynth (newly added reactions described ISC generation) was set to infinity, metabolic simulation was performed under the set aeration condition with the metabolic network of wild-type strain that does not include the gene deletion or the introduction of a heterologous pathway to record the ISC generation flux. Then, the upper limit of ISC generation reaction ISCsynth was set to the value which was recorded, metabolic distributions were calculated for the metabolic designs of the certain metabolite bio-production including the introduction or deletion of metabolic reactions. The total flux of ISC required reactions were constrained by the value of ISCsynth.

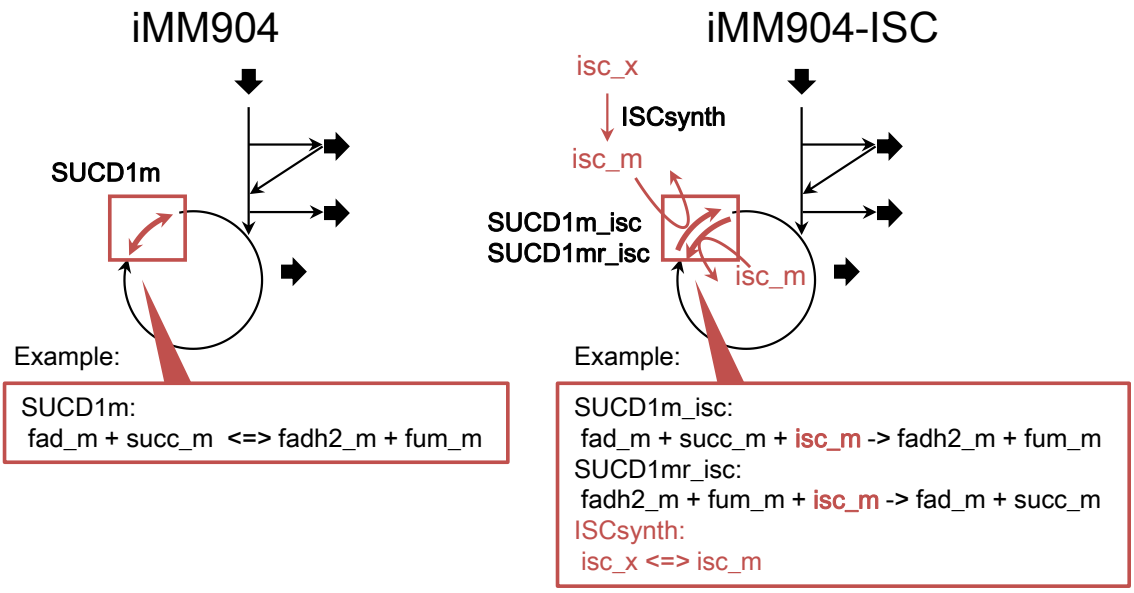

Figure 3-3-1 Example of the reconstruction of the metabolic model

The reactions required ISC shown in appendix table A4 page 131 were removed from the original genomic scale model iMM904. Then, the reactions are shown in appendix table A5 page 132 that newly including the terms of ISC were added to the model. In the new ISC reactions, all of the reversible reactions in the original model were described as the different reactions that consume ISC either of positive reaction or reverse reaction.

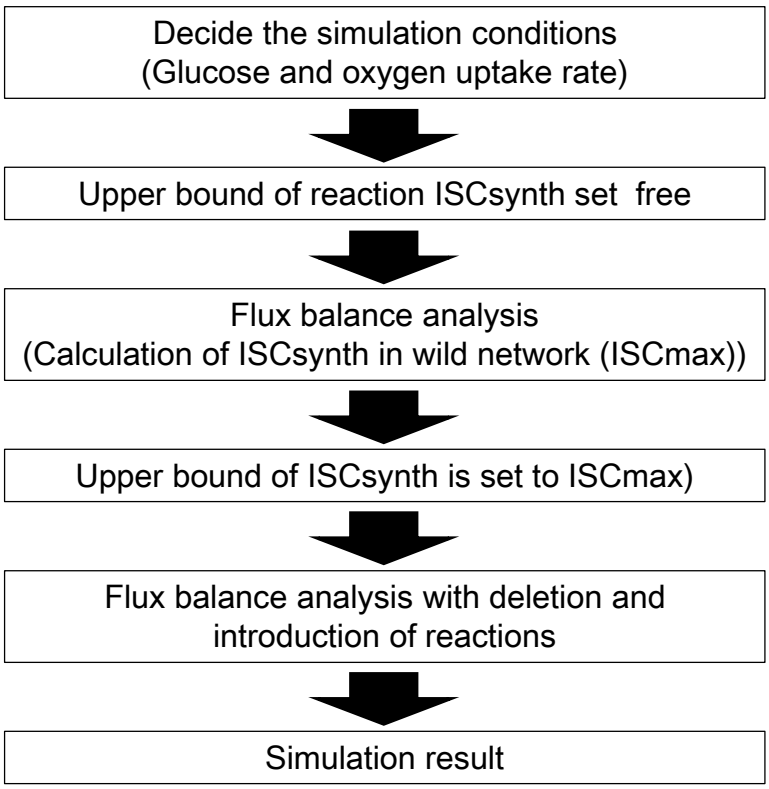

Figure 3-3-2 Procedure of the metabolic simulation with ISC constraint.

In the calculation, the upper bound of reaction ISCsynth was set to free. FBA metabolic simulation was conducted under certain conditions of glucose uptake rate and oxygen uptake rate that were wanted to be examined. Then, sum flux of all ISC dependent reactions is calculated as the value of reaction ISCsynth. Secondly, this value is used as the upper bound of the reaction ISCsynth for following simulations with genes knockout or introduction of heterologous pathways.

3-3-2 Strains and plasmids and yeast transformation

The yeast strains and plasmids used in this study were listed in appendix table A1 and table A2 page 125 and page 128 respectively. The lithium-acetate method was used for all yeast transformations. All strains were cultured in yeast extract peptone dextrose (YPD) medium (1% bacto yeast extract, 2% bacto peptone, 2% glucose) and synthetic dextrose (SD) medium (6.7% yeast nitrogen base without amino acids and 2%

or 0.5% glucose, as necessary, 0.06% leucine, 0.03% lysine hydrochloride, 0.02% histidine, 0.02% uracil, 0.04% tryptophan and 0.04% adenine hydrochloride) for transformations.

3-3-3 Fermentation test

For the 2,3-butanediol fermentation test, transformants were cultured for 72 h at 30°C with shaking at 150 rpm in 5 mL of SD medium containing 20 g/L glucose and required amino acids. The initial OD_{660} values for the main cultures were set at 1.0.

3-3-4 High-density fermentation test

For high-density fermentation, cells were inoculated into then inoculated into 50 mL of SD medium (containing 10% glucose, 6.7% yeast nitrogen base without amino acids and required amino acids) with 100 g/L glucose. The initial OD_{660} values were set at 20. Fermentation was performed at 30°C with mild agitation in 100-mL closed bottles equipped with a bubbling CO_2 outlet.

3-3-5 Measurement of RFP expression

The strains were pre-cultured with a 5 mL of 20 g/L glucose SD medium with required amino acids in a test tube. For the main culture, cells were harvested and inoculated to the fresh 200 μL of SD medium in a 96 well plate. The initial OD_{600} value was 0.1, and OD values and the fluorescence intensity of RFP were measured using the plate reader (excitation wavelength was 580 nm, the measured wavelength was 620 nm). In this experiment, 100 μg/L of the tryptophan was added to main culture medium for the tryptophan inducible promoter.

3-3-6 Micro-scale fermentation test

Transformants were inoculated in 2 mL of 20 g/L glucose SD medium in a 48 deep-well plate and pre-cultured at 30°C, and 150 rpm for 24 hours. The main culture was also performed for 48 hours with the same condition of pre-culture with 0.1 of initial OD_{600} value. In this experiment, inducers for the *ARO9* promoter (100 μg/L of tryptophan) and the *CUP1* promoter (20 mM of $CuSO_4$) were added to both pre-culture and main culture medium. The ethanol and the 2,3-butanediol concentration in the culture broth were measured using gas chromatography.

3-3-7 Repeated batch culture in a test tube

The strains were inoculated to 5 mL of 20 g/L glucose SD medium in a test tube with 30°C, and 150 rpm for 24 hours for pre-pre-culture. For the pre-culture, cells were inoculated to fresh medium with supplementation of 20 mM of $CuSO_4$ or 100 μg/L of tryptophan for gene expression induction. On the next day, the main culture was started with fresh medium at the initial OD was 0.1. After the 48 hours fermentation, whole cells were harvested and sub-cultured to fresh medium for next 48 hours fermentation. This operation was repeated three times, and the culture broth of each culture endpoint was analyzed to determine the alcohol concentrations by GC.

3-3-8 Analytical methods for culture broth

To determine the concentrations of glucose, ethanol, 2,3-butanediol, acetate, glycerol, and pyruvate in the culture medium, the supernatant was obtained by centrifugation at 15,000 rpm at 4°C for 5 min and applied to a gas chromatograph and

high-performance liquid chromatography (HPLC) system with same conditions described in chapter2.

3-4 Results and discussions

3-4-1 Reconstruction of the metabolic model for the flux balance analysis with iron-sulfur cluster constraint

In order to introduce the constraint of ISC dependent reactions into the genome-scale model iMM904, the following two constraints are newly established in addition to the usual constraints of FBA.

1. Cells do not produce the ISCs more than the amount required for their growth.
2. Introduction or deletion of metabolic pathways does not promote the ISC generation.

These constraints mean that the cells do not produce unnecessary products for their own growth. The maximum amount of ISC in yeast cells under certain culture conditions (in other words, the upper limit of the total flux of the ISC reactions) must not be exceeded the value of the wild-type strain (model iMM904) under the same conditions. According to these constraints, the model iMM904-ISC was reconstructed which was introduced the terms of ISC consumption to the ISC dependent reactions and the reaction for ISC biosynthesis (reaction ISCsynth in appendix table A5, page 132). In the calculations, first, the upper bound of ISCsynth was set to free, FBA metabolic simulation was conducted with no modification (deletion or introduction of the heterologous pathway) under certain conditions of glucose uptake rate and oxygen uptake rate. Then, the calculated value of the reaction ISCsynth was set to the upper bound of itself for the following simulations,

not to exceed the sum fluxes of the ISC dependent reactions (Figure 3-4-1).

The FBA metabolic simulation was conducted using the reconstructed model iMM904-ISC targeted for the isobutanol production in *S. cerevisiae*. In the calculations, the glucose and the oxygen uptake rate were set to 10 and 0.5 mmol gDW^{-1} h^{-1} respectively corresponding to the microaerobic condition. When the upper bound of the reaction ISCsynth was set to free, the isobutanol production was not observed in model iMM904-ISC. The summed flux of ISC dependent reactions was 2.2 mmol gDW^{-1} h^{-1} in these conditions. Without the upper bound of the reaction ISCsynth (conventional model iMM904), 54.2% of isobutanol yield was calculated with the deletion of the pyruvate decarboxylase (PDC) reaction which is responsible for ethanol production (Figure 3-4-2). Then, the upper bound of the reaction ISCsynth was set to the value which was recorded in the first simulation (2.2 mmol gDW^{-1} h^{-1}). The isobutanol yield was calculated as 11.7% with the deletion of the PDC reaction. This was 21.6% of the yield compared to the value with original model iMM904 without ISC constraint. It was suggested that the total flux of ISC reactions used in the usual yeast cells were too small to increase the isobutanol production. The calculated yield using the reconstructed model was 4.0 times higher than that of PDY055 strain constructed in chapter 2. The difference between the experimental yield and the simulation yield was decreased to 8.8% from 51.3% by the introduction of ISC constraints. It was suggested that there was still room to improve the isobutanol yield in PDY055 strain. However, even if the engineering for further improvement was conducted, the upper limit of the isobutanol yield was less than 12% due to the ISC production capacity. It was inevitable to conclude that the capacity of *S. cerevisiae* to produce the isobutanol was insufficient for massive production. Therefore, when using the *S. cerevisiae* for a bio-production host, other targets should be selected

which did not require ISC in its metabolic designs.

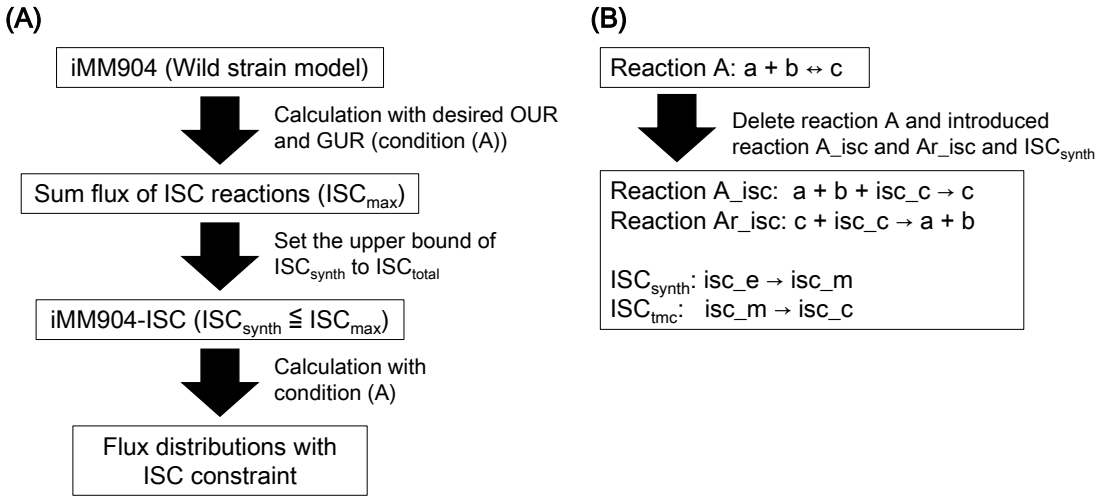

Figure 3-4-1 Scheme of flux balance analysis with reconstructed model

(A) The flow of the metabolic simulation with ISC constraint. (B) Reconstruction of the metabolic model iMM904-ISC.

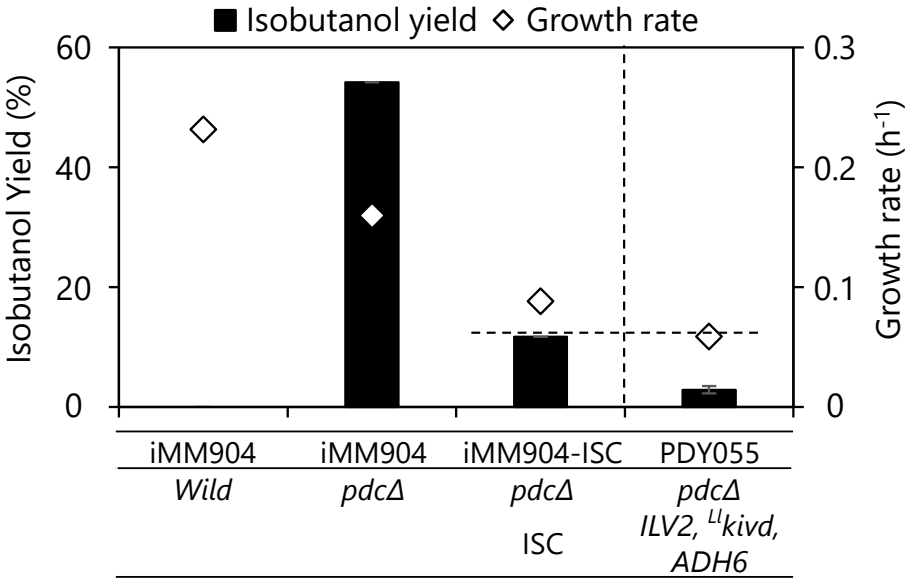

Figure 3-4-2 The isobutanol yield and the growth rate calculated using the model iMM904 and the model iMM904-ISC compared to the strain PDY055.

The black bars represent the production yield of isobutanol, and the open diamonds represent the growth rate. Error bars also showed the standard error of N = 3 independent experiments.

3-4-2 FBA metabolic simulation for various metabolite production

The simulation results of isobutanol production suggested that the metabolism in yeast strains could not produce sufficient ISC to function the introduced metabolic pathway including the ISC reactions. Therefore metabolites that required the large flux of ISC dependent reactions for their production should be avoided in the selection of target metabolites for bio-production in *S. cerevisiae*. In this section, metabolic pathways for the production of several metabolites were introduced to the reconstructed model iMM904-ISC in order to predict the target yields in *S. cerevisiae* under the constraints of ISC.

Figure 3-4-3 showed the yields of several target products such as 2,3-butanediol, 2-butanol, succinate, and lactate obtained from the metabolic simulations using the model iMM904-ISC. The 2,3-butanediol and the lactate are the targets that were not originally including the ISC reactions. On the other hand, 2-butanol production involves ISC dependent reaction in its biosynthesis pathway. Succinate is an intermediate metabolite of the TCA cycle involving the ISC dependent reaction of the succinate dehydrogenase. The 2,3-butanediol and the lactate were suggested that these target metabolite could be produced in yeast cells (58.9% and 170.2% mol mol-glucose^{-1} respectively). Actually, lactate production in *S. cerevisiae* has been highly achieved by the gene knockout related to the ethanol and glycerol production pathway [75]. On the other hand, the production yield of 2-butanol was predicted as 85.1% by the conventional FBA model. However, it was greatly decreased to 10.1% in the calculations using the reconstructed model like the case of isobutanol production. The 2-butanol is one of the bio-production targets which was tried to be produced using *S. cerevisiae* though its yield was still low. This simulation

result might suggest that the 2-butanol is a target which should not be produced using *S. cerevisiae*. The succinate is a target whose production in yeast has been tried for a long time. Regarding this target, the yield calculated by the conventional FBA model was only 2.8%, but it was increased to 71.2% by re-calculation with ISC constraints. This was probably due to the limitation of the solution space of FBA result because the reversible reaction such as the succinate dehydrogenase could not take an infinite value by the addition of the ISC constraint.

As described above, using the reconstructed model iMM904-ISC, it became possible to receive some suggestions about what kind of targets were suitable or not for the bio-production in yeast. In this chapter, 2,3-butanediol was selected as an example target, then the strains for 2,3-butanediol production were constructed in order to verify the simulation results by the reconstructed model.

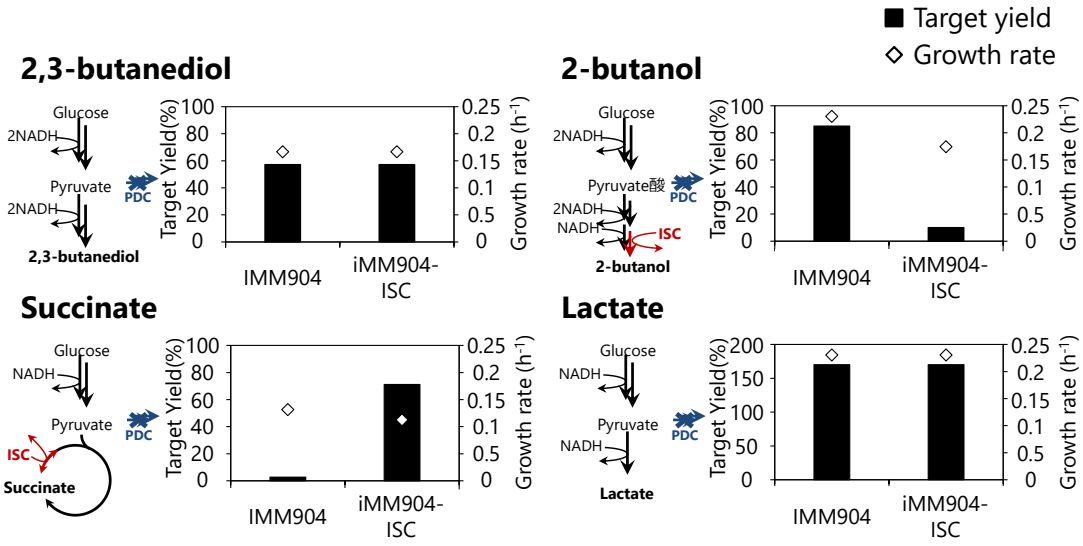

Figure 3-4-3 Yields of several target products such as 2,3-butanediol, 2-butanol, succinate, and lactate obtained from the metabolic simulations using the model iMM904 and model iMM904-ISC.

The black bars represent the production yield of 2,3-butanediol (23BD), and the open diamonds represent the growth rate.

3-4-3 Validation of metabolic model with 2,3-butanediol production

Construction of 2,3-butanediol production strain

The 2,3-butanediol is C4 alcohol harboring two hydroxyl groups, which can be used as a solvent and the raw material of synthetic rubber. The 2,3-butanediol is biologically synthesized from two molecules of pyruvate by four step reactions catalyzed by acetolactate synthase (ALS) and acetolactate decarboxylase (ALDC) and butanediol dehydrogenase (BDH).

In this thesis, the SCM043 strain for the 2,3-butanediol production was constructed based on *S. cerevisiae* BY4742 strain which was introduced the plasmid pATP426-alsLpOp-aldcLlOp-BDH1 which overexpresses the codon-optimized ALS and ALDC genes derived from *Lactobacillus plantarum* and *Lactococcus lactis* (als^{Lp}Op, $aldc^{Ll}Op$) and the BDH genes derived from *S. cerevisiae* (*BDH1*) (Figure 3-4-5). The strain SCM043 and the control strain SCM001 which was introduced the empty vector pGK426 were cultured under microaerobic conditions with 20 g/L glucose SD medium in test tubes. As a result, the 2,3-butanediol titers were increased 8.3±1.0 mg/L to 23.5±12.8 mg/L by the introduction of the expression plasmid, it was confirmed that the introduced 2,3-butanediol biosynthesis pathway was functioning.

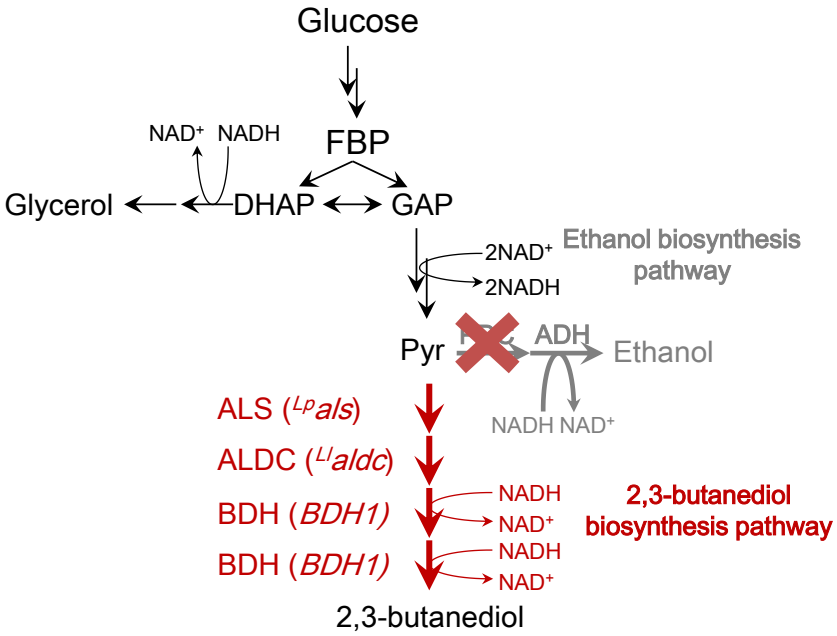

Figure 3-4-5 2,3-butanediol biosynthesis pathway

One molecule of 2,3-butanediol produced from two molecules of pyruvate by four metabolic reactions with three enzymes.

Comparison of the 2, 3-butanediol production yield of the strain to FBA result

The metabolic simulation based on FBA calculated the 58.9% of 2,3-butanediol production yield by the knockout of the pyruvate decarboxylase (PDC) genes that were responsible for ethanol production. The SCM070 strain was constructed based on the ethanol non-producing strain SD145-2 obtained in chapter 2 by the introduction of the plasmid pATP426-alsLpOp-aldcLlOp-BDH1. After the 96 hours of fermentation, 58.0±2.3% of the 2,3-butanediol yield was achieved (Figure 3-4-6). This yield was the almost the same yield calculated by metabolic simulation (58.9%). The redox cofactors required for the 2,3-butanediol production are two molecules of NADH. This must be one of the reasons why the 2,3-butanediol yield increased so easily because there were no other engineering was required to improve the redox balances of cofactors for the production. Furthermore, 2,3-butanediol biosynthesis was not required the ISC in its

pathway, these points might contribute to the great improvement of the 2,3-butanediol yield with deletion of PDC related genes. The specific growth rate of SCM070 strain was 0.059±0.029 h^{-1}. This value is three times smaller than the simulation result (0.167 h^{-1}), thus it took a very long time for the fermentation test of the SCM070 strain (96 hours). This was because the glucose uptake rate of SD145-2 strain became very small due to the mutations acquired in the adaptive laboratory evolution and original *MTH1-ΔT* mutations. However, a small glucose uptake rate is a great disadvantage for bioprocess from the viewpoint of productivity because it takes much more time to acquire a sufficient amount of cells for fermentation and lowers productivity. This is the weak point of SD145-2 strain constructed in chapter 2.

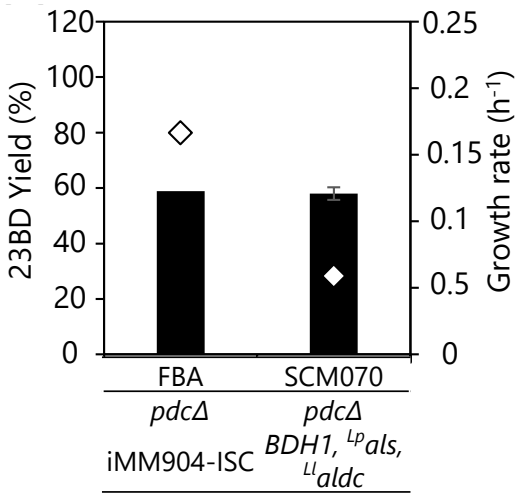

Figure 3-4-6 Comparison of 2,3-butanediol yield in the growth phase to simulation result.

The black bars represent the production yield of 2,3-butanediol (23BD), and the open diamonds represent the growth rate. Error bars also showed the standard error of N = 3 independent experiments.

2, 3-butanediol production in non-growth phase

In this section, the 2,3-butanediol yield of the SCM070 strain was investigated under the anaerobic and high cell density conditions. When yeast is inoculated at high density in this way, they do not grow and the most of glucose in the medium will be used for the alcohol production. In such non-growth coupled fermentation, the substrate used for the synthesis of cells was reduced, the target metabolite production can be increased in general. Although FBA is usually used to calculate the metabolic state of the mid-log growth phase, it is also possible to estimate the maximum production yield of the target product of non-growth phase from the stoichiometric matrix. When calculating the production yield of 2,3-butanediol under the no-growth condition, the maximum yield was 107.0% mol mol-glucose^{-1}. This value was greatly improved compared to the result of the mid-log growth phase (58.9% mol mol-glucose^{-1}), indicating that the no-growth condition was superior in fermentation process aiming for the mass production of target metabolites.

The anaerobic high-density fermentation was performed in the 100 g/L glucose SD medium. The initial OD value was set to 20 (Figure 3-4-7). The OD values represented by the open circles in the figure 3-4-7 were not significantly changed around at 20 after the inoculation, the growth was successfully stopped. After144 hours from the start of fermentation, 36.4±5.0 g/L of glucose remained in the culture broth. This might be the result of the low glucose uptake capacity due to the mutation in glucose sensors in SD145-2 strain. On the other hand, looking at the product, succinate was slightly produced (0.7±0.03 g/L) at 120 hours. Most of the products were the 2,3-butanediol and glycerol. The concentrations at 120 hours were 22.2±2.3 g/L and 20.7±1.5 g/L, respectively. The

yield of 2,3-butanediol was 70.5 ±2.5% mol mol-glucose^{-1}, which was improved to 1.2 times compared to the yield of growth phase culture (Figure 3-4-8). This value was 37% lower than the maximum yield of the FBA result (107.0% mol mol-glucose^{-1}). This gap probably due to the glycerol by-production. The glycerol yield was 64.3±1.8% mol mol-glucose^{-1}. Considering that two molecules of glycerol or one molecule of the 2,3-butanediol are produced from one molecule of glucose, the yield of the 2,3-butanediol was lowered by nearly 32% by the by-production of glycerol. Therefore, elimination of the glycerol production pathway was suggested to breed the strain with ideal metabolic distributions which were close to the FBA result.

In this section, the 2,3-butanediol production strains were constructed. 2,3-butanediol was predicted to be produced in *S. cerevisiae* by the metabolic simulation using the reconstructed FBA model iMM904-ISC taking into account the constraints of ISC reactions. The constructed strains were achieved high production yield close to the simulation results in the growth phase. Furthermore, strain with ideal metabolic distributions for the 2,3-butanediol production in non-growth phase was suggested by the knockout of glycerol biosynthesis related genes. This result indicated that the selections of producible targets in *S. cerevisiae* were really important in the metabolic engineering of yeast strains. The metabolic model iMM904-ISC developed in this thesis was considered to be beneficial for those target selections.

As shown in the results of the high-density culture, in the bioprocess, the fermentation without the cell growth is often superior to the fermentation in the growth phase for the target production. *S. cerevisiae* is robust for the stress of fermentation process compared to bacterial cells and suitable for multiple times of fermentation with no growth. However, the yeast strain which was constructed in chapter 2 resulted in the

decrease of glucose uptake rate due to the mutation of glucose sensors. This resulted in the remaining of a large amount of glucose in the culture medium and taking much time for fermentation. These problems would lower the productivity of the bioprocess and increase the costs of fermentation. Therefore, it should be solved to construct the more efficient fermentation process for the bio-production in *S. cerevisiae*.

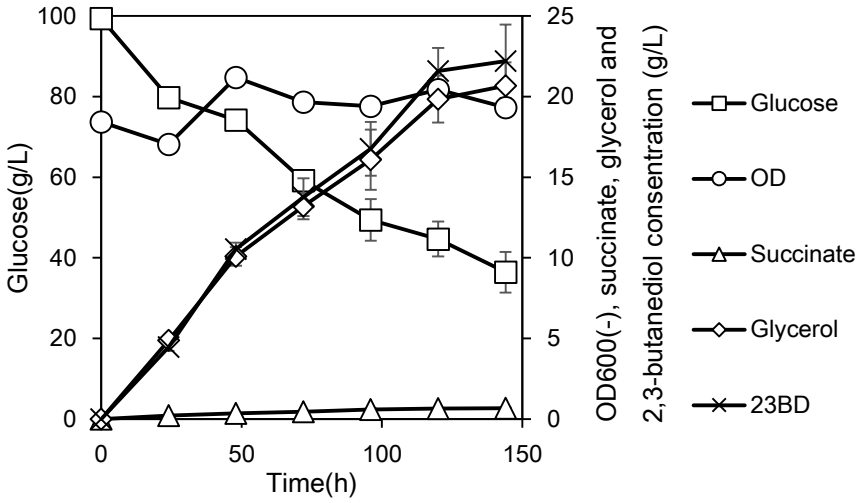

Figure 3-4-7 High-density culture for 2,3-butanediol production

The open circle, square, triangle, diamond and asterisk represents OD_{600} and glucose, succinate, glycerol, 2,3-butanediol concentration in the culture broth. Error bars also showed the standard error of N = 3 independent experiments.

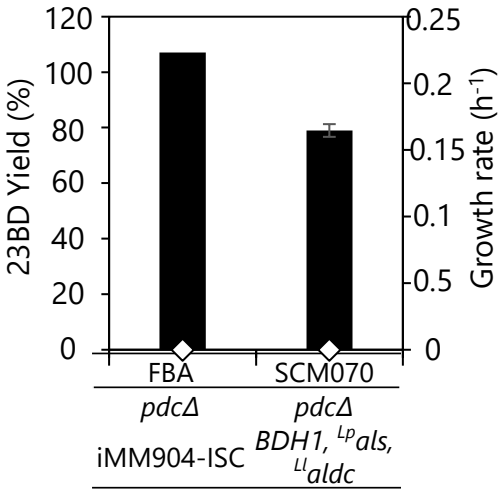

Figure 3-4-8 Comparison of 2,3-butanediol yield in non-growth phase to simulation result.

The black bars represent the production yield of 2,3-butanediol (23BD), and the open diamonds represent the growth rate. Error bars also showed the standard error of N = 3 independent experiments.

3-4-4 Regulation of ethanol fermentation for further improvement of productivity

Regulation of ethanol fermentation

For the efficient fermentation in yeast, an ideal process is acquiring the cells as soon as possible and then inoculating to main culture medium with high density for non-growth phase fermentation (Figure 3-4-9). The ethanol non-producing yeast strain SD145-2 constructed in chapter 2 was successfully reduced the ethanol production by the triple gene knockout of PDC. However, there were problems that it requires a lot of time for acquiring the cells to conduct the fermentation due to a low glucose uptake rate. Therefore, in order to solve the problems in SD145-2 strain, a new approach was proposed aiming to reduce the ethanol fermentation activity without the gene deletions of PDC.

In recent years, CRISPER-Cas9 (clustered regularly interspaced short palindromic repeats/ CRISPR associated proteins) which can cleave DNA double-stranded has been studied to be applied for the gene deletion and inserting the mutations. Inactive dead Cas9 (dCas9) is a mutant protein of CRISPER-Cas9 which can bind to the genomic sequence and suppressing the expression of the target gene instead of the ability to cleave the double-stranded DNA. In this section, the dCas9 expression system was constructed for the repression of ethanol fermentation (Figure 3-4-10). In *S. cerevisiae*, three pyruvate decarboxylase genes (*PDC1, PDC5,* and PDC6) were responsible for the ethanol fermentation, therefore the yeast strain lacking *PDC5* and *PDC6* of the YPH499 strain (pdc56Δ) was constructed. In this strain, the ethanol production relies on only *PDC1* expression, then an expression system that expresses dCas9 targeting *PDC1* was constructed aiming to inhibit the ethanol fermentation. The final goal of this system was to construct the strain which can rapidly grow in a growth phase with the ethanol

production and then repress the ethanol production in non-growth phase to improve target yield.

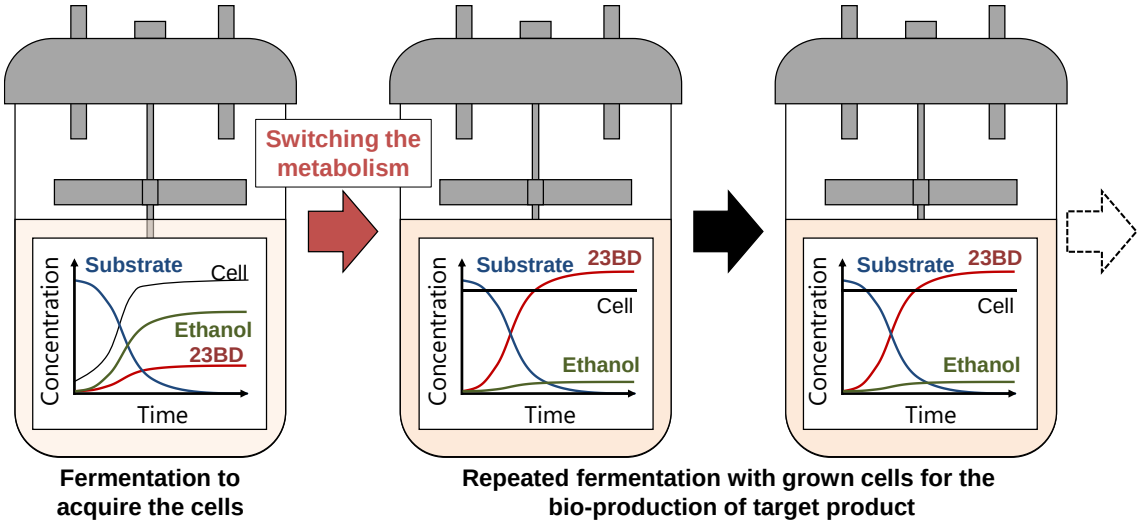

Figure 3-4-9 Ideal process to increase the target productivity switching the metabolism in yeast.

Acquiring the cells as soon as possible and then inoculating to main culture medium with high density for non-growth phase fermentation. In non-growth fermentation, substrates used for produce cell components are saved. If the ethanol fermentation repressed in non-growth fermentation phase, much more improvement of target productivity could be acquired

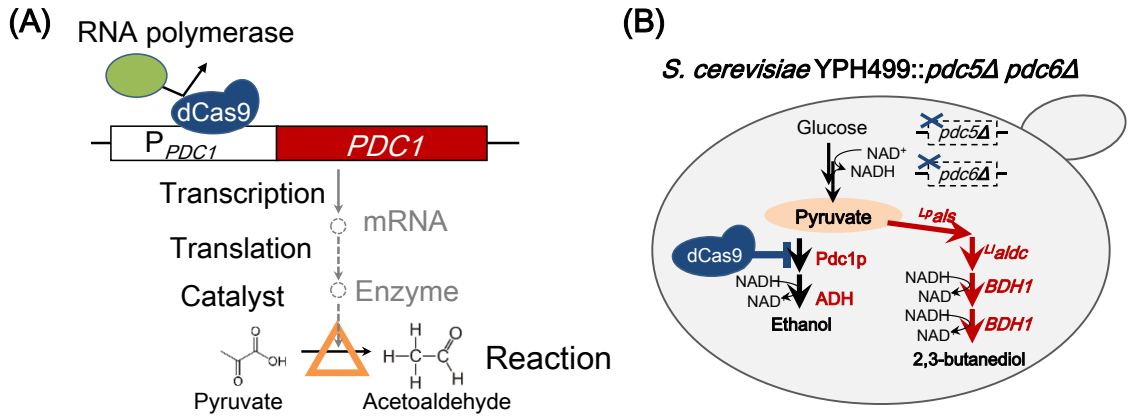

Figure 3-4-10 dCas9 expression system for the repression of ethanol fermentation

(A) Pyruvate decarboxylase (PDC) reaction which is the first reaction of ethanol biosynthesis from pyruvate was catalyzed by enzymatic protein Pdc1p. Binding of the dCas9 to the promoter region of *PDC1* inhibits the transcription of *PDC1* by RNA polymerase. Without the messenger RNA (mRNA) of *PDC1*, Pdc1p cannot be translated. Therefore enzymatic reaction of PDC was stopped due to the absence of Pd1p. (B) The ethanol production lacking *PDC5* and *PDC6* in *S. cerevisiae* completely relied on the Pdc1p. Therefore, repression of *PDC1* expression might decrease the ethanol biosynthesis and increase the 2,3-butanediol production without the triple gene knockout of PDC genes.

Construction of dCas9 expression system for PDC1 promoter control

In this system, arbitrary control of dCas9 expression is required for the repression of the *PDC1* expression in non-growth phase. It is also necessary to find the binding site of dCas9 which can effectively inhibit *PDC1* expression. In *S. cerevisiae*, *ARO9* promoter (pARO9) and *CUP1* promoter (pCUP1) were known that respond to the addition of tryptophan or Cu^{2+} to the medium turning on the gene expression respectively. These promoters were used for the expression of dCas9 in this study. Then, the binding sites of the dCas9 on the *PDC1* promoter (pPDC1) were examined for the effective repression of *PDC1* (Figure 3-4-11). Three plasmids were constructed for this experiment.

The plasmid pYK040 is expressing *mRuby2* coding red fluorescence protein under the control of pPDC1. The plasmid pYK044 is expressing dCas9 under the control of pARO9. The plasmid pYK045-PX (X = 0, 1, 2, 3, 5, 6, 7, 8 and 9) constantly express the nine kinds of gRNAs that lead the dCas9 to the proper binding sites of pPDC1. These plasmids were introduced to the *S. cerevisiae* BY4742 strain to acquire the transformants (SCM083 to 092 strain, P1 to P9 strain). Among these plasmids, the plasmid pYK045-P0 was a control plasmid which didn't include the target sequence of dCas9 for pPDC1. The constructed strains were cultured in a 96-well plate with a Synergy HTX multiplate reader for 50 hours with an initial OD_{600}=0.1. The fluorescence intensity of RFP was measured every an hour (Figure 3-4-12 (A) (B)). The tryptophan was added to all culture medium (final concentration was 100 μg/L) to induce the expression of dCas9. Figure 3-4-12 (A) and (B) showed the time course and final values of RFP fluorescence intensity of each strain. Each fluorescence intensities were corrected by subtracting the average value of the three control samples of medium without the cells as a background. The fluorescence intensities decreased in the strains P1 to P3 and P9 compared to the control strain (P0) which introduced no gRNA expression, but they showed a relatively high value. On the other hand, the intensities of P5 to P8 strain decreased to 1/3. Especially in the P8 strain, the fluorescence intensity of RFP was reduced to 20.1% comparing to that of control.

It was found that the too close binding sites to the initial codon (P1 to P3) and too far site (P9) were not effective to repress the gene expression under pPDC1 by dCas9. However, the regions that were 100 to 300 base pair from the initial codon of *PDC1* were the effective binding site of dCas9 for suppressing the gene expression under pPDC1.They might be included the binding site of the proteins such as RNA polymerase.

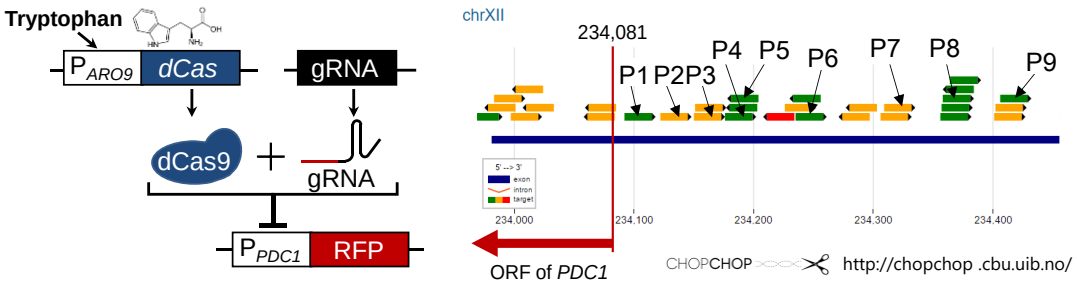

Figure 3-4-11 (A) Outline of the experiment. (B) The binding site of gRNA designed to suppress PDC1 expression by dCas9.

(A) Addition of tryptophan induces the dCas9 expression. Then complex of dCas9 and gRNA binds to the promoter region of *PDC1* where the specific site decided by the gRNA sequence. (B) A Web tool CHOPCHOP (http://chopchop.cbu.uib.no/) was used for the predicting of the binding site. Each site represented by P1 to P9 corresponded to the plasmids name such as pYK045-P1 in strain SCM083 (P1 strain).

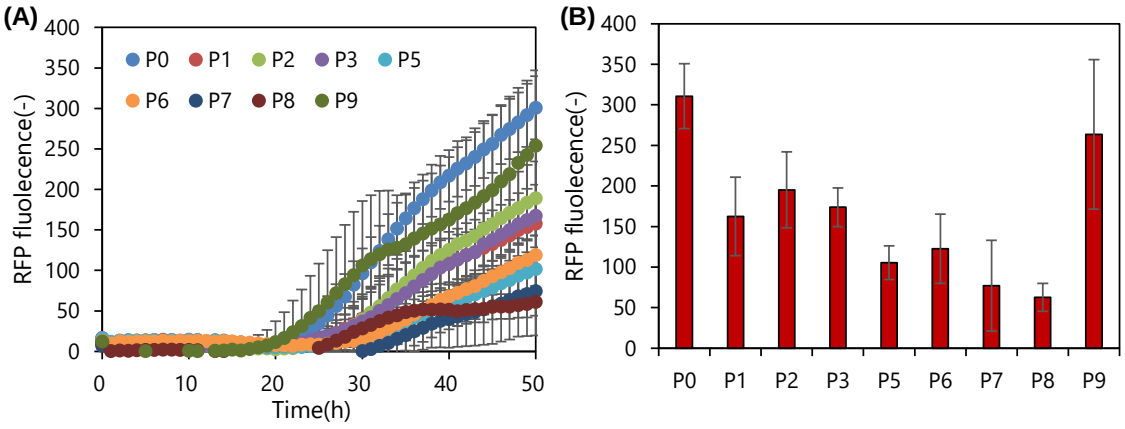

Figure 3-4-12 (A) Curves of the RFP fluorescence intensity and (B) the RFP fluorescence intensity at 50 hours.

P0 means the strain which was introduced plasmid pYK045-P0 (control plasmid without the target sequence of dCas9 for pPDC1). P1 to P9 mean the strains that were introduced plasmid including the target sequence of dCas9 for pPDC1 shown in figure 3-4-11 (B). Error bars also showed the standard error of N = 3 independent experiments.

Repression of ethanol production in 2, 3-butanediol production strain

To engineer the yeast ethanol fermentation depending on the only *PDC1* expression, the pdc56Δ strain was constructed lacking the two of three pyruvate decarboxylase (PDC) genes of *PDC5* and *PDC6*. The empty plasmid pGK424 and the plasmid pATP426-ALSLpOp-ALDCLlOp-BDH1 were introduced to the pdc56Δ strain for the 2, 3-butanediol production. Then, the plasmid pYK052-PX or pYK057-PX (X = 0, 5, 6, 7, 8) harboring the expression cassettes for four types of gRNA (P5-P8) and dCas9 under the control of pARO9 or pCUP1 were introduced to construct the engineered strain (SCM107-116). The SCM107 to 111 strains and the SCM112 to 116 strains were the tryptophan-inducible strain and the Cu^{2+}-inducible strains respectively. Transformants were cultured in 2 mL of 20 g/L glucose SD medium in 48 deep-well plate. In this fermentation, in order to promote the dCas9 expression from the early stage of cell growth, culture medium used in both of pre-culture and main culture were contained 100 μg/L tryptophan or 20 mM $CuSO_4$.

Figures 3-4-13 (A) and (B) showed the OD values, the ethanol and 2,3-butanediol concentrations of the SCM107 to 111 strains and the SCM112 to 116 strains at 48 hours after the start of fermentation, respectively. The tryptophan-inducible strains were shown in figure 3-4-13 (A). The strain whose dCas9 binding to the P6 position produced 91.7±16.1 mg/L of 2, 3-butanediol. It was significantly increased that of the control strain (P0, 29.4±50.9 mg/L). In addition, the 2,3-butanediol concentration in the strain with P8 gRNA, which was the most effective in the previous RFP fluorescence experiment, was reached at 118.0±8.8 mg/L. This was the highest concentration among these five strains and consistent to the previous RFP result. The Cu^{2+}-inducible strains

shown in figure 3-4-13 (B). The strain with P0 gRNA produced no 2, 3-butanediol, however, strains with P6 and P8 gRNA produced 122.3±20.1 mg/L and 197.4±14.7 mg/L of 2,3-butanediol similarly to the case of tryptophan type strains. With the P8 gRNA, the dCas9 expression under the control of pCUP1 was resulted in higher 2,3-butanediol titer compared to that of pARO9. However, the concentration of ethanol production was hardly changed in these cultures. Although the dCas9 was working to some extent increasing in the 2,3-butanediol production, it is considered that the suppression of *PDC1* expression was not sufficient.

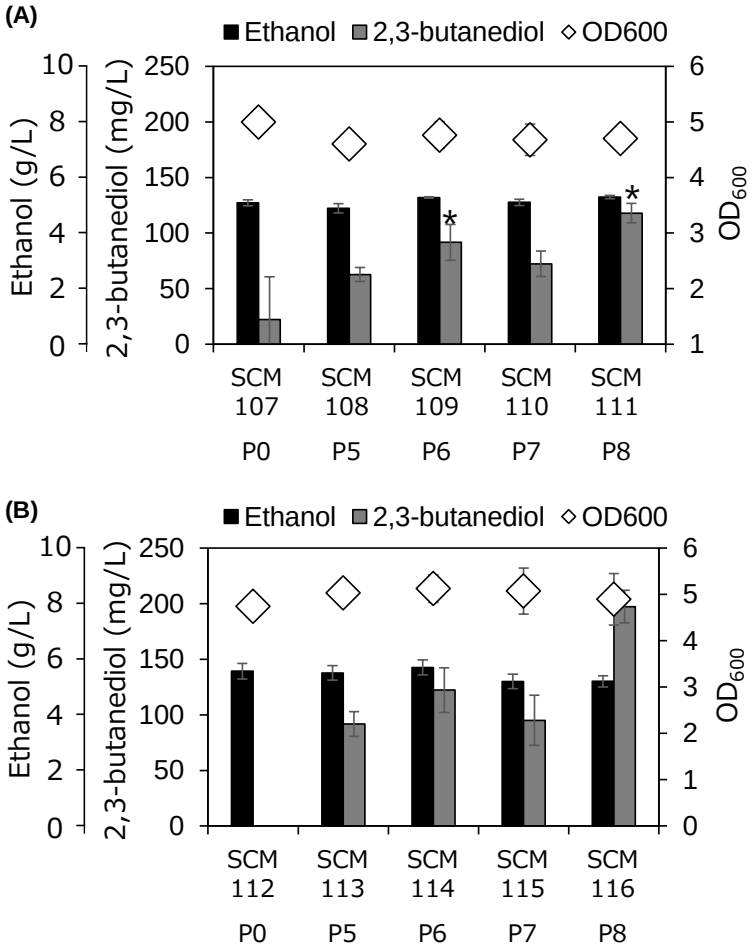

Figure 3-4-13 OD_{600}, ethanol and 2,3-butanediol concentration of (A) SCM107 to 111 strains and (B) SCM112 to 116 strains after the start of fermentation.

Error bars represent the standard deviation of the culture results of N=3 independent colonies, and * in (A) indicates that there was a significant difference ($P < 0.05$) in the T-test with control (P0).

Repeated batch culture in test tubes

The ethanol production was hardly decreased after the expression of dCas9. This result might be due to the residual of PDC protein (Pdc1p) keeping the ethanol bioproduction in the yeast cells because Pdc1p has a long half-life (11.5 hours) for degradation. If this assumption is correct, it is considered that the extension of the fermentation time leads to the degradation of Pdc1p and decrease of ethanol production. Therefore, in order to investigate the effect of the extension of fermentation time to the ethanol and the 2,3-butanediol fermentation ability, the repeated batch culture was conducted by inoculating the cells into a fresh medium several times.

The SCM112 strain and the SCM 116 strain that were introduced pYK057-P0 and pYK057-P8 were cultured in 20 g/l glucose SD medium containing 20 mM of Cu^{2+}. In this culture, whole cultured cells were harvested at 48 hours and re-inoculated into a fresh medium repeatedly, and the ethanol and the 2,3-butanediol concentrations were investigated every 48 hours (Figure 3-4-14). The OD values of both strains were continued to rise by inoculating the cells every 48 hours. In the control strain which did not express the gRNA for pPDC1, 2,3-butanediol production was not observed at all, whereas the SCM116 strain showed 695±7 mg/L of 2,3-butanediol production at the final round of culture. The ethanol concentrations were observed in both strains but differences appeared in the first round. Finally, SCM116 strain produced 6.28 ± 0.03 g/L of the ethanol which was about 1 g/L lower than that of control strain (7.20±0.09 g/L). These results suggested that the dCas9 expression certainly inhibited ethanol production. The 2,3-butanediol production was improved instead of the ethanol, and the influence of dCas9 expression was increased with time. However, ethanol production was not

drastically decreased probably due to the fact that Pdc1p was newly produced with the cell growth.

Figure 3-4-15 showed the comparison of the 2,3-butanediol yields and the growth rates between the FBA simulation and the SCM116 strain. The growth rate of the SCM116 strain in growth phase shown in figure3-4-15 (A) was slightly lower than that of FBA result, though it was a sufficiently large value of 0.2 h^{-1} compared to the triple gene knockout strain of PDC (SD145-2). However, in the non-growth phase shown in figure 3-4-15 (B) (data from the final sub-culture in figure 3-4-14), the 2,3-butanediol yield was only 7.0±0.02 mol mol-glucose^{-1} while the ethanol yield was 122.0±0.4% mol mol-glucose^{-1}. The strain constructed in this section was the first step of a new approach for the repression of ethanol production in *S. cerevisiae* without the gene deletion. However, the performance of the system was still far from the complete and further improvement was required in the future.

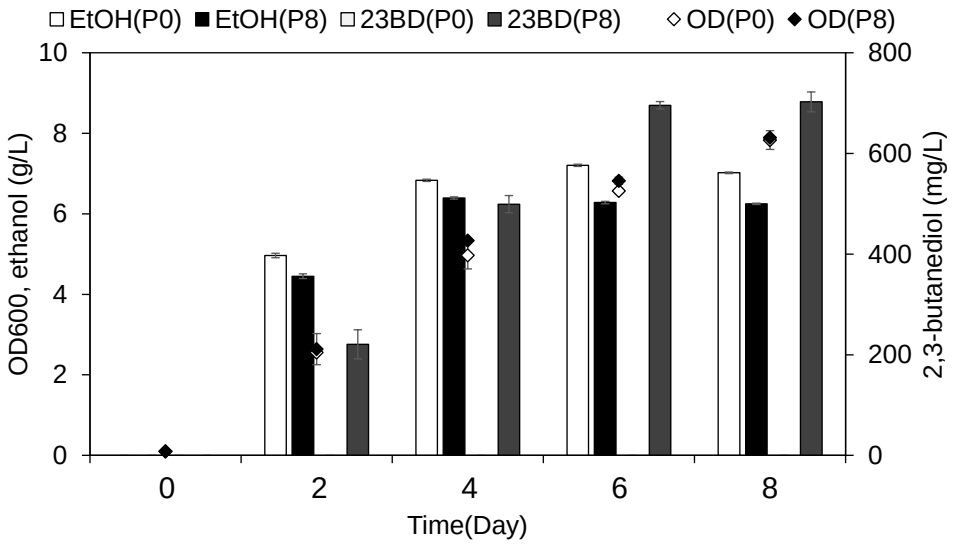

Figure 3-4-14 OD600, ethanol and 2, 3-butanediol concentration in repeated sub-culture.

Error bars also showed the standard error of N = 3 independent experiments.

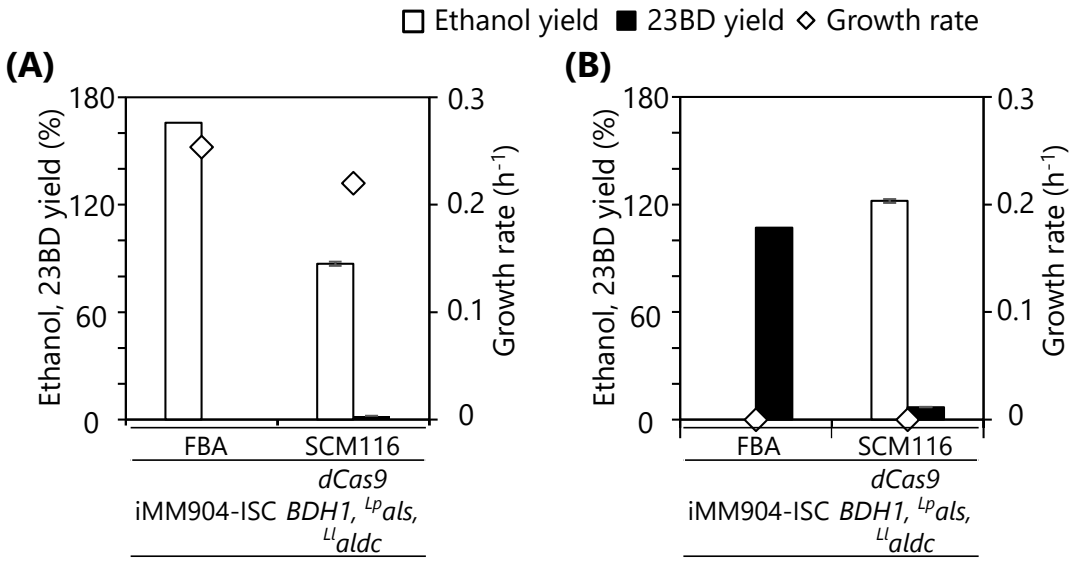

Figure 3-4-15 Growth rate and ethanol and 2, 3-butanediol yield at (A) the growth phase and (B) the non-growth phase.

The data of the growth phase was from first sub-culture and that of the non-growth phase was from the final sub-culture. Error bars also showed the standard error of N = 3 independent experiments.

3-5 Conclusion

In this chapter, based on the result of chapter 2, metabolic reactions requiring the ISC were considered that it was difficult to overexpress in *S. cerevisiae* cells. These reactions were considered as the rate-limiting steps in *S. cerevisiae* cells to create the discrepancy between the simulation result based on FBA and the experimental result of bred strains. Therefore metabolic model added the constraint of ISC reactions was newly constructed (model iMM904-ISC). Using the reconstructed model iMM904-ISC, the yield of isobutanol production was greatly reduced due to the ISC reactions, suggesting that the isobutanol is not suitable target metabolite to produce in *S. cerevisiae*. Then the target metabolites for the mass-production in yeast were investigated using a reconstructed model. It was suggested that the metabolites such as 2,3-butanediol were suitable for bio-production in yeast. The 2,3-butanediol production strain which was constructed based on the ethanol non-producing strain shown in chapter 2 achieved the same level of 2,3-butanediol yield compared to the FBA result in the growth phase. In addition, in order to utilize the carbons used for the cell synthesis to produce the target metabolite, non-growth coupled fermentation was carried out and compared to the FBA results. Although the production yield of the constructed strain was not reached to the maximum yield in the simulation, it was suggested that the possibility to improve the yield to a maximum value by the repression of the glycerol biosynthesis pathway. However, the knockout strain of pyruvate decarboxylase (PDC) genes constructed in chapter 2 required much time for fermentation due to the low glucose uptake rate. This property would decrease the capacity of bioprocesses and increase the costs, thus this problem should be solved. In this chapter, instead of the deletion of PDC genes, a new expressing system of dCas9 was constructed to repress the expression of the *PDC1* gene.

This system is aiming to allow the fast cell growth with ethanol production in the growth phase and to repress the ethanol by-production in non-growth phase for enhancement of target production. Although the constructed strain improved the 2,3-butanediol yield compared to the control strain without the system, the repression of ethanol production was the elementary level. Thus it is necessary to construct a more powerful inhibition system for ethanol biosynthesis.

The ability of yeast producing the ethanol rapidly from the glucose is called the Crabtree-effect. This ability was acquired from the long history of yeast evolution to survive the competition with other organisms, thus it is hard for modification. The Pdc1p is the main enzyme for the PDC reaction for ethanol biosynthesis. For the importance of ethanol production in yeast, a large amount of Pdc1 protein produced in the cell [78, 79]. The dCas9 expression system constructed in this chapter targeting the *PDC1* promoter. It was successfully reduced the expression level of the RFP gene to 20% under the control of the *PDC1* promoter. Therefore it is acceptable to consider that the transcription level of *PDC1* was also decreased to 20%. However, the ethanol production was still active with the repression system. The reason for this was insufficient repression of ethanol production probably due to the surviving Pdc1 proteins that were originally existed in the cell. In addition, since about 20% of gene expression was allowed, it is considered that the newly produced Pdc1 proteins were also remained in the yeast cells for a long time (half-life for degradation was nearly 12 hours). Therefore, for further improvement of this system, the approach to enhance the Pdc1 protein degradation is also required in order to decrease the amount of protein in the cell.

In this thesis, 2,3-butanediol production in yeast was only demonstrated which was estimated to be produced in the reconstructed FBA model. However, successful

examples have already been reported for the production of other targets such as lactate [75]. Succinate has also been produced in industrial scales by DSM (Netherlands) and ROQUETTE (France). These facts also indicated the effectiveness of this reconstructed model for the target selection. On the other hand, the isobutanol and the 2-butanol were suggested to be difficult to produce in yeast by this reconstructed model. There was no successful report for the production of these targets in yeast yet. The reasons for these results have mainly discussed the low activity of heterologous enzymes and imbalance of cofactor redox balance but ISC is rarely focused on. This might be due to the fact that FBA simulation tools have been developed mainly in bacteria whose cell structure is quite simple compared to eukaryotes. The bacterial cell is smaller rather than the eukaryotic cell such as yeast, so it can maintain the intracellular concentration of ISC without the mitochondria. The enzymes required ISC could be expressed anywhere in the bacterial cells, thus there is no need to consider about the ISC dependent reaction in the first place. The constraint of ISC dependent reactions presented in this thesis is a new noteworthy point which has tended to be overlooked for the metabolic engineering of yeast and other eukaryotes such as animal cells. Of course, this is one of the factors that can be considered for making a difference between simulations and experimental results. In the future, it is important to discover the other factors and improve both models and the breeding approach through the design, build, test and learn cycle. This research is considered to take the first step of the improvement.

Chapter 4: General conclusion and future perspective

4-1 General conclusion

The bioprocess by the metabolic reactions of microorganisms can be operated under mild conditions (at low temperature and pressure). Therefore, development of the bioprocess technology is desired to produce the useful substance from renewable resources and to reduce the environmental burden. In metabolic engineering, the well-known microorganisms such as *E. coli* and *S. cerevisiae* are often selected as the bio-production host because its genomes were already sequenced and easily accessing the data required for rational engineering. However, because of the network of genes and metabolic reactions are extremely enormous and complicated, it is very difficult to predict which genes could be the target of strain breeding.

In recent years, a metabolic simulation technique based on flux balance analysis account (FBA) has been developed. FBA calculates the metabolic flux distribution from the stoichiometric matrix of metabolic reactions by linear programming, under the conditions of maximizing the growth and the steady state of metabolism. Using FBA simulation, it becomes possible to calculate the influence of the local genetic engineering on the whole metabolism with a low calculation cost. FBA is a simplified metabolic model ignoring the factors such as the feedback regulation and kinetics of reactions, so the engineered strains often failed to present the result of FBA. For that reason, in metabolic engineering based on FBA requires the both of the design and breeding approaches to explore the problems by comparing the FBA simulation results and experimental data for

further improvement in the manner of the design-build-test-learn cycle.

FBA has been developed mainly targeting the simulation for bacterial species. Some examples have been reported that the metabolic engineering strategies using the metabolic simulation with great success improving the target productivity of *E. coli* which often used in the laboratory experiments. However, in *S. cerevisiae* which is used in industrial fermentation such as bio-ethanol production, the result of metabolic simulation by FBA and the yield of actually constructed strains are often different. This current situation is unfavorable because it decreases the reliability of metabolic engineering based on FBA in *S. cerevisiae*. Therefore in this thesis, to improve the computer-aided yeast breeding approach, strains were constructed based on FBA simulation result according to the design-build-test-learn cycle to verify whether the current model prediction capacities or the strain breeding approaches are insufficient for the specific bio-production targets. Then, a yeast FBA model was reconstructed including the constraint of the factor which was considered from the comparison, to propose the method for searching the suitable target metabolite for the bio-production in *S. cerevisiae*. The results of this thesis were summarized in figure 4-1-1.

In chapter 2, focusing on the isobutanol production, FBA simulations were conducted to elucidate the availability and limitation of metabolic engineering based on flux balance analysis in *S. cerevisiae*. In strain breeding, additional engineering was also conducted to complement the factors lack in FBA, for example, enhancing the expression of enzymes, releasing the feedback regulations and optimizing the metabolism by adaptive laboratory evolution.

For the improvement of the isobutanol production, addition of metabolic

pathways to support the regeneration of the cofactor NADPH were suggested, that are necessary for the biosynthetic reaction of isobutanol. Deletion of the competitive pathway (ethanol biosynthesis pathway) was also calculated to improve the isobutanol yield (Table 2-4-1 in chapter 2). Therefore, the yeast strains were constructed by the introduction of the phosphoenolpyruvate carboxylase (PPC) and the Entner-Doudoroff (ED) pathway that were suggested to improve the NADPH regeneration in *S. cerevisiae* by FBA simulation. The introduction of PPC improved isobutanol production yield 1.4 times (0.78% to 1.13% mol mol-glucose^{-1}, figure 2-4-4 in chapter 2). This was the first report that the expression of the *ppc* gene derived from *syn*6803 was beneficial for yeast isobutanol production. It was also suggested that the introduction of PPC improves the productivities of target metabolites requiring the NADPH for their biosynthesis.

On the other hand, the introduction of the ED pathway resulted in no change of production yield (figure 2-4-8 in chapter 2). The introduced ED pathway was confirmed that it was hardly functioning in yeast by the additional ^{13}C isotopic tracer experiment (table 2-4-3 in chapter 2).

Ethanol non-producing strain YSM021 with multiple knockouts of pyruvate decarboxylase (PDC) genes was constructed. The growth of this strain was significantly decreased, therefore, adaptive laboratory experiment (ALE) was conducted to optimize the yeast metabolism and improve the growth ability. The strain SD145-2 was acquired which growth was significantly improved (figure 2-4-15 in chapter 2). Isobutanol biosynthetic pathway was introduced to SD145-2 strain to obtain the transformants. However, this strain hardly produced isobutanol. In isobutanol production pathway, *ILV2* cording the enzyme for the first step of valine biosynthesis was repressed by the feedback regulation with Ilv6p. Therefore, the knockout strain of *ILV6* was constructed. This strain

produced 2.9% of isobutanol which was a comparable value to the highest isobutanol production yield in test tube scale culture (figure 2-4-18 in chapter 2). However, it was very low yield compared to the simulation result (54%) although the metabolic engineering approaches to complement the weaknesses of FBA were conducted. It suggested that the activity of the introduced isobutanol biosynthesis pathway was low in the first place. Considering about the isobutanol biosynthesis pathway and the ED pathway, these pathways with low activities in yeast include the iron-sulfur cluster (ISC) dependent reactions in pathways. ISC was mainly supplied in mitochondrion in yeast. Thus, it was estimated that the reactions requiring ISC might be the bottle-neck in yeast metabolism and the factor of cleaving the simulation and the experimental results. The FBA model has been developed on a bacteria without cell organelles, it did not take into account the constraint of ISC reactions. However, the ISC biosynthesis system is very complicated and hardly engineered. Therefore, the ISC dependent reactions should be avoided to use in yeast metabolic engineering and taken into account in FBA model.

In chapter 3, all reactions requiring the ISC in the FBA model iMM904 were rewritten with the terms of ISC generation and consumption. In this reconstructed model iMM904-ISC, the metabolic flux of the wild strain at the certain culture conditions is first calculated. The sum of total flux value of the ISC dependent reactions was set to the upper limit value for the next calculation with the engineered metabolic network for bioproduction. Using the reconstructed model, isobutanol production yield with the knockout of ethanol production was re-calculated. It resulted in a decrease of yield to 11.7%, which was lower than the original model and close to the yield of constructed strain (figure 3-4-2 in chapter 3). From the result, isobutanol was concluded as the

unsuitable metabolite for yeast production. Searching for the target metabolites that can be produced in yeast using the reconstructed model iMM904-ISC, several targets were found such as 2,3-butanediol (figure 3-4-3 in chapter 3).

The 2,3-butanediol biosynthesis related genes were introduced to the ethanol non-producing yeast SD145-2 strain constructed in chapter 2. The 2,3-butanediol yield was reached to 58.0% in the fermentation test in the growth phase, which was almost the same value of the simulation result (figure 3-4-6 in chapter 3)). However, the yield during the non-growth phase was 70.5%, suggesting that there was a room for further improvement compared to the simulated maximum yield of 107.0% (figure 3-4-8 in chapter 3).

The SD145-2 strain constructed in chapter 2 required much time for fermentation due to its poor growth and glucose uptake abilities. These characters would be the factors for lowering the productivity of the bioprocess and increasing the fermentation cost. To solve these problems in SD145-2 strain, a new system was tried to be constructed to inhibit the yeast ethanol fermentation only during the non-growth phase without gene deletion. In this system, the protein dCas9 targeting the *PDC1* promoter was expressed by the addition of the inducer for the inhibition of the mRNA transcription of the *PDC1* gene to repress the ethanol production. The constructed dCas9 expression system was validated using RFP that can be reduced to 20% of the expression levels of the gene under the *PDC1* promoter control (figure 3-4-12 in chapter 3). Then, inhibiting the *PDC1* expression of the 2,3-butanediol production strain with the dCas9 expression system, the production yield of 2,3-butanediol was resulted in only 7.0%, whereas 122% of ethanol was produced (figure 3-4-15 in chapter 3). The strain constructed in chapter 3 took the first step for a new method for the repression of ethanol production in *S. cerevisiae*

avoiding the decline of growth rate due to the *PDC1* deletion. However, the performance of the suppression system for ethanol production was still entry-level and further improvement would be necessary for the future bio-process.

In conclusion, this study first investigated the availability and limitation of metabolic engineering based on FBA through the simulation and strain breeding of yeast for isobutanol production. Then, a new yeast FBA model considering the ISC constraint and a new breeding approach for the repression of ethanol fermentation were proposed and verified through the 2,3-butanediol bio-production.

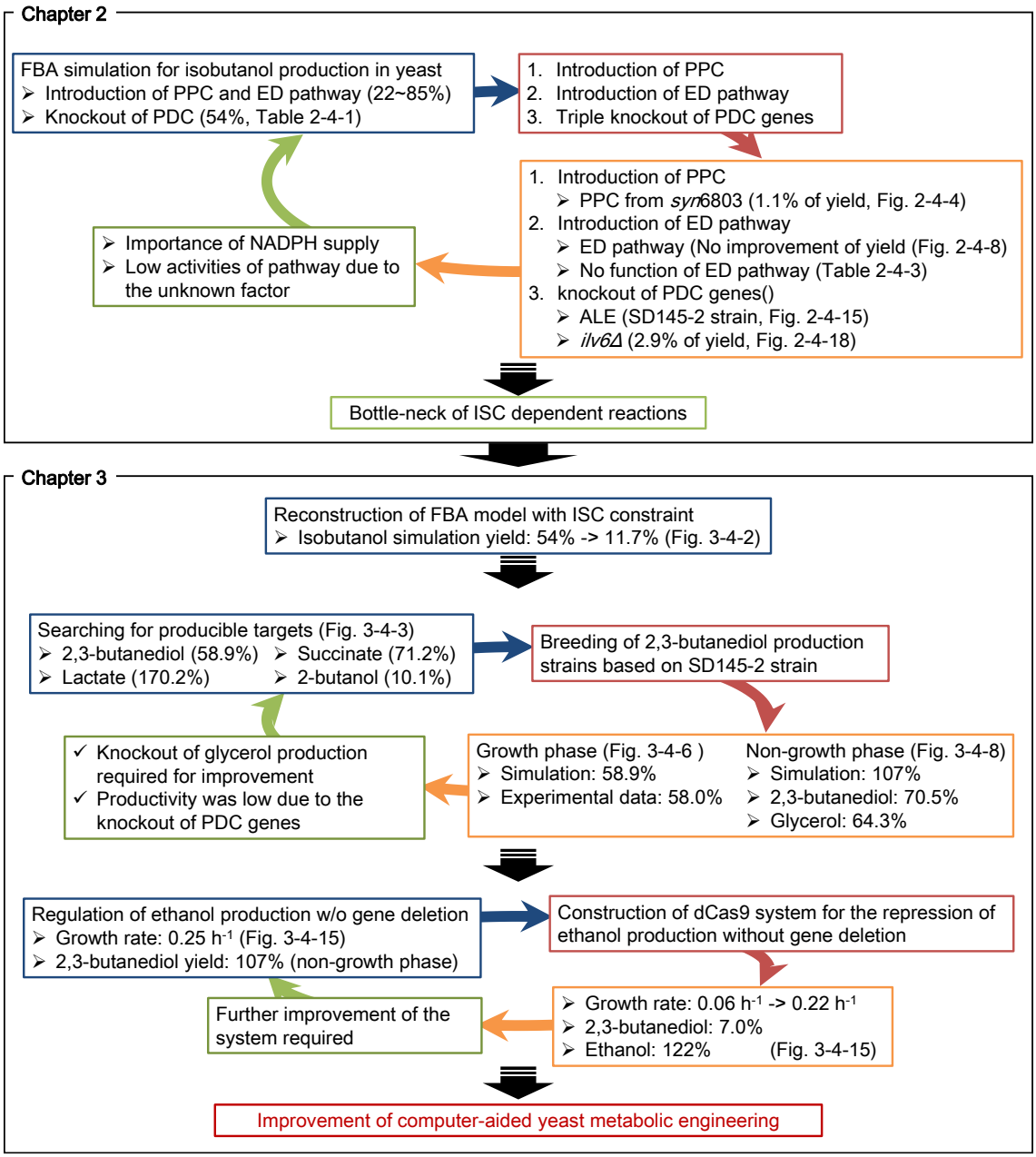

Figure 4-1-1 Summary of the thesis

4-2 Contribution of the present results for strain improvement

The present results in this doctor thesis demonstrated the availability and limitation of metabolic engineering of yeast based on current FBA simulation. Here, the contributions of the present results for strain improvement were discussed.

FBA is a simplified metabolic model ignoring some factors of reactions, so the engineering approaches for strain breeding often required the assist to complement the weak point of FBA to achieve the comparable experimental result to the simulation result. Also in this thesis, releasing the feedback repression which was not considered in FBA simulation for isobutanol production, constructed strain achieved the comparable yield to the world highest value in the test tube scale culture. However this experimental result was significantly lower than the simulation result, so it was suggested the overestimation of the FBA result or the incompletion of the strain breeding. From the viewpoint of breeding, constructed strains were optimized the metabolism by ALE to improve the growth without ethanol production, overexpressed the biosynthetic pathway genes, and even released the feedback regulation. It can be judged that all possible approaches have been tried to deal factors not taken into account in FBA simulation in some levels. Although in such situation, the low isobutanol yield must be due to the other factors that have never been considered inhibiting the isobutanol production. From the investigation of the reports and database, iron-sulfur cluster (ISC) dependence reactions were focused on in this thesis. Both enzymes of DHAD consisting the isobutanol biosynthesis pathway and EDD consisting the ED pathway are required the coordination of ISC to express their catalytic activities. Intracellular ISC is biosynthesized by the complex system in mitochondrion in the eukaryote. It is considered that these overexpressed ISC dependent

enzymes are limited their activity to some extent due to the lack of ISC. In the previous study on isobutanol production, Avalos *et al.* constructed the whole isobutanol biosynthetic pathway in mitochondrion achieving 1.54% of isobutanol yield. This improvement of isobutanol yield is considered due to the successful approach to localizing the biosynthetic pathway to ISC rich mitochondria. However, even in this approach, the production yield of isobutanol did not rise above a certain level. For one reason for this result, the pyruvate transport from cytosol to mitochondria may serve as a bottleneck but it is considered that the lack of ISC brings greater effect. For the cell, it must be a great burden to overproduce the ISC for improving isobutanol production by a complicated ISC generation system because such huge amount of ISC was never required in the regular life for yeast cells. Therefore, the report of Avalos *et al.* and the results of this thesis suggest that the ISC dependent reactions should not be excessively used for metabolic engineering in yeast.

The FBA model was reconstructed introducing the constraint to ISC dependent reactions in this thesis. Under this constraint, the summed flux of ISC dependent reactions is not allowed to exceed the value which was used for normal cell growth and maintenance. Using the reconstructed model, the flux value of the ISC dependent reaction which is normally used in yeast was found about 1/5 of the flux value required for the production of isobutanol. This result suggested the difficulty of isobutanol production in yeast. Then, searching for another producible target in yeast using the reconstructed FBA model, some chemicals such as 2,3-butanediol was found. The 2,3-butanediol production strain was constructed and achieved the comparable yield close to the FBA result, suggesting that the targets not required the ISC reaction for its biosynthesis could be mass-produced in yeast. Regarding other targets, the reconstructed model also suggested the

difficulty to produce the 2-butanol and the capacity to produce the lactate and the succinate. The 2-butanol has not yet been produced in yeast, in contrast, production of the lactate and the succinate have already been achieved in laboratory scale and industrial scale. From these examples, this model is considered to be capable of predicting the producible target in yeast and suggesting the metabolic engineering approaches that avoiding the use of ISC dependent reactions.

Regardless of the case of *S. cerevisiae*, this ISC constraint can be applied to other FBA metabolic models of eukaryotic microorganisms and animal cells such as mouse and humans because their cell structures are similar to yeast cells. On the other hand, ISC constraint might not be required in the bacterial metabolic model such as *E. coli*. Okahashi *et al.* reported the *E.coli* Entner-Doudoroff (ED) pathway could handle the 99% of glucose which was up-taken from outer the cell [80]. ED pathway is one of the natural ISC dependent reaction in *E.coli* cells, therefore, in bacterial cells, the amount of ISC should be plenty to function these ISC dependent reactions. However, the specific growth rate of the reported strain was decreased almost half (0.30 h^{-1} from 0.58 h^{-1}). Perhaps under the high growth rate conditions, resources for ISC formation are used for other reactions, and then, ISC dependent reactions might be restricted. If such case is experimentally observed, the introduction of ISC constraint into the bacterial metabolic model will be considered. Furthermore, ISC constraint should be taken into account to not only the static FBA model but also dynamic kinetic models when they deal the target pathways involving the ISC dependent reactions. Of course, the FBA model is not a complete model describing the intracellular reactions of cells. Therefore, there is a possibility to emerge a new problem other than ISC in the future through the comparison between the simulation result and experimental results of bred strains. This is what the

metabolic engineering premises to deal with the living cells with many unknown factors, therefore it should be welcomed as a trigger leading to new discoveries and improvements of hidden biological principles.

The most noteworthy achievement of this thesis is the improvement of the yeast FBA simulation model by introducing constraints of the ISC dependent reactions to predict the suitable target products in yeast. This result is supported by the comparison of the FBA simulation results using the reconstructed model and the experimental results of strain breeding based on the design-build-test-learn cycle of metabolic engineering. Of course, the FBA itself including some weaknesses to simplify the calculation, the proposed simulation model is not a perfect simulation model describing the entire metabolic behavior completely. However, it greatly contributed to the improvement of the rationality and reliability of the computer-aided yeast breeding approach. In eukaryotic cells, there are multiple types of ISC dependent reactions, therefore, constraints of the ISC dependent reactions in the reconstructed model can also be applied to other microbial species that classified as eukaryotes and animal cells derived from humans and mice. The results of this thesis contributed to making a step forward in the computer-aided metabolic engineering of eukaryotes.

4-3 Future perspective for strain improvement

Although the similar metabolic engineering approaches have been taken for both *E. coli* and *S. cerevisiae* for a long time, strategies considering the differences between those metabolisms would become more important in the future. Engineering of *E. coli* for the production of target metabolite is relatively easy compared to other microorganisms. However, the industrial operation of *E. coli* involves some demerits. *E. coli* requires pH control during the fermentation and must be grown for every time due to its low tolerance to fermentation stress. There is also the risk of the annihilation of the cells in the whole tank due to the phage contamination. These demerits are not serious in laboratory scale fermentation, however, in industrial scale fermentation, tons of medium, a substrate for cells and neutralization reagent are required. On the other hand, *S. cerevisiae* has the advantages such as the high tolerance to fermentation stress, high pH tolerance, and robustness withstanding to the repeated fermentation and safety impression. There is also no risk of phage contamination but the yeast has the disadvantage of difficulty to breed rather than *E. coli*. Therefore, either strain is never absolutely superior. These facts indicate that the important things for the improvement of bio-process are not only considering the ease of strain construction and the advantages of industrial fermentation. Understanding the advantages and disadvantages of organisms is necessary to select the proper hosts according to the circumstances. This thesis focused on *S. cerevisiae*. The metabolites such as 2,3-butanediol that were demonstrated to be produced by the reconstructed model were highly produced by the bred strains. This target product should be produced by yeast, however, metabolites like the isobutanol which was difficult to produce in yeast should be produced using *E. coli* as a host organism. Form this point of

view, the results of the thesis rewrote the features of microbial hosts shown in table 1-5-1 in chapter 1 to table 4-3-1 for the discussion of the production hosts. In table 4-3-1 was newly added the column for ISC dependent reactions to consider the metabolic engineering approaches in yeast. The consideration of this factor must be important in order to avoid unfeasible metabolic engineering strategies due to the ISC deficient for efficient yeast engineering. The proposed reconstructed FBA model in this thesis can contribute to select the proper microbial host strain against the target metabolite.

Repression of ethanol biosynthesis cannot be avoided in metabolic engineering research of *S. cerevisiae*. In chapter 2, the ethanol non-producing strain SD145-2 was constructed whose triple genes of the pyruvate decarboxylase were knocked out. Although the ethanol production was successfully reduced, this strain resulted in the low glucose uptake and the growth rate in the same manner of previous studies. Therefore, in chapter 3, the dCas9 expression system targeting the *PDC1* expression was constructed for the repression of ethanol production without *PDC1* deletion. However, the inhibition ability of ethanol production was elementary level, suggesting that further improvement was required in the future. In order to develop this system, the *PDC1* protein should be degraded immediately during the non-growth phase to lower the intracellular amount of enzyme. In recent years, methods to control the rate of protein degradation by adding a ubiquitination tag and the rate of the messenger RNA translation by forming a unique three-dimensional structure of mRNA molecule called as a riboswitch have been developed. Therefore it is expected that more efficient suppression system would be constructed using these upcoming engineering tools.

Recently, there was another new movement in the construction of ethanol non-producing yeast. Up until now, construction of ethanol non-producing yeast was

depended on the mutation in *MTH1* (*MTH1-ΔT*) which is a part of glucose sensor decreasing glucose uptake rate and enabling the yeast to grow without ethanol production. In the report in 2018, apart from the introduction of *MTH1-ΔT* mutation, an approach which introducing a new bypass pathway to supply the acetyl-CoA in the yeast cytosol achieved the ethanol non-producing yeast strain with high growth ability [81]. In this report, application for the target metabolite production such as 2,3-butanediol was not tested. Therefore it was still unclear whether or not its metabolism would behave ideally for the bio-production. However, the introduction of the bypass pathway of acetyl-CoA supply and the discovery of the genes functioning in yeast cells are very useful findings. Combining this bypass pathway with the dCas9 expression system proposed in this study might be helpful to release the burden on the yeast when the ethanol production was suppressed, thus, further development can be achieved in the future.

Table 4-3-1 Rewritten features of *E. coli* and *S. cerevisiae* to discuss the proper bio-production host and the engineering approaches in yeast

Features	*E. coli*	*S. cerevisiae*
Knowledge	◎	◎
Growth ability	◎	◎
pH tolerance	~5	~3
Physical robustness of cell	○	◎
Repeated fermentation	◎	◎
Risk of phage contamination	High	No risk
Complexity of cell structure	Low	High
Ease of engineering	◎	○
ISC dependent reactions	**◎**	**×**

Appendix

Table A1 Plasmids used in this study

Plasmids	Description	Ref.
pGK422	Yeast one gene expression vector containing *PGK1* promoter, *2μ* origin, *ADE2* marker, no expression (control plasmid)	[82]
pGK423	Yeast one gene expression vector containing *PGK1* promoter, *2μ* origin, *HIS3* marker, no expression (control plasmid)	[82]
pGK424	Yeast one gene expression vector containing *PGK1* promoter, *2μ* origin, *TRP1* marker, no expression (control plasmid)	[82]
pGK425	Yeast one gene expression vector containing *PGK1* promoter, *2μ* origin, *LEU2* marker, no expression (control plasmid)	[82]
pGK426	Yeast one gene expression vector containing *PGK1* promoter, *2μ* origin, *URA3* marker, no expression (control plasmid)	[82]
pATP422	Yeast three gene expression vector containing *ADH1*, *TDH3,* and *PGK1* promoters, *2μ* origin, *ADE2* marker, no expression (control plasmid)	[83]
pATP423	Yeast three gene expression vector containing *ADH1*, *TDH3,* and *PGK1* promoters, *2μ* origin, *HIS3* marker, no expression (control plasmid)	[83]
pATP424	Yeast three gene expression vector containing *ADH1*, *TDH3,* and *PGK1* promoters, *2μ* origin, *TRP1* marker, no expression (control plasmid)	[83]
pATP425	Yeast three gene expression vector containing *ADH1*, *TDH3,* and *PGK1* promoters, *2μ* origin, *LEU2* marker, no expression (control plasmid)	[83]
pATP426	Yeast three gene expression vector containing *ADH1*, *TDH3,* and *PGK1* promoters, *2μ* origin, *URA3* marker, no expression (control plasmid)	[83]
pGK422-PPCec	pGK422, co-expression of *E. coli PPC ppc*	This study
pGK422-PPCcg	pGK422, co-expression of *C. glutamicum ppc*	This study
pGK422-PPCsy	pGK422, co-expression of *Syn*6803 *ppc*	This study

Table A1 Plasmids used in this study (Continued)

Plasmids	Description	Ref.
pATP426-kivd-ADH6-ILV2	pATP426, co-expression of *L. lactis kivd*, *S. cerevisiae ADH6* and *ILV2* genes controlled by *ADH1*, *TDH3* and *PGK1* promoters	[51]
pGK423-Eceda	pGK423, expression of *E.coli eda* gene	This study
pGK425-Ecedd	pGK425, expression of *E.coli edd* gene	This study
pGK423-ZmedaOp	pGK423, expression of *Z.mobilis eda* gene optimized for yeast	This study
pGK425-ZmeddOp	pGK425, expression of *Z.mobilis edd* gene optimized for yeast	This study
pATP426-mtkivdOp-mtADH7Op-ILV2	pATP426, co-expression of *L. lactis kivd* and *S. cerevisiae ADH7* attaching the mitochondrial transit sequence and optimized for yeast (*mtkivdOp* and *mtADH7Op*), and *ILV2* genes controlled by *ADH1*, *TDH3,* and *PGK1* promoters	[51]
pILV532cytL	pATP425, co-expression of *S. cerevisiae ILV5c*, *ILV3c*, and *ILV2c* genes (lacking the sequence of the mitochondrial transit signal) controlled by *ADH1*, *TDH3,* and *PGK1* promoters	[51]
pATP426-kivd-ADH6-ALSLpOp	pATP426, co-expression of *L. lactis kivd*, *S. cerevisiae ADH6* and *ALSLpOp* controlled by *ADH1*, *TDH3* and *PGK1* promoters	This study
pATP425- ILV5c -ZmDHAD-ALSLpOp	pATP425, co-expression of *S. cerevisiae ILV5c, Z. mobilis ilvD* and *ALSLpOp* controlled by *ADH1*, *TDH3,* and *PGK1* promoters	This study
pATP425-KpKARI-ILV3c -ALSLpOp	pATP425, co-expression of *K. pneumoniae ilvC, S. cerevisiae ILV3c* and *ALSLpOp* controlled by *ADH1*, *TDH3* and *PGK1* promoters	This study
pATP426-23BD	pATP426, co-expression of *L. lactis aldc, L. plantarum als* and *BDH1* genes codon optimized for yeast.	[84]
pYK040	ConLS-pPDC1-mRuby2-tTDH1-ConR1-LEU2-2micron-KanR-ColE1	This study
pYK044	ConL2- pARO9-dCas9-tTDH1 -ConRE-HIS3-2micron-KanR-ColE1	This study
pYK045-P0	ConL1-gRNAcassette_no_target -ConR2-URA3-2micron-KanR-ColE1	This study
pYK045-P1	ConL1-gRNAcassette_P1 -ConR2-URA3-2micron-KanR-ColE1	This study
pYK045-P2	ConL1-gRNAcassette_P2-ConR2-URA3-2micron-KanR-ColE1	This study
pYK045-P3	ConL1-gRNAcassette_P3 -ConR2-URA3-2micron-KanR-ColE1	This study
pYK045-P4	ConL1-gRNAcassette_P4 -ConR2-URA3-2micron-KanR-ColE1	This study
pYK045-P5	ConL1-gRNAcassette_P5 -ConR2-URA3-2micron-KanR-ColE1	This study
pYK045-P6	ConL1-gRNAcassette_P6 -ConR2-URA3-2micron-KanR-ColE1	This study
pYK045-P7	ConL1-gRNAcassette_P7 -ConR2-URA3-2micron-KanR-ColE1	This study

Table A1 Plasmids used in this study (Continued)

Plasmids	Description	Ref.
pYK045-P8	ConL1-gRNAcassette_P8 -ConR2-URA3-2micron-KanR-ColE1	This study
pYK045-P9	ConL1-gRNAcassette_P9 -ConR2-URA3-2micron-KanR-ColE1	This study

Plasmids of pYK series were constructed based on MoClo-YTK plasmids [85].

Table A2 Strains used in this study

Name	Genotype	Ref
YPH499	*MATa ura3-52 lys2-801 ade2-101 trp1-Δ63 his3-Δ200 leu2-Δ1*	Stratagene
YKP001	YPH499/pATP426-kivd-ADH6-ILV2	This study
YKP002	YPH499/pGK423/pATP426-kivd-ADH6-ILV2	This study
YKP003	YPH499/pGK423/pATP426-kivd-ADH6-ILV2/pGK422	This study
YKP004	YPH499/pGK423/pATP426-kivd-ADH6-ILV2/pGK422-PPCec	This study
YKP005	YPH499/pGK423/pATP426-kivd-ADH6-ILV2/pGK422-PPCcg	This study
YKP006	YPH499/pGK423/pATP426-kivd-ADH6-ILV2/pGK422-PPCsy	This study
YED007	YPH499/pGK426/pGK425/pGK423	This study
YED008	YPH499/pGK426/pGK425-Ecedd/pGK423-Eceda	This study
YED009	YPH499/pATP426-kivd-ADH6-ILV2/pGK425/pGK423	This study
YED010	YPH499/pATP426-kivd-ADH6-ILV2/pGK425-Ecedd/pGK423-Eceda	This study
BY4742	*MATα his3 leu2 lys2 ura3*	Thermo Scientific
gnd1Δ	BY4742::*gnd1Δ*	Thermo Scientific
YKM013	BY4742/pGK423/pGK425/pGK426	This study
YKM015	BY4742/pGK423-Eceda/pGK425-Ecedd/pGK426	This study
YKM025	gnd1◿/pGK423/pGK425/pGK426	This study
YKM027	gnd1◿/pGK423-Eceda/pGK425-Ecedd/pGK426	This study
YKM040	gnd1◿/pGK423-ZmedaOp/pGK425-ZmeddOp/pGK426	This study
YSM021	YPH499::*pdc1Δ pdc5Δ pdc6Δ MTH1-ΔT*	This study
SD75-1	Laboratory evolved strain of YSM021	This study
SD75-2	Laboratory evolved strain of YSM021	This study
SD75-3	Laboratory evolved strain of YSM021	This study
SD145-1	Laboratory evolved strain of YSM021	This study
SD145-2	Laboratory evolved strain of YSM021	This study
SD145-3	Laboratory evolved strain of YSM021	This study
YSM046	SD145-2:: *ilv6Δ*	This study
PDY001	SD145-2/pATP426-kivd-ADH6-ILV2	This study
PDY005	SD145-2/pATP426-mtkivd-mtADH7-ILV2	This study
PDY007	SD145-2/pATP426-kivd-ADH6-ILV2/pILV532cytL	This study
PDY055	YSM046/pATP426-kivd-ADH6-ILV2/pILV532cytL	This study

Table A2 Strains used in this study (continued)

Name	Genotype	Ref
PDY074	YSM046/pATP426-kivd-ADH6-ALSLpOp/pATP425-ILV5cyt-ZmDHAD-ALSLpOp	This study
PDY079	YSM046/pATP426-kivd-ADH6-ALSLpOp/pATP425-KpKARI-ILV3cyt-ALSLpOp	This study
PDY082	YSM046/pATP426-kivd-ADH6-ALSLpOp/pILV532cytL	This study
SCM070	SD145-2:: pATP426-ALSLpOp-ALDCLlOp-BDH1	This study
SCM083	BY4742:: pYK040/ pYK044/ pYK045-P0	This study
SCM084	BY4742:: pYK040/ pYK044/ pYK045-P1	This study
SCM085	BY4742:: pYK040/ pYK044/ pYK045-P2	This study
SCM086	BY4742:: pYK040/ pYK044/ pYK045-P3	This study
SCM087	BY4742:: pYK040/ pYK044/ pYK045-P4	This study
SCM088	BY4742:: pYK040/ pYK044/ pYK045-P5	This study
SCM089	BY4742:: pYK040/ pYK044/ pYK045-P6	This study
SCM090	BY4742:: pYK040/ pYK044/ pYK045-P7	This study
SCM091	BY4742:: pYK040/ pYK044/ pYK045-P8	This study
SCM092	BY4742:: pYK040/ pYK044/ pYK045-P9	This study
pdc56Δ	YPH499:: *pdc5Δ pdc6Δ*	This study
SCM107	pdc56Δ:: pGK424/ pATP426-23BD/ pYK052-P0	This study
SCM108	pdc56Δ:: pGK424/ pATP426-23BD/pYK052-P5	This study
SCM109	pdc56Δ:: pGK424/ pATP426-23BD/pYK052-P6	This study
SCM110	pdc56Δ:: pGK424/ pATP426-23BD/pYK052-P7	This study
SCM111	pdc56Δ:: pGK424/ pATP426-23BD/pYK052-P8	This study
SCM112	pdc56Δ:: pGK424/ pATP426-23BD/pYK057-P0	This study
SCM113	pdc56Δ:: pGK424/ pATP426-23BD/pYK057P5	This study
SCM114	pdc56Δ:: pGK424/ pATP426-23BD/pYK057-P6	This study
SCM115	pdc56Δ:: pGK424/ pATP426-23BD/pYK057-P7	This study
SCM116	pdc56Δ:: pGK424/ pATP426-23BD/pYK057-P8	This study

Table A3 Introduced reactions to model iMM904 for the target production.

Name	Equation	LB*	UB*
PPCr	adp_c + co2_c + pep_c -> atp_c + oaa_c	0	999999
EDP	6pgc_c + isc_c -> g3p_c + pyr_c + h2o_c	0	999999
ACLSc	h_c + 2 pyr_c -> alac__S_c + co2_c	0	999999
KARA1ic	alac__S_c + h_c + nadph_c -> 23dhmb_c + nadp_c	0	999999
DHAD1c	23dhmb_c + isc_c -> 3mob_c + h2o_c	0	999999
ACLSc	h_c + 2 pyr_c -> alac__S_c + co2_c	0	999999
ACLO	alac__S_c + A -> diacetyl + AH2 + co2_c	0	999999
ALDC	alac__S_c -> actn__R_c + co2_c	0	999999
ActnOD	diacetyl + nadh_c + h_c -> actn__R_c + nad_c	0	999999
actnt	actn__R_c -> actn__R_e	0	999999
actnex	actn__R_e ->	0	999999
diol dehydratase	btd_RR_c + isc_c -> 2_butanone	0	999999
sec_alc dehydrogenase	2_butanone + nadh_c + h_c -> 2_butanol_c + nad_c	0	999999
2_butanol_t	2_butanol_c -> 2_butanol_e	0	999999
EX_2_butanol_e	2_butanol_e ->	0	999999

Table A4 Deleted reactions from model iMM904 for the reconstruction

Name	Equation	LB*	UB*
DHAD1m	23dhmb_m -> 3mob_m + h2o_m	0	999999
DHAD2m	23dhmp_m -> 3mop_m + h2o_m	0	999999
DHQTi	3dhq_c -> 3dhsk_c + h2o_c	0	999999
ECOAH11p	h2o_x + hxc2coa_x <=> 3hxccoa_x	-999999	999999
ECOAH4p	3hdcoa_x <=> dc2coa_x + h2o_x	-999999	999999
ECOAH5p	3hddcoa_x <=> dd2coa_x + h2o_x	-999999	999999
ECOAH6p	3htdcoa_x <=> h2o_x + td2coa_x	-999999	999999
ECOAH7p	3hhdcoa_x <=> h2o_x + hdd2coa_x	-999999	999999
ECOAH8p	3hodcoa_x <=> h2o_x + od2coa_x	-999999	999999
G5SADs	glu5sa_c <=> 1pyr5c_c + h_c + h2o_c	-999999	999999
G5SADrm	glu5sa_m <=> 1pyr5c_m + h_m + h2o_m	-999999	999999
IGPDH	eig3p_c -> h2o_c + imacp_c	0	999999
IPPMIa	3c2hmp_c <=> 2ippm_c + h2o_c	-999999	999999
MCITDm	hcit_m <=> h2o_m + b124tc_m	-999999	999999
MDRPD	5mdru1p_c -> h2o_c + dkmpp_c	0	999999
PPNDH	h_c + pphn_c -> co2_c + h2o_c + phpyr_c	0	999999
SUCD1m	fad_m + succ_m <=> fadh2_m + fum_m	-999999	999999
NADH2_u6cm	h_c + nadh_c + q6_m -> nad_c + q6h2_m	0	999999
NADH2_u6m	h_m + nadh_m + q6_m -> nad_m + q6h2_m	0	999999
2HMHMBQMTm	amet_m + 2hpmhmbq_m -> ahcys_m + h_m + q6_m	0	999999
CYOR_u6m	1.5 h_m + 2 ficytc_m + q6h2_m -> 1.5 h_c + 2 focytc_m + q6_m	0	999999
DHORD4i	dhor__S_c + q6_m -> orot_c + q6h2_m	0	999999
DXHPScm	h2o_c + spmd_c + q6_m -> 4abutn_c + 13dampp_c + q6h2_m	0	999999
FDNG	for_c + h_c + q6_m -> co2_c + q6h2_m	0	999999
NADH2_u6cm	h_c + nadh_c + q6_m -> nad_c + q6h2_m	0	999999
NADH2_u6m	h_m + nadh_m + q6_m -> nad_m + q6h2_m	0	999999
SUCD2_u6m	succ_m + q6_m <=> fum_m + q6h2_m	-999999	999999
SUCD3_u6m	fadh2_m + q6_m <=> fad_m + q6h2_m	-999999	999999

*LB: Lower bound, *UB: Upper bound

Table A5 Added reactions to model iMM904 for the reconstruction

Name	Equation	LB*	UB*
DHAD1m_isc	23dhmb_m + isc_m -> 3mob_m + h2o_m	0	999999
DHAD2m_isc	23dhmp_m + isc_m -> 3mop_m + h2o_m	0	999999
DHQTi_isc	3dhq_c + isc_m -> 3dhsk_c + h2o_c	0	999999
ECOAH11p_isc	h2o_x + hxc2coa_x + isc_x_1a -> 3hxccoa_x + isc_x_1b	0	999999
ECOAH11pr_isc	3hxccoa_x + isc_x_1b -> h2o_x + hxc2coa_x + isc_x_1a	0	999999
ECOAH4p_isc	3hdcoa_x + isc_x_2a -> dc2coa_x + h2o_x + isc_x_2b	0	999999
ECOAH4pr_isc	dc2coa_x + h2o_x + isc_x_2b -> 3hdcoa_x + isc_x_2a	0	999999
ECOAH5p_isc	3hddcoa_x + isc_x_3a -> dd2coa_x + h2o_x + isc_x_3b	0	999999
ECOAH5pr_isc	dd2coa_x + h2o_x + isc_x_3b -> 3hddcoa_x + isc_x_3a	0	999999
ECOAH6p_isc	3htdcoa_x + isc_x_4a -> h2o_x + td2coa_x + isc_x_4b	0	999999
ECOAH6pr_isc	h2o_x + td2coa_x + isc_x_4b -> 3htdcoa_x + isc_x_4a	0	999999
ECOAH7p_isc	3hhdcoa_x + isc_x_5a -> h2o_x + hdd2coa_x + isc_x_5b	0	999999
ECOAH7pr_isc	h2o_x + hdd2coa_x + isc_x_5b -> 3hddcoa_x + isc_x_5a	0	999999
ECOAH8p_isc	3hodcoa_x + isc_x_6a -> h2o_x + od2coa_x + isc_x_6b	0	999999
ECOAH8pr_isc	h2o_x + od2coa_x + isc_x_6b -> 3hodcoa_x + isc_x_6a	0	999999
G5SADs_isc	glu5sa_c + isc_c_7a -> 1pyr5c_c + h_c + h2o_c + isc_c_7b	0	999999
G5SADsrr_isc	1pyr5c_c + h_c + h2o_c + isc_c_7b -> glu5sa_c + isc_c_7a	0	999999
G5SADrm_isc	glu5sa_m + isc_m_8a -> 1pyr5c_m + h_m + h2o_m + isc_m_8b	0	999999
G5SADrmr_isc	1pyr5c_m + h_m + h2o_m + isc_m_8b -> glu5sa_m + isc_m_8a	0	999999
IGPDH_isc	eig3p_c + isc_c -> h2o_c + imacp_c	0	999999
IPPMIa_isc	3c2hmp_c + isc_c_9a -> 2ippm_c + h2o_c + isc_c_9b	0	999999
IPPMIb_isc	2ippm_c + h2o_c + isc_c_9b -> 3c2hmp_c + isc_c_9a	0	999999
MCITDm_isc	hcit_m + isc_m_10a -> h2o_m + b124tc_m + isc_m_10b	0	999999
MCITDmr_isc	h2o_m + b124tc_m + isc_m_10b -> hcit_m + isc_m_10a	0	999999
MDRPD_isc	5mdru1p_c + isc_c -> h2o_c + dkmpp_c	0	999999
PPNDH_isc	h_c + pphn_c + isc_c -> co2_c + h2o_c + phpyr_c	0	999999
SUCD1m_isc	fad_m + succ_m + isc_m_11a -> fadh2_m + fum_m + isc_m_11b	0	999999
SUCD1mr_isc	fadh2_m + fum_m + isc_m_11b -> fad_m + succ_m + isc_m_11a	0	999999

Table A5 Added reactions to model iMM904 for the reconstruction (continued)

Name	Equation	LB*	UB*
NADH2_u6cm_isc	h_c + nadh_c + q6_m + isc_m -> nad_c + q6h2_m	0	999999
NADH2_u6m_isc	h_m + nadh_m + q6_m + isc_m -> nad_m + q6h2_m	0	999999
2HMHMBQMTm_isc	amet_m + 2hpmhmbq_m + isc_m -> ahcys_m + h_m + q6_m	0	999999
CYOR_u6m_isc	1.5 h_m + 2 ficytc_m + q6h2_m + isc_m -> 1.5 h_c + 2 focytc_m + q6_m	0	999999
DHORD4i_isc	dhor__S_c + q6_m + isc_m -> orot_c + q6h2_m	0	999999
DXHPScm_isc	h2o_c + spmd_c + q6_m + isc_m -> 4abutn_c + 13dampp_c + q6h2_m	0	999999
FDNG_isc	for_c + h_c + q6_m + isc_m -> co2_c + q6h2_m	0	999999
SUCD2_u6m_isc	succ_m + q6_m + isc_m_12a -> fum_m + q6h2_m + isc_m_12b	0	999999
SUCD2_u6mr_isc	fum_m + q6h2_m + isc_m_12b -> succ_m + q6_m + isc_m_12a	0	999999
SUCD3_u6m_isc	fadh2_m + q6_m + isc_m_13a -> fad_m + q6h2_m + isc_m_13b	0	999999
SUCD3_u6mr_isc	fad_m + q6h2_m + isc_m_13b -> fadh2_m + q6_m + isc_m_13a	0	999999
ISCinput	isc_x <=>	-999999	0
ISCsynth	isc_x <=> isc_m	0	(999999)
ISCtmc	isc_m <=> isc_c	0	999999
ISCtxm	isc_m <=> isc_x	0	999999
ISC_1	isc_x_1a <=> isc_x_1	-999999	999999
ISC_2	isc_x_1b <=> isc_x_1	-999999	999999
ISC_3	isc_x_2a <=> isc_x_2	-999999	999999
ISC_4	isc_x_2b <=> isc_x_2	-999999	999999
ISC_5	isc_x_3a <=> isc_x_3	-999999	999999
ISC_6	isc_x_3b <=> isc_x_3	-999999	999999
ISC_7	isc_x_4a <=> isc_x_4	-999999	999999
ISC_8	isc_x_4b <=> isc_x_4	-999999	999999
ISC_9	isc_x_5a <=> isc_x_5	-999999	999999

Table A5 Added reactions to model iMM904 for the reconstruction (continued)

Name	Equation	LB*	UB*
ISC_10	isc_x_5b <=> isc_x_5	-999999	999999
ISC_11	isc_x_6a <=> isc_x_6	-999999	999999
ISC_12	isc_x_6b <=> isc_x_6	-999999	999999
ISC_13	isc_c_7a <=> isc_c_7	-999999	999999
ISC_14	isc_c_7b <=> isc_c_7	-999999	999999
ISC_15	isc_m_8a <=> isc_m_8	-999999	999999
ISC_16	isc_m_8b <=> isc_m_8	-999999	999999
ISC_17	isc_c_9a <=> isc_c_9	-999999	999999
ISC_18	isc_c_9b <=> isc_c_9	-999999	999999
ISC_19	isc_m_10a <=> isc_m_10	-999999	999999
ISC_20	isc_m_10b <=> isc_m_10	-999999	999999
ISC_21	isc_m_11a <=> isc_m_11	-999999	999999
ISC_22	isc_m_11b <=> isc_m_11	-999999	999999
ISC_23	isc_m_12a <=> isc_m_12	-999999	999999
ISC_24	isc_m_12b <=> isc_m_12	-999999	999999
ISC_25	isc_m_13a <=> isc_m_13	-999999	999999
ISC_26	isc_m_13b <=> isc_m_13	-999999	999999
ISC_27	isc_x <=> isc_x_1	-999999	999999
ISC_28	isc_x <=> isc_x_2	-999999	999999
ISC_29	isc_x <=> isc_x_3	-999999	999999
ISC_30	isc_x <=> isc_x_4	-999999	999999
ISC_31	isc_x <=> isc_x_5	-999999	999999
ISC_32	isc_x <=> isc_x_6	-999999	999999
ISC_33	isc_c <=> isc_c_7	-999999	999999
ISC_34	isc_m <=> isc_m_8	-999999	999999
ISC_35	isc_c <=> isc_c_9	-999999	999999
ISC_36	isc_m <=> isc_m_10	-999999	999999
ISC_37	isc_m <=> isc_m_11	-999999	999999
ISC_38	isc_m <=> isc_m_12	-999999	999999
ISC_39	isc_m <=> isc_m_13	-999999	999999

*LB: Lower bound, *UB: Upper bound

Acknowledgments

This study was carried out in Metabolic Engineering Laboratory, Graduate School of Information Science and Technology, Osaka University. I am extremely thankful for my supervisor, Professor Dr. Hiroshi Shimizu for his guidance, passion and scientific lead. I really appreciate for his giving the opportunity for me to study about strain improvement in his laboratory.

I am also thankful to Professor Dr. Fumio Matsuda, Analytical Biotechnology Laboratory, Graduate School of Information Science and Technology, Osaka University for giving the constructive discussions, comments, advice, and encouragements. Professor Dr. Matsuda has also trained me to become a researcher for a long time in Metabolic Engineering Laboratory with his kind guidance on my study.

I am also thankful to each member of my thesis advisory committee: Professor Dr. Taro Maeda, Professor Dr. Hideo Matsuda, and Professor Dr. Naoki Wakamiya, Department of Bioinformatic Engineering, Graduate School of Information Science and Technology, Osaka University for all their constructive comments and advice on my study.

I would like to thank Assistant Professor Dr. Yoshihiro Toya, Metabolic Engineering Laboratory, Department of Bioinformatic Engineering, Graduate School of Information Science and Technology, Osaka University for his many constructive comments and suggestions, and Dr. Mas3akazu Toyoshima for his kind advice on my

study. And I am also especially thankful to all members in Metabolic Engineering Laboratory for every supports in my student life.

I am thankful for the staffs and students in the Humanware innovation program, Osaka University for their supports, helps, passions and kindness.

Finally, I would like to thank my family, familiars and my beloved for their support, love and continuous encouragements throughout many years.

Reference

1. Campbell G **Fermented foods - a world perspective** *Food Research International* 1994, **27:**253-257
2. Sykes R **Penicillin: from discovery to product.** *Bull World Health Organ.* 2001, **79:**778-9
3. A. K. Mohanty , M. Misra, L. T. Drzal **Sustainable Bio-Composites from Renewable Resources: Opportunities and Challenges in the Green Materials World** *Journal of Polymers and the Environment* 2002, **10:**19-26
4. J. Michael Cherry, Caroline Adler, Catherine Ball, Stephen A. Chervitz, Selina S. wight, Erich T. Hester, Yankai Jia, Gail Juvik, TaiYun Roe, Mark Schroeder, Shuai Weng, David Botstein: **SGD: *Saccharomyces* Genome Database** *Nucleic Acids Res* 1998, **26**:73–79.
5. Kanehisa M, Goto S: **KEGG: kyoto encyclopedia of genes and genomes**. *Nucleic Acids Res* 2000, **28**:56–59.
6. Keseler IM, Collado-Vides J, Gama-Castro S, Ingraham J, Paley S, Paulsen IT, Peralta-Gil M, Karp PD: **EcoCyc: a comprehensive database resource for *Escherichia coli*.** *Nucleic Acids Res* 2005, **33**:334–337.
7. Lederberg J. **Cell genetics and hereditary symbiosis.** *Physiol Rev.* 1952, 32:403-30.
8. Bailey JE: **Toward a science of metabolic engineering**. *Science* 1991, **252**:1668–1675.9
9. Stephanopoulos GN, Aristidou AA, Nielsen J: **Metabolic Engineering. Principles and methologies.** San Diego. USA: Academic Press; 1998. ISBN ISBN 0-12-666260-6.
10. Savinell J, Palsson B: **Network analysis of intermediary metabolism using linear optimization.I.Development of mathematical formalism**. *J Theor Biol* 1992, **154**:421–454.
11. Schuster S, Dandekar T, Fell DA: **Detection of elementary flux modes in biochemical networks : a promising tool for pathway analysis and metabolic engineering**. 1999, **17**:53–60.
12. Csete ME, Doyle JC **Reverse engineering of biological complexity** *Science* 2002, 295 pp. 1664-1669
13. Loew LM, Schaff JC **The virtual cell: a software environment for computational cell biology** *TRENDS Biotechnol*. 2001, 19 (10) 401-406
14. Morgan JA, Rhodes D **Mathematical modeling of plant metabolic pathways** *Metab. Eng.* 2002,4, 80-89

15. Olivier BG, Snoep JL **Web-based kinetic modelling using jws online** *Bioinformatics* 2004, 20, 2143-2144
16. Snoep JL **The silicon cell initiative: working towards a detailed kinetic description at the cellular level** *Curr. Opin. Biotechnol*. 2005, 16, 336-343
17. Steuer R **Computational approaches to the topology, stability and dynamics of metabolic networks.** *Phytochemistry*. 2007, 68(16-18)
18. Hanly TJ, Henson MA. **Dynamic model-based analysis of furfural and HMF detoxification by pure and mixed batch cultures of *S. cerevisiae* and *S. stipitis.*** *Biotechnol Bioeng*. 2014, 111(2):272-84
19. Tran LM, Rizk ML, Liao JC **Ensemble modeling of metabolic networks** *Biophys J*. 2008, Dec 15;95(12):5606-17
20. Orth J, Thiele I, Palsson B: **What is flux balance analysis?** *Nat Biotechnol* 2010, **28**:245–248.
21. Jeremy S. Edwards, Markus Covert, Bernhard Palsson **Metabolic modelling of microbes: the flux-balance approach** *Environmental Microbiology* 2002, **4:** 33–140
22. Jong Min Lee, Erwin P.Gianchandani and Jason A. Papin **Flux balance analysis in the era of metabolomics** *Briefings in Bioinformatics* 2006, **7:**140-150
23. Amit Varma, Bernhard O. Palsson **Metabolic Flux Balancing: Basic Concepts, Scientific and Practical Use** *Nature Biotechnology* 1994, 12: 994-998
24. Zupke, C., and Stephanopoulos, G. **Modeling of isotope distributions and intracellular fluxes in metabolic networks using atom mapping matrices**. *Biotechnol Prog* 1994, 10: 489–498.
25. Wiechert, W., and De Graaf, A.A. **In vivo stationary flux analysis by 13C labeling experiments.** *Adv Biochem Eng/Biotechnol* 1996, 54:489-498
26. Sauer, U., Hatzimanikatis, V., Bailey, J., Hochuli, M., Szyperski, T., and Wuthrich, K. **Metabolic fluxes in riboflavin-producing *Bacillis subtilis***. *Nature Biotechnol* 1997, 15: 448–452.
27. Klapa, M.I., Park, S.M., Sinskey, A.J., and Stephanopoulos, G. **Metabolite and isotopomer balancing in the analysis of metabolic cycles. I. Theory**. *Biotechnol Bioeng* 1999, 62: 375–391.
28. Feist AM, Henry CS, Reed JL, Krummenacker M, Joyce AR, Karp PD, Broadbelt LJ, Hatzimanikatis V, Palsson BØ: **A genome-scale metabolic reconstruction for Escherichia coli K-12 MG1655 that accounts for 1260 ORFs and thermodynamic information.** *Mol Syst Biol* 2007, 3:121.
29. Yoshikawa K, Kojima Y, Nakajima T, Furusawa C, Hirasawa T, Shimizu H: **Reconstruction and verification of a genome-scale metabolic model for *Synechocystis* sp. PCC6803**.

Appl Microbiol Biotechnol 2011, 92:347–358.

30. Shinfuku Y, Sorpitiporn N, Sono M, Furusawa C, Hirasawa T, Shimizu H: **Development and experimental verification of a genome-scale metabolic model for *Corynebacterium glutamicum*.** *Microb Cell Fact* 2009, 8:43.
31. Schellenberger J, Que R, Fleming RMT, Thiele I, Orth JD, Feist AM, Zielinski DC, Bordbar A, Lewis NE, Rahmanian S, Kang J, Hyduke DR, Palsson BØ: **Quantitative prediction of cellular metabolism with constraint-based models: the COBRA Toolbox v2.0**. *Nat Protoc* 2011, **6**:1290–1307.
32. Alper H, Jin Y-S, Moxley JF, Stephanopoulos GN: **Identifying gene targets for the metabolic engineering of lycopene biosynthesis in *Escherichia coli***. *Metab Eng* 2005, 7:155–164.
33. Park JH, Lee KH, Kim TY, Lee SY: **Metabolic engineering of *Escherichia coli* for the production of L-valine based on transcriptome analysis and in silico gene knockout simulation**. *Proc Natl Acad Sci U S A* 2007, 104:7797–802.
34. Lee SJ, Lee D-Y, Kim TY, Kim BH, Lee J, Lee SY: **Metabolic engineering of *Escherichia coli* for enhanced production of succinic acid, based on genome comparison and in silico gene knockout simulation.** *Appl Environ Microbiol* 2005, 71:7880–7887.
35. Hjersted JL, Henson MA. **Steady-state and dynamic flux balance analysis of ethanol production by *Saccharomyces cerevisiae.*** *IET Syst Biol* 2009;**3:**167–79.
36. Brochado AR, Matos C, Moller BL, Hansen J, Mortensen UH, Patil KR. **Improved vanillin production in baker's yeast through in silico design**. *Microb Cell Fact* 2010 **9:**84
37. Tokuyama K, Ohno S, Yoshikawa K, Hirasawa T, Tanaka S, Furusawa C, Shimizu H **Increased 3-hydroxypropionic acid production from glycerol, by modification of central metabolism in *Escherichia coli*.** *Microb Cell Fact.* 2014, 13:64
38. Tokuyama K, Toya Y, Horinouchi T, Furusawa C, Matsuda F, Shimizu H. **Application of adaptive laboratory evolution to overcome a flux limitation in an *Escherichia coli* production strain.** *Biotechnol Bioeng.* 2018, 115(6):1542-1551.
39. Förster J1, Famili I, Fu P, Palsson BØ, Nielsen J. **Genome-scale reconstruction of the Saccharomyces cerevisiae metabolic network.** *Genome Res.* 2003, 13(2):244-53. Förster J1, Famili I, Fu P, Palsson BØ, Nielsen J.
40. Duarte NC, Herrgård MJ, Palsson BØ **Reconstruction and validation of Saccharomyces cerevisiae iND750, a fully compartmentalized genome-scale metabolic model** *Genome Res.* 2004, 14(7):1298-309.
41. Dobson PD, Smallbone K, Jameson D, Simeonidis E, Lanthaler K, Pir P, Lu C, Swainston N, Dunn WB, Fisher P, Hull D, Brown M, Oshota O, Stanford NJ, Kell DB, King RD,

Oliver SG, Stevens RD, Mendes P. **Further developments towards a genome-scale metabolic model of yeast** *BMC Syst Biol.* 2010, 28;4:145

42. Osterlund T, Nookaew I, Nielsen J. **Fifteen years of large scale metabolic modeling of yeast: developments and impacts** *Biotechnol Adv.* 2012, 30(5):979-88
43. Nookaew I, Olivares-Hernández R, Bhumiratana S, Nielsen J **Genome-scale metabolic models of Saccharomyces cerevisiae.** *Methods Mol Biol.* 2011;759:445-63
44. Mo ML, Palsson BO, Herrgård MJ **Connecting extracellular metabolomic measurements to intracellular flux states in yeast.** *BMC Syst Biol.* 2009, **3:**37
45. Asadollahi MA, Maury J, Patil KR, Schalk M, Clark A, Nielsen J **Enhancing sesquiterpene production in *Saccharomyces cerevisiae* through in silico driven metabolic engineering**. *Metab Eng.* 2009, 11(6):328-34
46. Hjersted JL, Henson MA, Mahadevan R. **Genome-scale analysis of *Saccharomyces cerevisiae* metabolism and ethanol production in fed-batch culture.** *Biotechnol Bioeng.* 2007, 97(5):1190-204.
47. Xu G, Zou W, Chen X, Xu N, Liu L, Chen **Fumaric acid production in *Saccharomyces cerevisiae* by in silico aided metabolic engineering.** J.*PLoS One.* 2012, 7(12)
48. Agren R, Otero JM, Nielsen J.**Genome-scale modeling enables metabolic engineering of *Saccharomyces cerevisiae* for succinic acid production.** *J Ind Microbiol Biotechnol*. 2013, 40(7):735-47
49. Atsumi S, Hanai T, Liao JC: **Non-fermentative pathways for synthesis of branched-chain higher alcohols as biofuels.** *Nature* 2008, 451(7174):86–89.
50. Matsudahimizu H, Kondo A: **Engineering strategy of yeast metabolism for higher alcohol production.** *Microbial Cell Factories* 2011, 10:70
51. Matsuda F, Ishii J, Kondo T, Ida K, Tezuka H, Kondo A.: **Increased isobutanol production in *Saccharomyces cerevisiae* by eliminating competing pathways and resolving cofactor imbalance.** *Microbial Cell Factories* 2013, 12:119.
52. Thomas Wallner, Scott A. Miers and Steve McConnell **A Comparison of Ethanol and Butanol as Oxygenates Using a Direct-Injection, Spark-Ignition Engine** *Journal of Engineering for Gas Turbines and Power* 2009 **131:**9
53. Atsumi S, Higashide W, Liao JC: **Direct photosynthetic recycling of carbon dioxide to isobutyraldehyde**. *Nat Biotechnol* 2009, 27(12):1177–1180.
54. Atsumi S, Li Z, Liao JC: **Acetolactate synthase from *Bacillus subtilis* serves as a 2-ketoisovalerate decarboxylase for isobutanol biosynthesis in *Escherichia coli*.** *Appl Environ Microbiol* 2009, 75(19):6306–6311.

55. Atsumi S, Wu TY, Eckl EM, Hawkins SD, Buelter T, Liao JC: **Engineering the isobutanol biosynthetic pathway in *Escherichia coli* by comparison of three aldehyde reductase/alcohol dehydrogenase genes.** *Appl Microbiol Biotechnol* 2010, 85(3):651–657.
56. Smith KM, Cho KM, Liao JC: **Engineering *Corynebacterium glutamicum* for isobutanol production.** *Appl Microbiol Biotechnol* 2010, 87(3):1045–1055.
57. Baez A, Cho KM, Liao JC: **High-flux isobutanol production using engineered *Escherichia coli*: a bioreactor study with in situ product removal.** *Appl Microbiol Biotechnol* 2011, 90(5):1681–1690.
58. Higashide W, Li Y, Yang Y, Liao JC: **Metabolic engineering of *Clostridium cellulolyticum* for production of isobutanol from cellulose**. *Appl Environ Microbiol* 2011, 77(8):2727–2733.
59. Bastian S, Liu X, Meyerowitz JT, Snow CD, Chen MM, Arnold FH: **Engineered ketol-acid reductoisomerase and alcohol dehydrogenase enable anaerobic 2-methylpropan-1-ol production at theoretical yield in *Escherichia coli.*** *Metab Eng* 2011, 13(3):345–352.
60. Blombach B, Riester T, Wieschalka S, Ziert C, Youn JW, Wendisch VF, Eikmanns BJ: ***Corynebacterium glutamicum* tailored for efficient isobutanol production.** *Appl Environ Microbiol* 2011, 77(10):3300–3310.
61. Li S, Wen J, Jia X: **Engineering *Bacillus subtilis* for isobutanol production by heterologous Ehrlich pathway construction and the biosynthetic 2-ketoisovalerate precursor pathway overexpression.** *Appl Microbiol Biotechnol* 2011, 91(3):577–589.
62. Yamamoto S, Suda M, Niimi S, Inui M, Yukawa H: **Strain optimization for efficient isobutanol production using *Corynebacterium glutamicum* under oxygen deprivation.** *Biotechnol Bioeng* 2013, 110(10):2938–2948.
63. Kondo T, Tezuka H, Ishii J, Matsuda F, Ogino C, Kondo A: **Genetic engineering to enhance the Ehrlich pathway and alter carbon flux for increased isobutanol production from glucose *by Saccharomyces cerevisiae***. *Journal of Biotechnology* 2012, 159(1–2):32–37.
64. Chen X, Nielsen KF, Borodina I, Kielland-Brandt MC, Karhumaa K: **Increased isobutanol production in *Saccharomyces cerevisiae* by overexpression of genes in valine metabolism.** *Biotechnol Biofuels* 2011, 4:21.
65. Avalos JL, Fink GR, Stephanopoulos G: **Compartmentalization of metabolic pathways in yeast mitochondria improves the production of branched-chain alcohols**. *Nat*

Biotechnol 2013,**4**:335-341.

66. Lee W, Seo S, Bae Y, Nan H, Jin Y, Seo J: **Isobutanol production in engineered *Saccharomyces cerevisiae* by overexpression of 2-ketoisovalerate decarboxylase and valine biosynthetic enzymes.** *Bioproc Biosyst Eng* 2012, **9:**1467-1475.
67. Matsuda F, Kondo T, Ida K, Tezuka H, Ishii J, Kondo A: **Construction of an artificial pathway for isobutanol biosynthesis in the cytosol of *Saccharomyces cerevisiae*.** *Biosci Biotechnol Biochem* 2012, 76(11):2139–2141.
68. Brat D, Weber C, Lorenzen W, Bode HB, Boles E: **Cytosolic re-localization and optimization of valine synthesis and catabolism enables inseased isobutanol production with the yeast *Saccharomyces cerevisiae*.** *Biotechnol Biofuels* 2012, 5(1):65.
69. Brat D, Boles E: **Isobutanol production from D-xylose by recombinant Saccharomyces cerevisiae.** *FEMS Yeast Res* 2013, **2:**241-244.
70. Langmead, B., Salzberg, S. L., 2012. **Fast gapped-read alignment with Bowtie 2**. Nat Methods. 9**,** 357-9.
71. Li, H., Handsaker, B., Wysoker, A., Fennell, T., Ruan, J., Homer, N., Marth, G., Abecasis, G., Durbin, R., Genome Project Data Processing, S., 2009. **The Sequence Alignment/Map format and SAMtools**. Bioinformatics. 25**,** 2078-9.
72. Robinson, J. T., Thorvaldsdottir, H., Winckler, W., Guttman, M., Lander, E. S., Getz, G., Mesirov, J. P., 2011. **Integrative genomics viewer**. Nat Biotechnol. 29**,** 24-6.
73. Tyrrell Conway **The Entner-Doudoroff pathway: history, physiology and molecular biology** *FEMS Microbiology Letters* 1992 **103:**1-28
74. F Benisch, E Boles - **The bacterial Entner–Doudoroff pathway does not replace glycolysisin *Saccharomyces cerevisiae* due to the lack of activity of iron–sulfurcluster enzyme 6-phosphogluconate dehydratase** *Journal of biotechnology* 2014, **171**:45–55
75. Yoshihiro Ida, Takashi Hirasawa, Chikara Furusawa, Hiroshi Shimizu **Utilization of Saccharomyces cerevisiae recombinant strain incapable of both ethanol and glycerol biosynthesis for anaerobic bioproduction** *Applied Microbiology and Biotechnology* 2013, **97**:4811-4819
76. Soo-Jung Kima, Seung-Oh Seoc, Yong-Su Jinc, Jin-Ho Seo **Production of 2,3-butanediol by engineered *Saccharomyces cerevisiae*** *Bioresource Technology* 2013, **146:** 274–281
77. Braymer JJ, Lill R **Iron-sulfur cluster biogenesis and trafficking in mitochondria** *J Biol Chem.* 2017, 292(31):12754-12763
78. Nagaraj N, Kulak NA, Cox J, Neuhauser N, Mayr K, Hoerning O, Vorm O, Mann M. **System-wide perturbation analysis with nearly complete coverage of the yeast proteome by single-shot ultra HPLC runs on a bench top Orbitrap.** *Mol Cell Proteomics.*

2012, 11(3)

79. Liebermeister W1, Noor E, Flamholz A, Davidi D, Bernhardt J, Milo R. **Visual account of protein investment in cellular functions.** *Proc Natl Acad Sci USA*. 2014 Jun 10; 111(23):8488-93.
80. Okahashi N, Matsuda F, Yoshikawa K, Shirai T, Matsumoto Y, Wada M, Shimizu H **Metabolic engineering of isopropyl alcohol-producing *Escherichia coli* strains with ^{13}C-metabolic flux analysis** *Biotechnol Bioeng.* 2017, 114(12):2782-2793.
81. Dai Z, Huang M, Chen Y, Siewers V, Nielsen J **Global rewiring of cellular metabolism renders *Saccharomyces cerevisiae* Crabtree negative** *Nat Commun.* 2018,9(1):3059
82. Ishii J, Izawa K, Matsumura S, Wakamura K, Tanino T, Tanaka T, Ogino C, Fukuda H, Kondo A **A simple and immediate method for simultaneously evaluating expression level and plasmid maintenance in yeast.** *J Biochem* 2009, **145:**701–708.
83. Ishii J, Kondo T, Makino H, Ogura A, Matsuda F, Kondo A **Three gene expression vector sets for concurrently expressing multiple genes in *Saccharomyces cerevisiaeI.*** *FEMS Yeast Research* 2014, **14:**399 – 411
84. Ishii J, Morita K, Ida K, Kato H, Kinoshita S, Hataya S, Shimizu H, Kondo A, Matsuda F.**A pyruvate carbon flux tugging strategy for increasing 2,3-butanediol production and reducing ethanol subgeneration in the yeast *Saccharomyces cerevisiae*** *Biotechnol Biofuels.* 2018, 26, 11:180
85. Lee ME, DeLoache WC, Cervantes B, Dueber JE **A Highly Characterized Yeast Toolkit for Modular, Multipart Assembly.** *ACS Synth Biol*. 2015, 18; 4(9):975-86.